1
}
\ 
ĺ
j
: ' '
; ; ;
·
i
(
Î
ن.

## FLEXURAL ELASTIC CHARACTERISTICS OF CROSS-SHAPED STRUCTURAL JOINTS

by

Shantilal Chaturbhai Patel

## AN ABSTRACT

Submitted to the School for Advanced Graduate Studies of Michigan State University of Agriculture and Applied Science in partial fulfillment of the requirements for the degree of

DOCTOR OF PHILOSOPHY

Department of Civil Engineering

1959

Approved: Carl Z. Shermer

A knowledge of the energy distribution characteristics of the joints is important for an analysis of indeterminate framed structures with deep-short members. This dissertation determines the characteristics of cross-shaped joints (internal joints of the framed structure) subjected to flexural action. The members of the frame are of rectangular cross section and the stress distribution is assumed to be plane.

The Airy's stress function Ø inside the cross-shaped region is determined by solving the biharmonic differential equation by the numerical finite difference method. The stresses and the elastic energy per unit beam length are determined. The equivalent depth distribution is calculated, i.e., the depth distribution which when used in the evaluation of the energy by the conventional beam theory formulas will give the true elastic energy. The effects, of the fillets at the joint, of the dimensions of the cross shape, and of the variations in the Poisson's ratio, on the equivalent depth are studied.

The column portion of the cross shape is also analyzed with an assumed linear bending stress distribution and a uniform shear stress distribution at the beam to column junction. The analysis is made by taking the stress function in the form of a series. The comparison of equivalent depth curves, inside the column portion, calculated by the finite

difference method and by the series method shows a fair agreement as far as the shape of the equivalent depth curve is concerned. The series method is also used to investigate the effect of the different proportions of the cross shape on the equivalent depth inside the column.

It is concluded that the exact value of the equivalent depth depends upon the proportions of the cross shape, the type of the loading, and the radius of the fillet. For practical use, an approximate equivalent depth line is suggested, which can be used for any kind of loading and any proportions of the cross shape. In an example, worked out with the suggested approximation and the beam theory formulas. the total energy of the joint differs from the energy calculated by the finite difference method by less than 11%. This is a much smaller error than that which results from using either of the assumptions commonly made: that the equivalent depth at any section inside the joint is the same as the depth at the face of the joint or alternatively that the moment of inertia at any section inside the joint is infinity. Either of these assumptions leads to errors of about 100% in the total energy of the joint.

# FLEXURAL ELASTIC CHARACTERISTICS OF CROSS-SHAPED STRUCTURAL JOINTS

bу

Shantilal Chaturbhai Patel

A THESIS

Submitted to the School for Advanced Graduate Studies of Michigan State University of Agriculture and Applied Science in partial fulfillment of the requirements for the degree of

DOCTOR OF PHILOSOPHY

Department of Civil Engineering

To My
Late Father,
and

Younger Brother, Anu

## ACKNOWLEDGMENTS

The author wishes to express his sincere appreciation and thanks to his major Professor, Dr. Carl L. Shermer, for his invaluable assistance and guidance throughout this investigation.

Sincere appreciation is also expressed to Dr. L. E. Malvern for his keen interest, invaluable help, and illuminating inspiration throughout the study.

He is indebted to Dr. Charles E. Cutts for his valuable remarks. Thanks are also expressed to Dr. R. H. J. Pian for his many suggestions.

The writer would like to express thanks to Dr. Charles
O. Harris for his cooperation in making the facilities
available for the experimental investigation.

Thanks are also expressed to Mrs. G. B. Reed and Dr. G. P. Weeg for their assistance in preparation of Digital Computer programs, and to Dr. V. G. Grove who acted on the guidance committee.

## TABLE OF CONTENTS

CHAPTER									PA	AGE
I.	INTRO	DUCI	ON	•	•				•	1
II.	PRINC	CIPLE		•	•				•	9
III.	EXPER	RIMEN	'AL ANALYSIS	•	•	•	•	•		19
IV.	NUMER	RICAI	METHOD	•	•		•	•	•	32
	Part	I.	ure Bending Moment	Con	diti	on	•		•	35
		Α.	ross shape having $b = 3.0$ , $d/b = 1$ .	L/b O an	= 2. d r/	o, d =	: 1/	<b>'</b> 3	•	36
		В.	quivalent depth re/b of the cross sh		d to	ra •	tio •	•	•	49
		С.	ross shape having $b/b = 2.333$ , $d/b = 2.333$	L/b 1.0	= 1. and	333 r/d	, =	0		54
		D.	ffect of Poisson's quivalent depth .		io c		•	•	•	55
	Part	II.	ariable Bending Mo Shear-Loading Case				ion	•		56
	•	Α.	ross shape having $a/b = 2.333$ , $d/b =$	L/b 1.3	= 1. and	333 r/d	, =	1/3	· •	<b>5</b> 6
		в.	cross shape having $a/b = 2.333$ , $d/b =$	L/b 1.0	= 1. and	333 <b>r/</b> d	, =	0		60
		С.	ffect of Poisson's quivalent depth .	rat	io c	n •	•	•	•	61
	Part	III.	nterpretation of F	Resul	.ts	•			•	61
		Α.	quivalent depth ra	atio					•	61
		В.	contribution of she he total energy .							66
		С.	tresses on the fac	e of	col	.umn	١.	•	•	66

CHAPTER													F	PAGE
v.	SERI	ES SC	LUTIO	N.		•	•	•	•	•	•	•	•	110
	Part	I.	Gene	ral	Solu	ıtio	n.	•		•	•	•	•	111
	Part	II.	Pure	Ber	nding	Mo	ment	Cor	ndi	tior	١.	•	•	118
	Part	III.	Vari (She		e Ber Loadi								•	126
	Part	IV.	Inte Meth											131
		Α.	Pure	bend	ding	mom	ent	•	•	•	•	•	•	131
		В.	Varia loadi	ble n <b>g</b> d	bend case)	ling	mom.	ent •	(s)	hear •	•	•	•	132
	Part	v.			natic ent f								•	132
VI.	SUMM	ARY A	ND CO	NCLU	JSION	Ι.	•	•	•	•	•	•	•	156
APPENDIX	Α.		rmal gon.	Mapr	_		a Cr			_		•	•	159
APPENDIX	В.	Finit	ce Dif	fere	ence	Equ	atic	ns	•	•	•	•	•	171
APPENDIX	C.	Tota	C Com al Ene Colum	rgy	Alor	ıg t	he E	Beam	Se	ctic	n c		•	
			ent Ac									•	•	174
BIBLIOGRA	APHY.	•		•			•	•	•	•	•			185

## LIST OF TABLES

TABLE	P	AGE
4.1	$\emptyset$ values for the cross shape having L/b = 2.0, h/b = 3.0, d/b = 1.0, and r/d = 1/3 subjected to pure bending moment	70
4.2	Bending stress	71
4.3	Comparison of resisting and applied moments $M_y$ for the cross shape having $d/b=1.0$ and $r/d=1/3$ subjected to pure bending moment	72
4.4	$\emptyset$ values for the cross shape with graded net having $L/b = 1.333$ , $h/b = 2.333$ , $d/b = 1.0$ , and $r/d = 1/3$ subjected to pure bending moment.	73
4.5	Bending stresses $y$ for the cross shape having $d/b = 1.0$ and $r/d = 1/3$ subjected to pure bending moment (graded net)	74
4.6	Comparison of resisting and applied moments $M_y$ for a cross shape having $d/b = 1.0$ and $r/d = 1/3$ subjected to pure bending moment (graded net)	75
4.7	Bending stress $\sqrt[4]{y}$ for a cross shape having $d/b = 1.0$ and $r/d = 1/3$ subjected to pure bending moment (higher order difference formula, graded net)	76
4.8	Comparison of resisting and applied moments $M_y$ for a cross shape having $d/b=1.0$ and $r/d=1/3$ subjected to pure bending moment (higher order difference formula, graded net).	77
4.9	Normal stress $\mathcal{L}_{x}$ and shearing stress $\mathcal{L}_{xy}$ for the cross shape having $d/b = 1.0$ and $r/d = 1/3$ subjected to pure bending moment (graded net).	78
4.10	Computation of the energy for the cross shape having $d/b = 1.0$ and $r/d = 1/3$ subjected to pure bending moment (Poisson's ratio = 0.30)	79

TABLE		PAGE
4.11	Ratio R, the equivalent depth $d_e$ to the depth 2d of the beam, for the cross shape having $L/b = 1.333$ , $h/b = 2.333$ , $d/b = 1.0$ and $r/d = 1/3$ subjected to pure bending moment (Poisson's ratio = 0.30).	79
4.12	$\emptyset$ values for the cross shape having L/b = 2.5, h/b = 3.5, d/b = 1.5 and r/d = 1/3 subjected to pure bending moment	80
4.13	Stress values for the cross shape having $d/b = 1.5$ and $r/d = 1/3$ subjected to pure bending moment	81
4.14	Computation of the energy for the cross shape having $d/b = 1.5$ and $r/d = 1/3$ subjected to pure bending moment (Poisson's ratio = 0.30) .	82
4.15	Ratio R, the equivalent depth $d_e$ to the depth 2d of the beam for the cross shape having $L/b = 2.5$ , $h/b = 3.5$ , $d/b = 1.5$ and $r/d = 1/3$ subjected to pure bending moment (Poisson's ratio = 0.30)	82
4.16	$\emptyset$ values for the cross shape having L/b = 1.333, h/b = 2.333, d/b = 1.0 and r/d = 0 subjected to pure bending moment	83
4.17	Stresses for the cross shape having $d/b = 1.0$ and $r/d = 0$ subjected to pure bending moment .	84
4.18	Computation of the energy for the cross shape having $d/b = 1.0$ and $r/d = 0$ subjected to pure bending moment (Poisson's ratio = 0.30)	85
4.19	Ratio R, the equivalent depth $d_e$ to the depth 2d of the beam for the cross shape having $L/b = 1.333$ , $h/b = 2.333$ , $d/b = 1.0$ and $r/d = 0$ subjected to pure bending moment (Poisson's ratio = 0.30).	85
4.20	Ratio R, the equivalent depth $d_e$ to the depth 2d of the beam, for the cross shape having $L/b = 1.333$ , $h/b = 2.333$ , $d/b = 1.0$ and $r/d = 1/3$ subjected to pure bending moment (Poisson's ratio = 0.15)	86

TABLE		PΑ	GE.
4.21	$\emptyset$ values for the cross shape having L/b = 1.333, h/b = 2.333, d/b = 1.0 and r/d = 1/3 subjected to variable bending moment	•	86
4.22	Stress values for the cross shape having $d/b = 1.0$ and $r/d = 1/3$ subjected to variable bending moment	•	87
4.23	Comparison of applied and resisting forces for the cross shape having $L/b = 1.333$ , $h/b = 2.333$ , $d/b = 1.0$ and $r/d = 1/3$ subjected to variable bending moment	•	88
4.24	Computation of the energy for the cross shape having $d/b = 1.0$ and $r/d = 1/3$ subjected to variable bending moment (Poisson's ratio = 0.30)	))	89
4.25	Ratio R, the equivalent depth $d_e$ to the depth 2d of the beam, for the cross shape having $L/b = 1.333$ , $h/b = 2.333$ , $d/b = 1.0$ and $r/d = 1/3$ subjected to variable bending moment (Poisson's ratio = 0.30)	•	89
4.26	$\emptyset$ values for the cross shape having $1/b = 1.333$ , $h/b = 2.333$ , $d/b = 1.0$ and $r/d = 0$ subjected to variable bending moment	•	90
4.27	Stresses for the cross shape having $d/b = 1.0$ and $r/d = 0$ subjected to variable bending momen	nt	91
4.28	Computation of the energy for the cross shape having $d/b = 1.0$ and $r/d = 0$ subjected to variable bending moment (Poisson's ratio = 0.30)	)	92
4.29	Ratio R, the equivalent depth $d_e$ to the depth 2d of the beam, for the cross shape having $L/b = 1.333$ , $h/b = 2.333$ , $d/b = 1.0$ and $r/d = 0.0$ subjected to variable bending moment (Poisson's ratio = 0.30)	3	92
4.30	Ratio R, the equivalent depth $d_e$ to the depth 2d of the beam, for the cross shape having $L/b = 1.333$ , $h/b = 2.333$ , $d/b = 1.0$ and $r/d = 1/3$ subjected to variable bending moment (Poisson's ratio = 0.15)	•	93

TABLE		PAGE
5.1	Stresses for a column having b=d=0.42856h subjected to pure bending moment	. 137
5.2	Energy and ratio R for a column having b=d=0.42856h subjected to pure bending moment	. 139
5.3	Center line deflection u, slope curvature and ratio R based on curvature	. 140
5.4	Values of ratio R for various b, d, and h. Pure bending moment condition	. 141
5.5	Values of ratio R for various b, d, and h keeping L constant. Shear loading condition	. 142
5.6	Values of ratio R for different span length L, keeping b, d, and h constant. Shear loading condition	. 143
A.1	Coefficients of the series of the mapping function	. 163
A.2	Z-values of the transformed shape for a cross shape having $a_1 = e^{-i(\pi/2)}$ , $a_2 = e^{-i(\pi/2)}$ , $a_3 = e^{-i(\pi/2)}$	. 164
A.3	Z-values of the transformed shape for a cross shape having $a_1 = e^{\frac{1}{2} \cos(\pi/2)}$ , $a_3 = e^{\frac{1}{2} \cos(\pi/2)}$ .	. 165
A.4	Z-values of the transformed shape for a cross shape having $a_1 = e^{\frac{1}{2}(\pi/2)}$ , $a_2 = e^{\frac{1}{2}(\pi/2)}$ , $a_3 = e^{\frac{1}{2}(\pi/2)}$ .	. 166

## LIST OF FIGURES

FIGURE	•	PAGE
2.1	Linear and non-linear stress distribution	17
2.2	Stress block	17
2.3	Cross-shaped joint subjected to flexural action	18
3.1	Polariscope set-up	27
3.2	Model mounted in loading frame	28
3.3	Model form	29
3.4	Isochromatic fringes of the cross shape subjected to pure bending moment	30
3.5	Isochromatic fringes of the cross shape subjected to variable bending moment (shear-loading case)	31
4.1	Cross shape having $I/b = 2.0$ , $h/d = 3.0$ , $d/b = 1.0$ and $r/d = 1/3$	94
4.2	Bending stress of curves for various beam sections of the cross shape having b=d=0.333h.(Pure bending moment)	95
4.3	Cross shape with graded net having $L/b = 1.333$ , $h/b = 2.333$ , $d/b = 1.0$ and $r/d = 1/3$	
4.4	Bending stress $\sigma_y$ curves for various beam sections of a cross shape having b=d=0.42856h. (Pure bending moment. Graded net)	97
4.5	ov curves for beam sections for a cross shape having b=d=0.42856h. (Pure bending moment)	98
4.6	Equivalent depth diagram for a cross shape having $d/b = 1.0$ and $r/d = 1/3$ subjected to pure bending moment	99
4.7	Cross shape having $L/b = 2.5$ , $h/b = 3.5$ , $d/b = 1.5$ and $r/d = 1/3$	100

FIGURE	·	PAGE
4.8	Equivalent depth diagram for a cross shape having $d/b = 1.5$ and $r/d = 1/3$ subjected to pure bending moment	. 101
4.9	Equivalent depth diagram for a cross shape having $d/b = 1.0$ and $r/d = 0$ subjected to pure bending moment	. 102
4.10	Cross shape subjected to variable bending moment	. 103
4.11	Equivalent depth diagram for a cross shape having $d/b = 1.0$ and $r/d = 1/3$ subjected to variable bending moment	. 104
4.12	Equivalent depth diagram for a cross shape having $d/b = 1.0$ and $r/d = 0$ —subjected to variable bending moment	. 105
4.13	Qualitative distribution of $\sigma_y$ and $\sigma_y^2$ on beam section at the face of column	. 106
4.14	Cross shape having $d/b = 1.0$ , $h/d = 2.333$ , $r/d = 1/3$ and $I/d$ greater than 1.333 subjected to variable bending moment	. 107
4.15	for stress distribution for beam section #3 for a cross shape having $b=d=0.42856h$ and $r/d=0$ . (Pure bending moment)	. 108
4.16	Actual and assumed shear stress distribution on the face of a column due to shear force V	. 109
5.1	Boundary forces on the column	. 144
5.2	Bending stress of curves for various beam sections of a column, having b=d=0.42856h, subjected to pure bending moment	. 145
5.3	Center line (Y-axis) deflection, slope, and curvature for a column, having b=d=0.42856h, subjected to pure bending moment	. 146
5.4	Equivalent depth as calculated by energy and curvature concept for b=d=0.42856h. (Pure bending moment)	. 147
5.5	Equivalent depth curves for different column widths with d=0.2h. (Pure bending moment) .	. 148

FIGURE		PAGE
5.6	Equivalent depth curves for different beam depths with b=0.42856h. (Pure bending moment) .	. 149
5.7	Equivalent depth curves as calculated by series method and numerical method. (Pure bending moment)	. 150
5.8	Equivalent depth curves as calculated by series method and numerical method. (Shear loading)	. 151
5.9	Equivalent depth curves for different column widths with $d=0.2h$ and $L=0.57143h$ . (Shear loading)	. 152
5.10	Equivalent depth curves for different beam depths with b=0.42856h. (Shear loading)	. 153
5.11	Equivalent depth curves for different beam span lengths with b=d=0.42856h. (Shear loading)	. 154
5.12	Approximated equivalent depth diagram for rectangular flexural members intersecting at a rigid joint	. 155
A.1	Cross-shaped region on complex Z and 🕻 planes.	167
A.2	Mapped region for a cross shape with $a_1 = e^{-i(\pi/2)}$ , $a_2 = e^{-i(\pi/2)}$ , $a_3 = e^{-i(\pi/2)}$ .	. 168
A.3	Mapped region for a cross shape with $a_1 = e^{\frac{1}{2} \cdot \frac{1}{2}}$ , $a_2 = e^{\frac{1}{2} \cdot \frac{1}{2}}$ , $a_3 = e^{\frac{1}{2} \cdot \frac{1}{2}}$ .	169
A.4	Mapped region for a cross shape with $a_1 = e^{0.01/\pi/2}$ , $a_2 = e^{0.51/\pi/2}$ , $a_3 = e^{0.991/\pi/2}$ .	170

#### NOTATION

- A -- Cross-sectional area of the beam.
- $A_o$  -- Constant in Fourier series of shear stress  $Z_{xy}$ .
- $A_{m}$  -- Constant in Fourier series of shear stress  $Z_{xy}$ .
- $a_1$ ,  $a_2$ ,  $a_3$  --  $\xi$  values for corners of the cross shape.
- B<sub>m</sub> -- Constant in Fourier series of normal stress  $\sigma_{v}$ .
- b -- Half width of the column.
- C<sub>n</sub> -- Constants in the mapping series.
- $c_{1m}$ ,  $c_{2m}$ ,  $c_{3m}$ ,  $c_{4m}$  -- Constants in stress function  $\emptyset$  series.
- D -- Depth of the beam.
- d -- Half depth of the beam.
- de -- Equivalent depth of the beam.
- E -- Modulus of elasticity in tension or compression.
- e<sub>x</sub>, e<sub>y</sub>, e<sub>z</sub> -- Unit extension (longitudinal strain) in.
  x, y and z directions respectively.
- F -- Correction factor.
- $F_y$  --  $Y/K_bh$
- F(x)-- Function of x only, describing the distribution of y on y = b.
- $f_m(y)$  Function of y only. Also function of integer m which varies from 1 to  $\infty$
- $f_m(y)$  Second derivative of  $f_m(y)$ .
- $f_m(y)$  Fourth derivative of  $f_m(y)$ .
- G -- Modulus of elasticity in shear.
- G(x) Function of x only, describing the distribution of  $\mathbf{z}_{xy}$  on y = b.

h -- Half height of the column of the cross shape.

I -- Moment of inertia.

 $K_1$  -- Constant in the bending stress  $\sigma_y$  function.

 $K_2$  -- Constant in the shear stress  $\tau_{xy}$  function.

 $K_b -- b = K_b h$ 

 $K_d$  --  $d = K_d h$ 

L -- Distance from the face of a column to the end of a beam of the cross shape.

L<sub>1</sub> -- Distance from the face of a column to the point on the beam through which concentrated load is applied.

L<sub>2</sub> -- Distance from the face of a column to the point of the beam through which applied loads are resisted.

L<sub>3</sub> -- Portion of beam span greater than 1.333d.

M -- Bending moment.

 $M_V$  -- Bending moment due to stress distribution  $\sigma_V$ .

m -- Integer, varying from 1 tc ℃.

 $N_{x}$  -- Normal force in X-direction.

 $P_0$  -- Constant in series of the stress function  $\emptyset$ .

R -- Ratio of the equivalent depth  $d_e$  to the depth 2d of the beam.

r -- Radius of fillet.

s -- Ungraded mesh size.

U -- Elastic strain energy

u -- Displacement in X-direction

V -- Shear force.

 $V_{x}$  -- Shear force in X-direction.

v -- Displacement in Y-Direction.

X, Y, Z -- Three dimensional axes.

-- In Appendix A, it is complex variable plane.  $\mathbf{z}$ 

ΔS -- Small segment of the beam.

-- Strain energy of the small volume element. dU

o<sub>1</sub>; o<sub>2</sub> -- Principal stresses.

 $\sigma_x$ ,  $\sigma_y$ ,  $\sigma_z$  -- Normal stress in x, y, and z directions, respectively.

Txy -- Shear stress in Y-direction, acting on the plane
perpendicular to X-axis. Similar meaning for Tvz, Tzv.

 $\mathbf{Y}_{\mathbf{X}\mathbf{y}}$ ,  $\mathbf{Y}_{\mathbf{y}\mathbf{z}}$ ,  $\mathbf{Y}_{\mathbf{Z}\mathbf{X}}$  -- Shearing strains.

M -- Poisson's Ratio.

 $\nabla^2$  -- Laplace's operator =  $\frac{3}{3\chi^2} + \frac{3^2}{3\gamma^2}$ .  $\nabla^4$  --  $\frac{3^4}{3\chi^4} + 2\frac{3^4}{3\chi^23\gamma^2} + \frac{3^4}{3\gamma^4}$ .

 $\theta$  --  $\xi = e^{i\theta}$ 

 $\theta_1$ ;  $\theta_2$  -- Angle of relative rotation at the neutral axis.

 $\emptyset$  -- Airy's stress function.

 $\emptyset'$ , $\emptyset''$  -- First and second derivatives of  $\emptyset$ , respec-

<т- m т/h.

**B** -- An angle which approximated equivalent depth line makes with the horizontal line.

← Complex number.

TK: -- Interior angles at vertices of the polygon.

Equations, tables, and figures in this dissertation are identified by the following notation: The character before full stop represents chapter or appendix number in which it appears. The number after full stop represents the sequence number of the equation, or table, or figure, of that particular chapter or appendix. As for example: Equation 2.3 is the third equation of Chapter II. Tables and figures of each chapter or appendix are located at the end of the chapter or appendix.

#### CHAPTER I

#### INTRODUCTION

Developments in concrete technology and connection methods in metal structures have created confidence among engineers in the validity of the assumption of rigidity of joints in frame structures. Hence, engineers design them in accordance with this assumption. Rigid frame structures are those which have beams and columns as the principal resisting members with the joints providing continuity. This dissertation describes the interaction between structural members rigidly connected at their joints. It is limited to frame structures in which the cross section of the members is rectangular and does not vary abruptly, except that there may be small fillets at the joints. The intersection angle is 90 degrees. This dissertation is further limited to frame structures in which the flexural deformation is the primary distortion. Shear and axial are secondary deformations. Procedures for the analysis of a frame structure which is of indeterminate nature have been known for many years. However, the flexural action of joints is not clearly understood even today. This dissertation presents a study of the flexural interaction at the joint of members rigidly connected. For this study, the structure has been assumed in state of plane stress.

For many years the bending deformation characteristics of beams has been understood. Theoretically the relative rotation of the end faces of the small segment

△S of the structural member of uniform cross section subjected to pure bending moment M is equal to M ( S/EI) This relative rotation is often interpreted in terms of curvature, since M/EI is equal to curvature. The bending energy can be written as (M)(rotation)/2. Hence the bending energy reduces to  $M^2(\Delta S/2EI)$ . In practice there will be few structures in which the beam is under a pure bending moment condition, i.e. in which the bending moment is constant along the span of the beam. Hence, shear energy will form part of the total energy. Also, axial energy will be a part of the total. Usually the shear energy and the axial energy will be insignificant compared with the bending energy. Hence, the last two factors are neglected for computing the total energy. So bending energy is usually taken as the total energy for practical purposes. Whatever method may be used to study the deformation characteristic of the structure necessary to analyze the indeterminate structure, the evaluation of the energy is a required step directly or indirectly.

For the evaluation of the total energy of members, the above discussed tending energy relationship has been used in the clear span zone by engineers. In the region of the joint two procedures are being used. The first

considers that the depth, i.e. the moment of inertia, at any point in the joint, to be used for evaluating total energy, is the same as at the face of the column. The second procedure uses the depth of the column as the effective depth from the face of the column through the joint, or in frames, since the column height is considerably larger than the depth of the beam, infinity is used as the value for the moment of inertia.

A review of engineering literature indicates that since 1900 many investigations have been conducted on rigid frames, joints, and knees. These investigations are focused on the validity of the assumptions of structural behavior as calculated by the elastic theory. The effect of various sizes and types of fillets on the distribution of the stresses in the joint and its effect on the other part of the frame have been studied. In concrete structures, factors such as the amount of reinforcement and its distribution have been studied. In steel structures, joint conditions and buckling properties have been taken into account. However, very little has been learned about the interaction of the column and the beam in the joint zone.

Inge Lyse and W. E. Black have calculated the angular change of the knee faces from the observed principal

lnge Lyse and W. E. Black, "An Investigation of Steel Rigid Frames," Transactions of American Society of Civil Engineers, 107 (1942), pp. 143-144.

stress distribution. This angular change agreed closely with the one calculated from the information of the observed shear forces. They have also calculated the theoretical bending deformation on the assumption that the moment of inertia at any point in the knee zone is the same as that at the face. This calculated deformation is twice that of the one calculated from the observed principal stress distribution. These two authors have concluded that if, however, the effect of the shear is neglected through the frame (as would be done in the design) the large bending deformation assigned to the knee tends to offset the neglect of shear deformation in the frame as a whole.

This conclusion explains the reasons for the use of the first procedure. This matter of compensation is justified in frames in which the span length of the member is very large compared with the depth of the member, so that the effect of the shear is small. Does this compensation idea give the correct results for the frame analysis where the spans are very small? In other words is the contribution of the knee significant in such a case? Since it is known that the knee contributes very little to the tending deformation of the frame as a whole the application of the second procedure seems to be the natural choice. This will necessitate the need for taking into account the shear energy in the evaluation of total energy. However,

most engineers usually neglect shear energy thereby increasing the error in the total energy.

The second procedure was suggested by L. T. Evans.<sup>2</sup>
In setting up the column coefficients for the slopedeflection he mentioned that if the beam is deep with
respect to the height of the column, then it is evident
that the column cannot bend in the knee zone. And this
assumption is equivalent to assuming an infinite moment
of inertia in the knee zone. Evans and others have prepared many tables and graphs charting different functions
such as stiffness factors, carry-over factors and fixed-end
moments for different loading conditions. Evans' assumption
means that the moment of inertia increases abruptly at the
face of the column.

Can there by any sudden change in the moment of inertia at the face of the knee? A similar question has been raised by Ralph E. Spaulding. Discussing the article, "An Analysis of Stepped-Column Mill Bents," by Daniel S. Ling, he pointed out that the effective moment of inertia does not change suddenly when the cross section changes

<sup>&</sup>lt;sup>2</sup>L. T. Evans, "The Modified Slope Deflection Equations," Proceedings of American Concrete Institute, 28 (September 1931--April 1932), p. 118.

<sup>&</sup>lt;sup>3</sup>Ralph E. Spaulding, Discussion on "An Analysis of Stepped-Column Mill Bents," by Daniel S. Ling, <u>Transactions of American Society of Civil Engineers</u>, 113 (1948), p. 1099.

suddenly. The effective cross section for M/EI analysis has been sketched by him. He did not furnish a computational analysis for this, but mentioned that the photoelastic and the strain gauge analysis revealed that there are dead areas in the corner of the wider part.

Joseph A. Wise analyzed the inverted U-frame in which he assumed that the moment of inertia at any point in the knee is the moment of inertia at the face multiplied by the third power of the ratio of half the width of the column to the distance of the point under consideration from the center line of the column. He indicated the need for further investigation of frames with wide members.

This literature indicated that the followers of both procedures are in general agreement that the bending deformation of the knee is very small. Hence they neglect the knee or the joint entirely as far as the bending energy is concerned. The follower of the first procedure compensates for the shear energy of the frame while the follower of the second procedure will take the shear energy separately if it is of significant magnitude compared with the total. The questions remaining unanswered about the joint are:

What is the shape of the moment of inertia curve within the joint? Will the neutral axis curvature within the joint

Joseph A. Wise, "Corner Effects in Rigid Frames," Proceedings of American Concrete Institute, 35 (September 1938--June 1939), pp. 190-191.

zone represent the true effective moment of inertia to be used in the deformation analysis of the structure? If not, what is the true representation? What are the factors that affect the true effective moment of inertia? The answers to these questions are important when the spans are short. The aim of this dissertation is to bring forth answers by studying the interaction of the column to the team subjected to pure bending moment conditions and variable tending moment conditions. The investigation made in this study is limited to cross-shaped joints although it is possible from the results to infer something about the behavior of "T" shaped and "L" shaped joints.

In Chapter II the principles involved in the analysis of indeterminate structures are discussed. It is concluded that the energy variation should be studied for analysis of indeterminate structures, which in turn reduces the problem to the evaluation of stresses. The problem has been specifically outlined for the evaluation of stresses by elasticity theory. Chapter III discusses the experimental method used to investigate the limits of the interaction zone of the cross-shaped joint. From photoelastic analysis it has been concluded that in the beam and in the column the limit extends a distance equal to half the column width and half the beam depth respectively from the faces of the joint. A numerical method for the evaluation of stresses

is discussed in Chapter IV. Using these stresses the internal energy has been calculated at various sections. The equivalent depth is defined as the one which if used in the evaluation of the energy by the conventional beam theory formulas would give the true elastic energy. equivalent depth increases toward the center of the column up to a maximum of 1.40 times the beam depth for pure bending loading and up to 1.59 times the beam depth if shear forces and bending moment are transmitted across the joint. Chapter V discusses the Fourier series application to evaluate stresses and energy in the column zone. This method is used to compare the results with the numerical method and also to study the effect on the equivalent depth of changing the ratio of the beam depth to the column width. Chapter VI summarizes the results and conclusions of the study.

#### CHAPTER II

## PRINCIPLES

For the analysis of indeterminate structures the only basic understanding required by the engineer is how to determine the deflection, linear or rotational, at any point. The determination of deflections generally reduces to the problem of computing the internal elastic energy of the structure. Because of the importance of the energy it will be appropriate to look into principles and the assumptions involved in the commonly used expressions for the energy. The bending energy of a small segment is  $M^2$  ( $\triangle$  S/2EI) as mentioned in Chapter I. This expression of energy has been derived by using the following assumptions: (1) Hooke's Law is valid and the elastic limit is not exceeded during distortion. (2) Sections are plane after bending, i.e. the strain varies linearly across the cross section. The first assumption is valid since the most commonly used materials obey Hooke's Law and the analysis considered here applies to structures in which the elastic limit is not exceeded. The second one, although sufficiently accurate in most cases, is certainly not valid for sections within a joint.

Even in beams where the top and the bottom fibers deviate only a little from parallel, the distribution of the stresses as determined by the ordinary beam theory is not true as was shown by William R. Osgood. He has derived the stress formulas for the beam with non-parallel surfaces by the application of the wedge theory. The use of the ordinary beam theory will not cause a large error in the stresses as long as the angle between the two non-parallel sides does not exceed 10 degrees. In the frame structure the beam from the face of the column inwards could be considered as a beam having a wedge angle of 180 degrees formed by the top and the bottom non-parallel surfaces. Therefore, the stress distribution determined by the ordinary beam theory will not be valid. Beginning at the face of the column the stresses will be distributed fan-like through the joint. This will result in the non-linearity of stresses in the joint zone.

Since the assumption of linearity is not satisfied, the ordinary formula for bending energy should not be used. This also indicates that the concept of geometric moment of inertia should not be used to evaluate the total energy. Also the conventional energy equation is often written in

William R. Osgood, "A Theory of Flexure for Beams with Non-Parallel Extreme Fibers," Transactions of American Society of Mechanical Engineers, 61 (1939), <u>Journal of Applied Mechanics</u>, pp. A-122--A-126.

terms of the neutral axis curvature. Many engineers evaluate the energy by using the neutral axis curvature and the external moment M irrespective of the stress distribution. The implication of this practice is illustrated by the assumed linear and non-linear stress distribution produced by the same moment M as shown in Figure 2.1. The angle of relative rotation at the neutral axis will not be equal in the two cases. Applying the conventional formulas the bending energy of the segment shown in Figure 2.1b will be evaluated as  $M\Theta_2$ . The error involved in evaluating the energy by this approach is enormous. Hence, it is incorrect to think that the bending energy can always be computed in terms of neutral axis curvature.

In the beam of variable section, i.e. non-parallel surfaces, there will be shear stresses even in the case of pure bending moment, as shown by William R. Osgood. Accordingly, there will be shear energy in the pure bending moment case, which should be taken into account to evaluate total energy. Its significance will not be considered at this stage. The 180 degrees wedge analogy discussed above suggests that there will be shear stresses in the column zone of the frame structure subjected to pure bending. Also in beams subjected to variable moment along the span

<sup>&</sup>lt;sup>2</sup><u>Ibid.</u>, p. A-125.

there will be shear stresses. Due to non-linearity of bending stresses in the column zone the shear stresses will not be distributed in the parabolic shape even when the cross section is a rectangle. Hence, the shear energy if taken into account should not be evaluated by the conventional formula  $1.2 \text{ V}^2/2\text{GA}$ .

If the stresses are not distributed as assumed in beam theory, then the total energy at any cross section can be evaluated by the integration of the strain energy density along the depth or by the summation of the strain energy of the small volume elements. The strain energy dU of the small volume element shown in Figure 2.2 can be written as follows:

$$d\mathbf{U} = \frac{1}{2} (\sigma_{\mathbf{x}} e_{\mathbf{x}} + \sigma_{\mathbf{y}} e_{\mathbf{y}} + \sigma_{\mathbf{z}} e_{\mathbf{z}} + C_{\mathbf{x}\mathbf{y}} Y_{\mathbf{x}\mathbf{y}} + C_{\mathbf{y}\mathbf{z}} Y_{\mathbf{y}\mathbf{z}} + C_{\mathbf{z}\mathbf{x}} Y_{\mathbf{z}\mathbf{x}}) d\mathbf{x}. d\mathbf{y}. d\mathbf{z}.$$
(2.1)

where  $\mathcal{L}_{x}$ ,  $\mathcal{L}_{y}$ ,  $\mathcal{L}_{z}$  are the normal stresses,  $\mathcal{L}_{xy}$ ,  $\mathcal{L}_{yz}$ ,  $\mathcal{L}_{zx}$  are shear stresses,  $\mathcal{L}_{x}$ ,  $\mathcal{L}_{y}$ ,  $\mathcal{L}_{z}$  are unit extensions and  $\mathcal{L}_{xy}$ ,  $\mathcal{L}_{yz}$ ,  $\mathcal{L}_{zx}$  are shear strains. By using the stress-strain relationship the strain energy equation can be written in terms of stress as follows:

$$dU = \left[\frac{1}{2E} \left(\sigma_{x}^{2} + \sigma_{y}^{2} + \sigma_{z}^{2}\right) - \frac{1}{2E} \left(\sigma_{x}\sigma_{y} + \sigma_{z}\sigma_{x} + \sigma_{y}\sigma_{z}\right) + \frac{1}{2E} \left(\tau_{xy}^{2} + \tau_{yz}^{2} + \tau_{zx}^{2}\right)\right] dx.dy.dz.$$
(2.2)

<sup>3</sup>Chi-Teh Wang, Applied Elasticity (New York: McGraw-Hill Book Company, 1953), p. 37.

where E is Young's modulus, G is the shear modulus, and

is Poisson's ratio.

When the width of the beam is small compared with the depth, the beam may be regarded as being an example of plane stress. 4 In such a case the energy of the small segment per unit width will be reduced to

$$dU = \left[\frac{1}{2E}\left(\sigma_{x}^{2} + \sigma_{y}^{2} - 2m \cdot \sigma_{x}\sigma_{y}\right) + \frac{1}{2G}\cdot C_{xy}^{2}\right]dx \cdot dy. \tag{2.3}$$

It is to be noted that by taking  $\sigma_{\!_{X}}$  and  $\tau_{\!_{X,y}}$  as zero and assuming the linear bending stress condition for  $\sigma_y$ , the conventional bending energy formula in terms of moment and the moment of inertia results from the plane stress formulation after integration over the depth. By the use of the strain energy formula of the plane stress condition the variation of the energy in the joint zone of the frame can be evaluated provided the actual stress condition can be determined at various points by some means. Information on the energy variation in the joint will be enough to determine the contribution of the various sections of the column to the deformation of the rest of the frame. Knowing the energy at any section in the joint zone and also the moment and the shear force, one can evaluate the equivalent moment of inertia or an equivalent depth. With this equivalent depth information the conventional formulas can be used to

<sup>&</sup>lt;sup>4</sup><u>Ibid</u>., p. 46.

evaluate the deflection, or the functions related to it, necessary for the analysis of an indeterminate structure. It is to be understood that the interpretation in terms of equivalent depth is a matter of convenience to explain the behavior in the conventional form.

The essential problem for evaluating the energy by the elasticity theory reduces to the determination of stresses in the structure. This can be done experimentally or theoretically. In either case it would be essential to investigate the boundary conditions which have to be imposed in order to produce the desired distortion in the structure. For the investigation of the interaction of columns with beams in the frame structures or specifically for the study of the energy variation in the internal joint subjected to flexural action, it will be enough to study the cross-shaped structure subjected to flexural action as shown in Figure 2.3. The  $\sigma_x$  stresses on ends are distributed so as to produce zero bending moment. The distribution of boundary  $\sigma_{x}$ ,  $\sigma_{v}$ , and  $\sigma_{xy}$  will be discussed in Chapter III. Due to the nature of the imposed boundary conditions as shown in Figure 2.3 the column part of the frame will act as part of the horizontal beam, i. e. there would not be any bending of the center line of the column itself. Referring to Figure 2.3, it is implied that there will not be any bending moment on horizontal cross sections of the column. The difference between the usual knee study which

is more a study of arch action and the study of the joint subjected to flexural action should be clearly noted. Even though the geometric shape of frames in the two studies appears to be the same the boundary conditions will be entirely different. The boundary forces shown in Figure 2.3 are the arbitrarily-imposed conditions used in this study.

In order to determine the state of the stress in an elastic body by the Theory of Elasticity it is necessary to solve the equations of equilibrium expressed in terms of stresses<sup>5</sup> together with Beltrami-Michell compatibility equations<sup>6</sup> subjected to proper boundary conditions. The alternative approach is to solve the equations of equilibrium expressed in terms of displacement<sup>7</sup> subject to proper boundary conditions. Considering the case of plane stress and the plane strain condition in the X and Y directions and introducing the Airy's stress function such that the

$$\sigma_{x} = \frac{3^{2}}{4}, \quad \sigma_{y} = \frac{3^{2}}{4}, \quad C_{xy} = -\frac{3^{2}}{4}$$
 (2.4)

compatibility equations will be reduced to the biharmonic

<sup>&</sup>lt;sup>5</sup>Wang, <u>op. cit.</u>, p. 6.

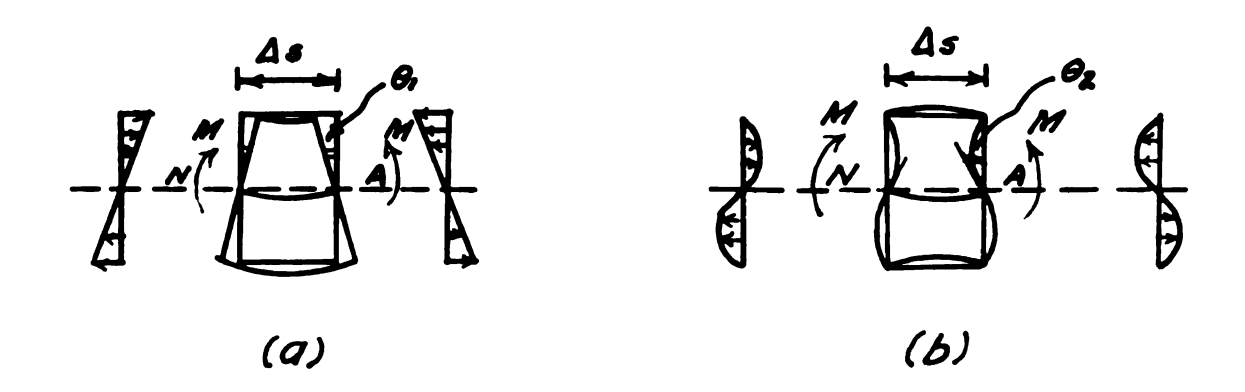
<sup>6&</sup>lt;sub>Ibid</sub>., p. 33.

<sup>7&</sup>lt;sub>Ibid., p. 34.</sub>

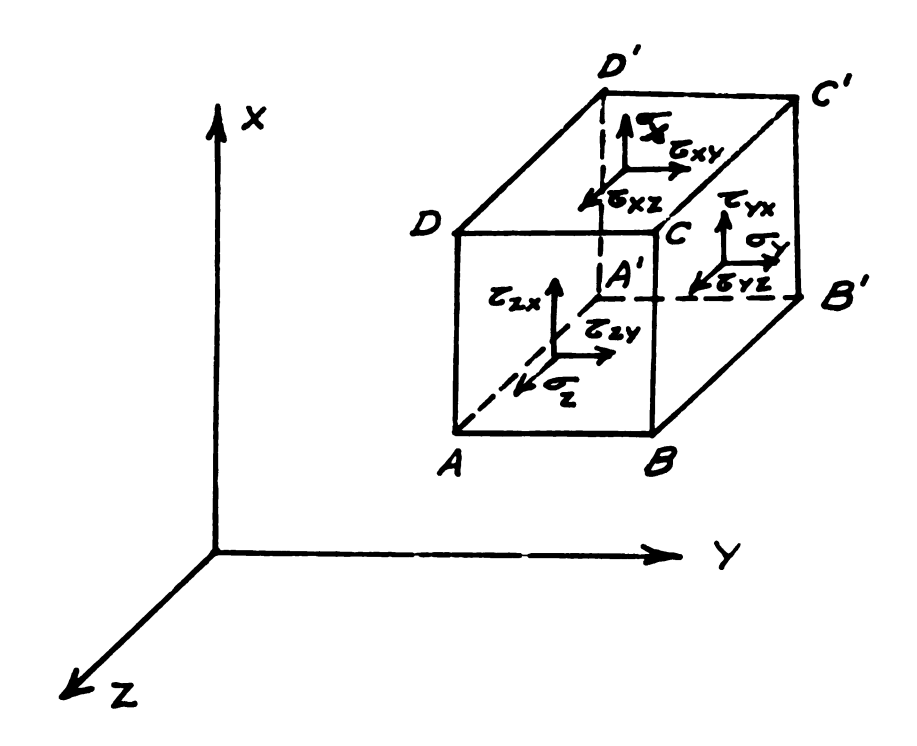
equation. This biharmonic equation is written as

$$\nabla \overset{4}{\phi} = 0 \tag{2.5}$$

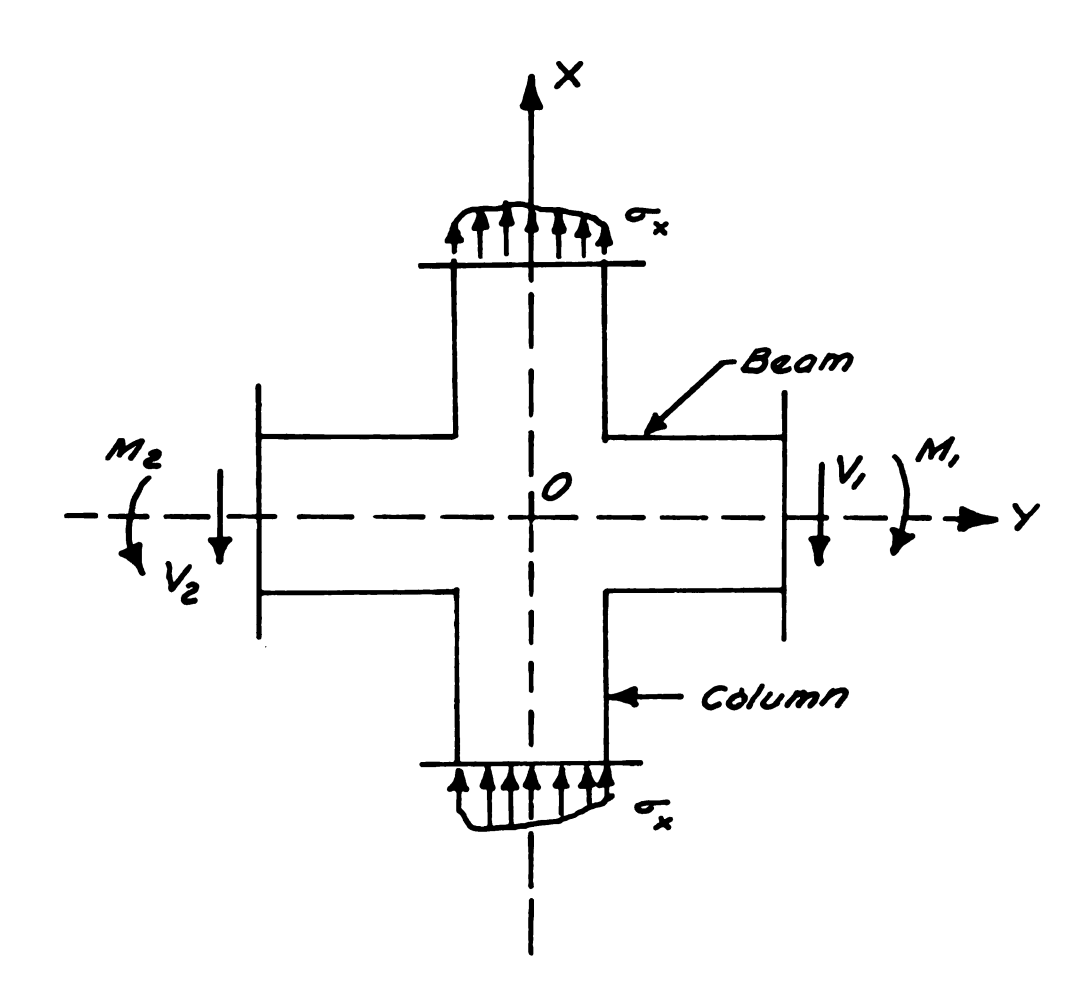
where  $\nabla^2$  is Laplace's operator. The equations of equilibrium are satisfied identically. Hence, the problem of determining stresses in the elastic body reduces to finding the solution of the biharmonic equation satisfying the boundary conditions of the elastic body.



# LINEAR AND NON-LINEAR STRESS DISTRIBUTION FIGURE 2.1



STRESS BLOCK
FIGURE 2.2



CROSS-SHAPED JOINT SUBJECTED TO FLEXURAL ACTION

FIGURE 2.3

#### CHAPTER III

#### EXPERIMENTAL ANALYSIS

As discussed in Chapter II, the interaction of the column with the beam at an internal joint can be studied by analyzing the cross-shaped structure. This analysis requires basically the determination of stress distribution. This could be done experimentally by measuring strains or displacements, by determining stresses by optical methods such as photoelasticity, or theoretically by evaluating Airy's stress function of or computing displacements u and v. In either case it is essential to investigate the limit of the interaction in the cross-shaped joint, i.e. the point beyond which the conventional (beam theory) mode of stress distribution is valid. Hence, the aim of this experiment is to investigate the limit. As the aim of the experiment is of qualitative nature, the photoelastic method has been selected for the purpose.

# Photoelastic Method

The photoelastic method was developed by David Brewster in 1812. He discovered that an optically isotropic transparent solid becomes optically anisotropic upon forced deformation. It has been shown that in the plane stress condition the difference between the principal indices of

refraction is proportional to the difference between the principal stresses in the deformed material and that the optical axes of the deformed material coincide with the principal stress directions. To apply this principle, two optical systems are used in the photoelastic method. In one system a circular polariscope with monochromatic light is used to determine the lines of constant relative retardation, i.e. isochromatic lines, which are the lines of constant principal stress difference or lines of constant maximum shear stress in the photoelastic model. The second system consists of a cross polarizer and analyzer and uses white light which is suitable for the determination of isoclinic lines, i. e. the lines of constant inclination of principal stresses.

#### Equipment

The optical system known as a photoelastic polariscope consists of a polarizer, two quarter wave plates, model, analyzer, and the camera. It also includes an attachment for loading specimens. The arrangement of all parts has been standarized and presented in many books. In this study a commercial polariscope, Chapman 5" Photoelastic Polariscope, as shown in Figure 3.1 is used. The loading

lsee for example, George Harmor Lee, An Introduction to Experimental Stress Analysis (New York: John Wiley and Sons, Inc., 1950), p. 163.

frame with the model mounted in it is shown in Figure 3.2. The loading frame was designed in such a way that the span of the beam of the cross-shaped frame could be varied. This feature was kept so as to investigate the effects of the span length.

# Material of the Model

For determination of isochromatic fringes of the cross-shaped model, CR-39 was selected due to the following favorable properties:

- 1. It has polished surfaces.
- 2. It does not develop machining stresses even under relatively high cutting speeds. Also the machinability is fair.
- 3. Aging effect is small.
- 4. Elastic properties are good. Modulus of elasticity is 300,000 psi. Stress-strain curve is linear up to 3,000 psi. Ultimate strength is 6,000 psi.
- 5. Photoelastic constant is 84 psi. per fringe per inch of thickness. Hence for a 1/4" thick specimen the first order of the fringe will develop at a stress of 336 psi. and linearity will hold good up to a fringe order of 9.
- 6. The effect of temperature on physical and optical properties is very small.

#### Model Form

The model dimensions are shown in Figure 3.3. shown in the figure, the horizontal part will act as the beam and the vertical portion will act as the column. top and bottom parts of the column are unequal for equipment convenience. But as the lengths of the top column and the bottom column are large compared with the depth of the beam, the inequality will not affect the experiment. small fillets of r = 1/16" were provided to relax the stress concentration. Dimensions were selected in the model to make the maximum use of the space and the loading capacity of the Chapman Polariscope. The loads are applied through points P, Figure 3.3, by means of a loading frame, and resisted at points Q. Figure 3.2 is a photograph of the set-up. It is to be noted that when the applied loads P are resisted only by loads Q there will not be any shear forces in the BC portion of the structure and the system is under pure bending moment in zone BC. When the shear forces are desired in the system, a pin is introduced in the hole made in the lower part of the column, which is rigidly connected to the loading frame. This will produce an axial force in the column and hence shear forces in the portion BC of the system. —The system in such a case will not be symmetrical about the horizontal axis due to unsymmetrical axial forces in the column.

## Procedure

As discussed previously, for determination of isochromatic lines, a circular polariscope is used which contains a polarizer, analyzer, and two quarter wave (mica) plates. In the Chapman polariscope all parts are housed in the optical barrel. As illustrated in Figure 3.1, the optical barrel is arranged so that the loading frame with model will be between the mica plates. Spans  $\rm L_1$  and  $\rm L_2$  are 2.5" and 1", respectively. In the case of pure bending moment in portion BC, the load P is 41.25 lbs. A photograph taken of the isochromatic fringes with this loading condition is given in Figure 3.4. Span L<sub>2</sub> was varied to investigate the effect of it on the distribution of stresses. It was found that the use of a span  $L_2$  greater than 1" did not change the mode of stress distribution from the one obtained in Figure 3.4. In the second case the shear forces were introduced in the portion BC of the system by introducing the pin in the column so that the applied loads P are resisted by supporting forces Q and an axial force through the pin. Spans  $L_1$  and  $L_2$  were kept the same and the load P was 55 lbs. The photograph of the isochromatic fringes is given in Figure 3.5.

# Discussion and Conclusion

In Figure 3.4 for pure bending moment loading, the order for isochromatic fringes increases linearly from the

neutral axis at the beam section located 1/4" from the face of the column, i.e. at a section located away from the column face a distance equal to half the width of the column. This means, from the definition of isochromatic fringes, that  $(\sigma_1 - \sigma_2)/2$  varies linearly. ( $\sigma_1$  and  $\sigma_2$ are the principal stresses.) At a beam section far away from the face of the column one cannot expect to find shear stresses or vertical normal stresses because this portion will behave like a beam of uniform section under pure bending moment. Since the isochromatic fringes at the section 1/4" from the face of the column appear identical to the ones far away from the face of the column, i.e. to the case of the uniform beam subjected to pure bending moment, it is to be concluded that there are no shear stresses or vertical normal stresses on the section 1/4" from the face of the column. Hence,  $\sigma_1$  will be equal to  $\sigma_y$  and  $\sigma_z$  will be equal to  $\sigma_x$ . Since the stress  $\sigma_x$ is zero,  $\sigma_y$  varies linearly, and the stress distribution on this section is of conventional form.

In the column zone at the horizontal sections 1/4" above or below the faces of the beam the order of isochromatic fringes is zero. This means that the section is stress free and that the flexural action of the beam is not carried into the column beyond a section located half the depth of the beam from the top or bottom of the beam.

From the linearity of the bending stresses beyond the section 1/4" from the face of the column it is deduced that when a shear force does exist there, then the shear stresses vary in a parabolic manner. Hence, the isochromatic fringes in this region should be the same as those of a beam similarly loaded but of constant cross section (not interrupted by an integrally-attached column). This is verified by comparing Figure 3.5 with results for the conventional case as given by Frocht.<sup>2</sup> The two agree outside the section 1/4" from the column face. In the lower column the order of the isochromatic fringes is constant except for some slight disturbance due to machining stresses. At the cross section 1/4" from the face of the joint it was found that in the pure bending moment case there were no bending stresses. It is to be expected there will not be any shear stresses at any cross section in the column beyond this line. means that the horizontal section is a principal plane. Hence,  $\sigma_1$  and  $\sigma_2$  will be equal to  $\sigma_x$  and  $\sigma_y$ . will be zero since  $\sigma_{V}$  is zero. Therefore, the same order of the fringe along the horizontal cross section, which means that  $(\frac{\sqrt{1-\sqrt{2}}}{2})$  is constant, implies that  $\sqrt{\sqrt{2}}$  is distributed uniformly.

<sup>&</sup>lt;sup>2</sup>Max Mark Frocht, Photoelasticity (New York: John Wiley and Sons, Inc., 1941), p. 148.

From the above experimental investigation and discussion it is concluded that the interaction of the column with the beam extends to the vertical cross section half the width of column from the face of the column, and the interaction of the beam with the column extends into the column to the horizontal cross section half the beam depth from the face of the beam. Hence, the conventional theories of stress distribution hold beyond this interaction zone.

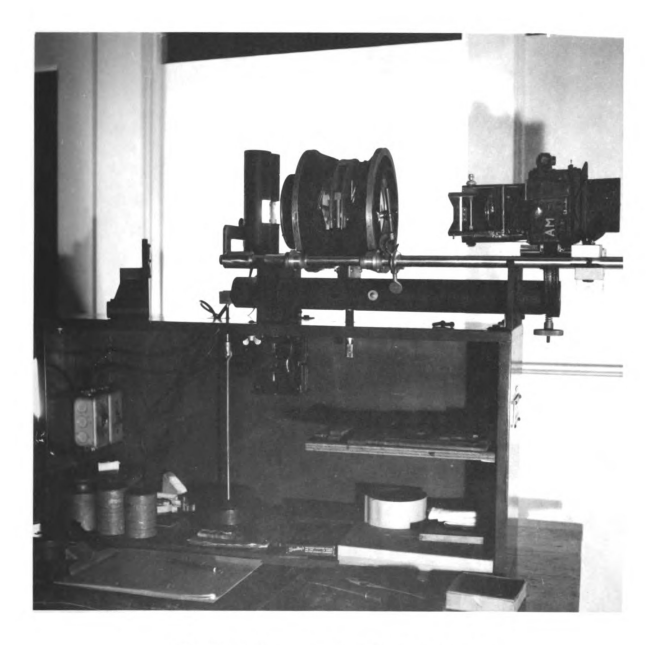


FIGURE 3.1 Polariscope set-up.

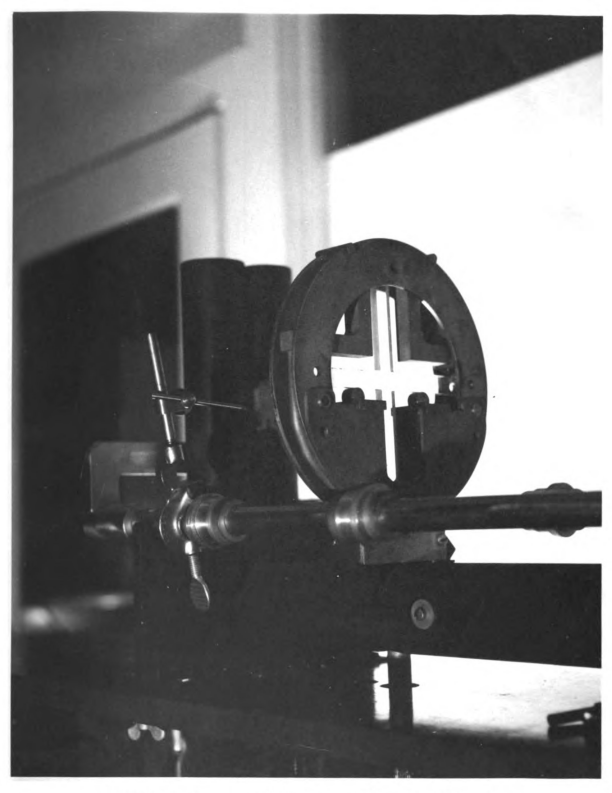
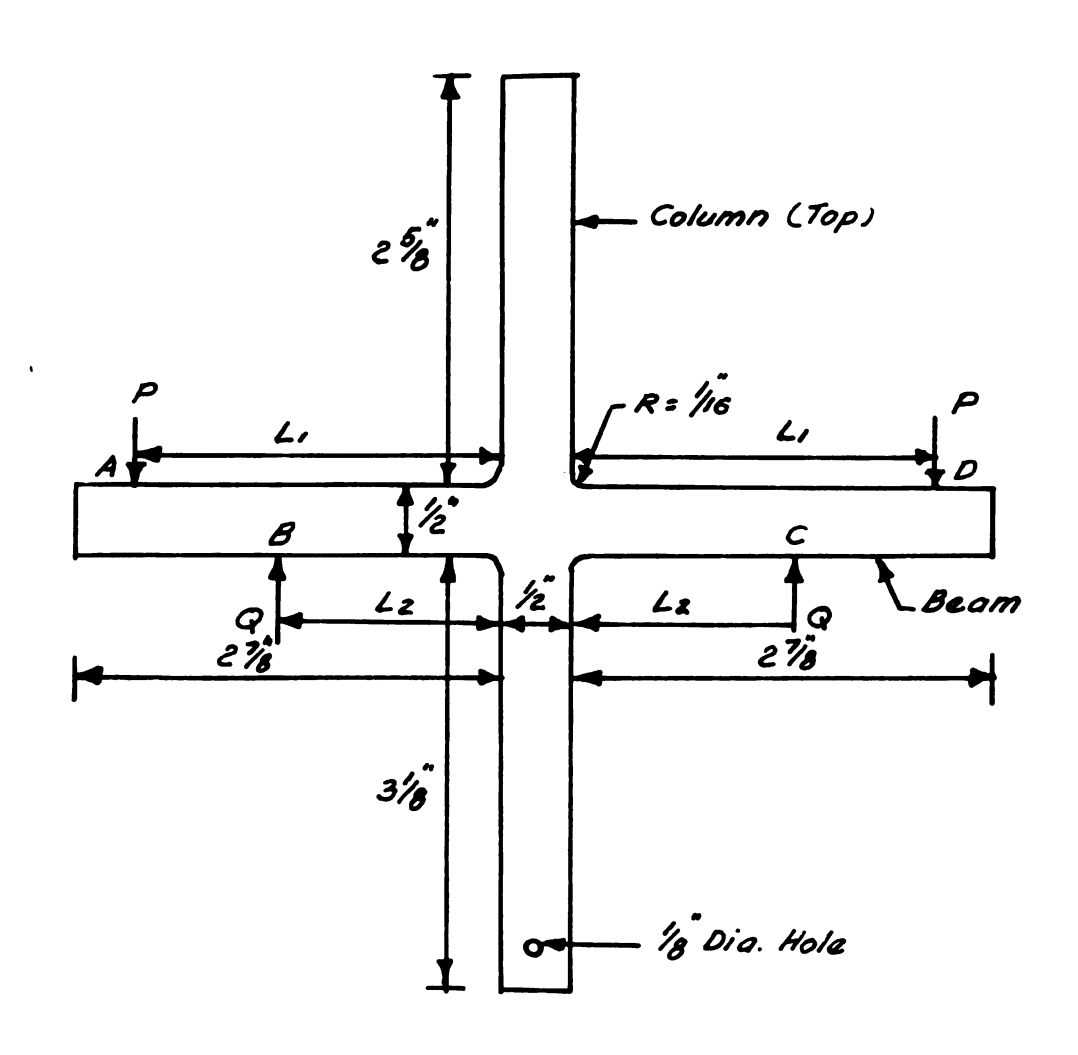


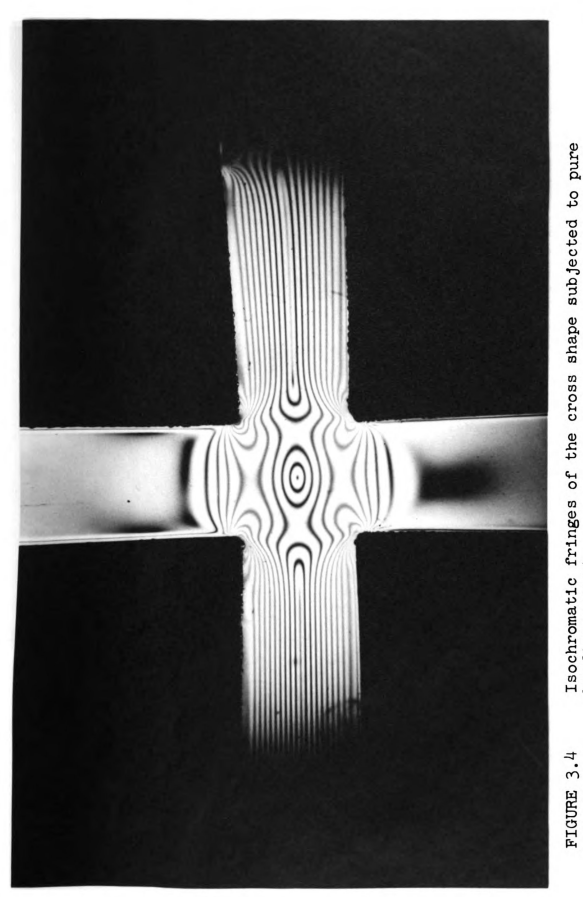
FIGURE 3.2 Model mounted in loading frame.



Model thickness = 1/4"

MODEL FORM

FIGURE 3.3



Isochromatic fringes of the cross shape subjected to pure bending moment.

Isochromatic fringes of the cross shape subjected to variable bending moment (shear loading case).

FIGURE 3.5

#### CHAPTER TV

#### NUMERICAL METHOD

The general solution of the biharmonic differential equation, as discussed in Chapter II, satisfying the boundary conditions, is usually quite difficult. Some problems of practical interest can be solved by an inverse method, making some assumptions regarding the stress distribution. This will lead to an expression for Airy's stress function  $\emptyset$  with some undetermined coefficients. Another method often used is to assume the stress function in terms of a series with undetermined coefficients. These undetermined coefficients are determined from the boundary conditions of the elastic body, which sometimes can be expanded in Fourier series.

In the absence of any notion of the stress function, the solution of the fundamental biharmonic boundary value problem can be made to depend upon a certain general representation of the biharmonic function by means of two analytic functions of a complex variable. The original presentation of this method was made by E. Goursat in 1898.

<sup>&</sup>lt;sup>1</sup>I. S. Sokolnikoff, <u>Mathematical Theory of Elasticity</u> (New York: McGraw-Hill Book Co., Inc., 1956), p. 262.

While this method will present calculation difficulties for certain types of boundaries, general formulas have been written for the case when the boundary of the region is a circle. It is possible to apply the formulas, derived for the case of a circular region, for any simply-connected region by introducing the mapping function which maps the particular region of complex Z-plane conformally onto the unit circle. An attempt to evaluate the mapping function for the cross shape is discussed in Appendix A. This method was abandoned because of convergence difficulties with the infinite series representation of the mapping function.

Because of the difficulty of the analytical solution for the elasticity problem, approximate numerical methods were used. The method of finite difference, which was first applied in elasticity problems by C. Rung in 1908, is a numerical method widely used in recent years. The wide use of this approach is due to the development of computers for the solution of simultaneous equations and the development of the relaxation method, which is used in the absence of computer facilities. In the method of finite differences one replaces the partial differential equation and the equation defining the boundary conditions by finite difference equations. Then the problem reduces to the solution of simultaneous linear algebraic equations.

<sup>&</sup>lt;sup>2</sup>Ibid., p. 145. <sup>3</sup>Wang, op. cit., p. 136.

In elasticity problems the boundary conditions are expressed in terms of either the stresses or the displacements or a combination of both. For the plane stress condition the governing differential equation solved is  $\nabla^4 \not \ni = 0$ , where  $\not \ni$  is Airy's stress function. Hence, it will be necessary to express the boundary conditions in terms of Airy's stress function. This can be done by application of relations of Airy's stress function with the stresses, 4 and the relations of the stresses to strains,5 and the strains to displacements. 6 The cross-shaped region will be studied with two loading conditions. In part I of this chapter the boundary conditions are of such a nature that the entire structure is under a pure bending moment condition. In this part there is also given considerable detail on the numerical procedure. In part II, the boundary conditions are of such a nature that there will be external shear forces at any cross section of the beam. For each loading condition, the cross shape will be analyzed both with and without fillets at the re-entrant angles. The pure bending case will be analyzed for two different ratios of beam depth to column width. In part III, results are summarized and their interpretation is discussed.

<sup>4&</sup>lt;u>Ibid.</u>, p. 43.

<sup>&</sup>lt;sup>5</sup>Ibid., p. 30.

<sup>6&</sup>lt;u>Ibid</u>., p. 17.

#### I. PURE BENDING MOMENT CONDITION

The cross shape to be studied in this case is shown in Figure 4.1. The clear spans of the beam and the columns are taken equal to the width of the column inasmuch as it was concluded in Chapter III that the interaction range extends, at the most, approximately half the width of the column into the beam as well as into the column. Hence, on the boundary AB of the cross shape subjected to pure bending moment, the bending stress will vary linearly. Also the ratio of the beam depth to the column width will affect the interaction. For the present the ratio is taken as unity, and the effect of different ratios will be discussed later on. In many structures, specifically concrete structures, there will be construction fillets at the reentrant angles formed by the junction of the beam and the column. These construction fillets will relieve the stress concentrations at the re-entrant angles, but will not have any radical effect upon the distribution of the stresses in the beam or the column far from the junction. shape having the ratio of beam depth to column width as one and the ratio of the radius of the fillet to the half depth of the beam as 1/3 has been analyzed at this point. The effect of the removal of the fillet on the interaction will be studied later on.

# A. Cross Shape Having $\frac{L}{b} = 2.0$ , h/b = 3.0, d/b = 1.0 and r/d = 1/3

Boundary conditions. Because of the loading conditions, the Airy's stress function  $\beta$  in the cross shape is antisymmetrical about the Y-axis and symmetrical about the X-axis. Therefore, it will only be necessary to study one-quarter of the entire region as shown in Figure 4.1b. The region has been divided as shown in the figure for setting up the finite difference equations. The boundary conditions can be summarized as follows:

On AB, 
$$\sigma_y = K_1 x$$
;  $T_{xy} = 0$ .  
On OA,  $\sigma_y = 0$ .

On OF, 
$$\mathbf{Z}_{xy} = 0$$
.

On BCDEF the normal stress and the shear stresses are zero.

On such a traction-free boundary, the partial derivatives

and  $\frac{3}{5}$  of the stress function are constant. Since the stress function is in any case only determined up to an arbitrary additional linear function of x and y, it was possible without loss of generality to set the boundary conditions in such a way that  $\frac{3}{5}$  =  $\frac{3}{5}$  = 0 on BCDEF. Then replacing the stresses by their expressions

<sup>7</sup>S. Timoshenko and J. N. Goodier, Theory of Elasticity (New York: McGraw-Hill Book Co., 1951), pp. 484-485.

in terms of Airy's stress function by Equation (2.4) and maintaining the continuity of all functions, such as Airy's function and its derivatives, on the boundary ABCDEF, the boundary condition can be reduced as follows:

On AB,  $\beta = K_1 x^3/6 - K_1 x d^2/2$ , Normal derivative is zero.

On BCDEF  $\emptyset = -K_1 d^{3/3}$ , Normal derivative is zero.

On OA,  $\emptyset = 0$ 

On OF, Normal derivative is zero.

The implication of zero normal derivative in terms of finite difference equations can be explained by the following example:

$$\left(\frac{\partial \phi}{\partial Y}\right)_{6,3} = 0$$

$$\therefore (\phi_{6,4} - \phi_{6,2})/2 \cdot \Delta Y = 0$$

$$\therefore \phi_{6,4} = \phi_{6,2}.$$
(4.1)

The subscript 6,3 used here identifies the node which is located at X = 6 and Y = 3 mesh units. The number before the comma represents the value of X and the number after the comma represents the value of Y. The same notation is used through the text.

From Figure 4.1b it can be seen that the  $\nearrow$  value of point 4,4 can be evaluated by any of the normal derivative conditions at 3,4; 4,3 and n. In this solution it has been

ev te n

j÷

5

e:

5

5 ...

. .

evaluated by taking the average of the slope written in terms of forward difference and backward difference at point n and equating this average to zero, which is the normal derivative condition at n.

Biharmonic differential equation. The finite difference equation of the Biharmonic differential equation for a typical interior node 2,2 as shown in Figure 4.1b can be written as follows:

Similar equations can be set up for each interior node of the region shown in Figure 4.1b. At first these equations will have many unknowns of the nodes which are outside the region. By the application of the boundary conditions discussed above and the known functional values on the boundary all equations can be stated in terms of unknown functions at interior nodes only. Hence, there will be 37 equations with 37 unknowns. These equations have been solved by using the L2 program in the MISTIC digital

<sup>&</sup>lt;sup>8</sup>Wang, <u>op. cit.</u>, p. 111.

<sup>&</sup>lt;sup>9</sup>Mistic Library, <u>L2 Program</u> (East Lansing: Computer Laboratory, Michigan State University, 1958).

computer at Michigan State University. The results of these equations are given in Table 4.1.

Bending stress and bending moment. From the  $\emptyset$  values the bending stress  $\sigma_y$  at any point can be calculated by its relationship expressed in the finite difference form. 10

e.g. 
$$(\sigma_{y})_{2,l} = (\frac{\partial^{2}\phi}{\partial x^{2}})_{2,l}$$
  

$$= \frac{(\phi_{3,l} - 2\phi_{2,l} + \phi_{l,l})}{(\Delta x)^{2}}$$
(4.3)

The results for the bending stress are recorded in Table 4.2. Its distribution on each section is given in graphical form in Figure 4.2. From the bending stress distribution the bending moment at any section can be calculated. Since the stress distribution is available in graphical form, the bending moment has been calculated by the graphical method. The X-axis of the stress distribution curves in Figure 4.2 has been divided into tenths of an inch. The bending moment at any section was calculated by the summation of products of the stress area of the one-tenth inch ordinate by the moment arm measured from the Y-axis to the middle of the stress segment. The results for the resisting

<sup>10</sup>Wang, op. cit., p. 110.

bending moments at various cross sections calculated by the described method are given in Table 4.3. Also the applied moments are given. The percentage errors compared with applied moment at various sections have been evaluated.

From Table 4.3 it appears that the errors at the face of the column and at the section where the fillet starts are the greatest. This indicates that there is considerable error in the stress distribution in the vicinity of the junction of the beam and the column. Due to the sudden change in the cross section at the junction the stress function will vary sharply. Hence, in order to determine the stress function more precisely it will be necessary to have a finer network for setting up the finite difference equations. It is to be expected that the stresses calculated will be considerably in error only in the vicinity of the fillet. Hence, the stress distribution obtained using a finer network throughout the region would not be much different from the one obtained by finer grading only in the vicinity of the fillet.

Graded net. The solution of simultaneous equations is done by MISTIC computer L2 program which is limited to a maximum of 39 equations. The finer grading around the fillet for the cross shape shown in Figure 4.1b would exceed the limit for MISTIC. Consequently it was necessary to make some modifications in the dimensions of the cross

shape shown in Figure 4.1. From Figure 4.2 it seems that at beam sections #6, #7, and #8 the  $\sigma_v$  stress distribution is very close to a straight line. Also in the column beyond the cross section parallel to Y-axis at 6 there are practically no stresses. This agrees with the photoelastic study in Chapter III. Hence, it will be appropriate to take the cross shape as shown in Figure 4.3 for the interaction study. The graded net around the fillet is shown in Figure 4.3b. While setting up the finite difference Equation like Equation 4.2 for points such as 3.23. 11 there will be many nodes like 34,2 which are not considered as unknowns. Hence, it will be necessary either to guess the value of such nodes or relate such nodes with neighboring unknown nodes. These means are possible only if some assumption is made. This difficulty can be avoided by re- $\nabla^4$  by  $(\nabla^2)(\nabla^2)$  and setting up placing the operator the finite difference operators separately for each  $\nabla^2$ . The net size used for setting up the  $\nabla^2$  operators need not be the same for different nodes or even for the two successive operators at the same node. This procedure was

Node 3,23 is identified as the one which is located at X=3 units and Y=2.5 units, i.e. located halfway between Y=2 and Y=3 units. The same notation applies when two numbers are before the comma. This notation is used throughout the text to identify the nodes which are between regular nodes.

first used by Allen and Dennis. <sup>12</sup> As an example the finite difference equation for point 23,23 shown in Figure 4.3b has been derived in Appendix B and is written as follows:

32 
$$\beta_{23,23}$$
 - 22  $\beta_{3,3}$  - 11  $\beta_{3,2}$  - 10  $\beta_{2,2}$  - 11  $\beta_{2,3}$  + 4  $\beta_{34,3}$  + 4  $\beta_{3,23}$  + 4  $\beta_{23,3}$  + 4  $\beta_{3,34}$  +  $\beta_{4,2}$  +  $\beta_{3,1}$  +  $\beta_{2,1}$  +  $\beta_{1,2}$  +  $\beta_{1,3}$  +  $\beta_{2,4}$  = 0 (4.4)

In a similar way the finite difference equation can be set up at each point where Equation 4.2 is not applicable. The boundary condition and its implication in terms of finite difference form is the same as that of the ungraded net except for point 34,34 which is evaluated in Appendix B. The finite difference equations for the graded region shown in Figure 4.3b were solved by the MISTIC computer. The values of the  $\emptyset$  obtained are given in Table 4.4.

From the stress function values the stresses were calculated by the finite difference Equation 4.3 and from this information the bending moments at various cross sections were calculated by a graphical method. The results are given in Table 4.6.

<sup>12</sup>D. N. De. G. Allen and S. C. R. Dennis, "Graded Nets in Harmonic and Biharmonic Relaxation," Quart. Journal Mech. and Applied Maths., Vol. IV, Pt. 4 (1951), pp. 439-443.

Effect of graded net on bending moments. With the understanding that the distribution of the stresses in the region shown in Figure 4.3b will not be materially different from that of the region shown in Figure 4.1b the bending moment evaluations of Tables 4.3 and 4.6 can be compared to study the effect of the graded net. At beam sections #5, #6, and #7 the error has been increased at the most by 0.30%. At beam sections #3 and #4 the error is reduced by 5.49% and 10.20%, respectively. At beam section #2 the error is increased by 0.78%. The slight increase or decrease in the percentage error at sections #2, #5, #6, and #7 from Table 4.3 to Table 4.6 is not significant. The bending moments were calculated by a graphical method in which the stress values are read from the graph. Hence, any slight errors in the stresses when multiplied by the lever arm for evaluation of the moment may be responsible. but they are not significant. But from comparison of the results at sections #3 and #4 it can be concluded that the graded net improves the results considerably.

Higher order differences. Further improvement can be made in the finite difference approximation by taking a finer net. This will increase the number of simultaneous equations. An alternative approach in which higher order finite difference approximation formulas are used was

suggested by Fox. 13 The finite difference equation, set up by considering the higher order finite difference approximation for the biharmonic equation could be used for evaluation of stress functions. This would involve considerable labor in setting up the equations. In general, by using the standard first order difference formulas, the accuracy in the stress function obtained is always better than in the derivatives of the function. Hence, even if the stress functions are obtained by standard first order formulas, the improvement in the results will be considerable with little extra labor if the derivatives are calculated by higher order differences and used for evaluation of stress.

For bending stress  $\sigma_y$  the finite difference formula using the higher order difference is as follows:

e.g. 
$$(\sigma_{y})_{2,l} = (\frac{\partial^{2}\phi}{\partial x^{2}})_{2,l}$$
  

$$= \frac{1}{(\Delta X)^{2}} \left[ \nabla^{2}\phi_{2,l} - \frac{1}{12} \nabla^{4}\phi_{2,l} + \frac{1}{90} \nabla^{6}\phi_{2,l} \cdots \right]$$
(4.5)

The first term of the formula is the contribution of the standard first order difference application. The first

 $<sup>^{13}</sup>$ L. Fox, "Some improvements in the use of relaxation methods for the solution of ordinary and partial differential Equations," Proceedings, Royal Society (London), A, Vol. 190 (1947), pp. 31-59.

<sup>&</sup>lt;sup>14</sup>Wang, <u>op. cit.</u>, p. 125.

factor has already been evaluated in Table 4.5. The second term is evaluated separately using the stress functions given in Table 4.4. Only the first two terms are taken in the formula (4.5) as the terms beyond this will be insignificant. The results of the bending stress evaluated by the formula (4.5) are given in Table 4.7. These results have been plotted in Figure 4.4. The bending moments have been calculated graphically using Figure 4.4. The comparison of the results is given in Table 4.8.

The effect of application of higher order difference in the stress distribution can be studied by looking into results of the percentage error in the calculated resisting moments given in Tables 4.6 and 4.8. There is practically no improvement in the result at beam section #3. Inside the column, i. e. at beam sections #3, #1, #2 the errors have been reduced almost to zero. The change in the errors at sections #4, #5, #6, and #7 is not important as far as the interaction of the column and beam is concerned. Looking into the values of the stresses in Table 4.5 and Table 4.7 it can be summarized that there is significant difference only at the node point of the maximum stress on a section. Inside the column zone there is quite a difference percentage-wise at the nodes close to the top boundary, but as far as the area of the stress diagram is concerned this will not be of any importance. Hence, in conclusion the only way to improve the error in the stresses near the

fillet is to have a very fine net around the fillet. This will increase considerably the number of equations. As the problem involves the joint region as a whole and the error in the stresses near the fillet will not greatly change the results, it will not be justifiable to spend more time for the solution of more simultaneous equations. In the subsequent calculations the values  $\sigma_y$  are calculated by higher order differences, while the normal stress  $\sigma_x$  and the shearing stress  $\tau_{xy}$  are calculated by the standard first order difference.

Normal stress  $\sigma_x$  and shearing stress  $T_{xy}$ . The finite difference formulas for  $\sigma_x$  and  $T_{xy}$  stresses for the typical node 2,2 as shown in Figure 4.3b can be written as follows:  $^{15,16}$ 

$$(\sigma_{X})_{2,2} = (\frac{\partial^{2}\phi}{\partial y^{2}})_{2,2} = \frac{(\phi_{2,3} - 2\phi_{2,2} + \phi_{2,1})}{(\Delta Y)^{2}}$$

$$(\tau_{XY})_{2,2} = -(\frac{\partial^{2}\phi}{\partial x \cdot \partial y})_{2,2} = -\frac{[(\phi_{3,3} - \phi_{3,1}) + (\phi_{1,1} - \phi_{1,3})]}{4 \cdot \Delta X \cdot \Delta Y}.$$
(4.6)

Using the Formula 4.6 the  $\mathcal{L}_x$  and  $\mathcal{L}_{xy}$  stresses are calculated with the help of the stress function  $\emptyset$  given in Table 4.4. The results of these are given in Table 4.9.

<sup>&</sup>lt;sup>15</sup>Ibid., p. 113.

<sup>16&</sup>lt;sub>F</sub>. S. Shaw, An Introduction to Relaxation Methods (New York: Dover Publications, Inc., 1953), p. 36.

Energy. Knowing the stress distribution at various sections the energy can be evaluated by the formula discussed in Chapter II. The energy formula for a segment of unit length in the Y-direction is

$$U = \int \left[\frac{1}{2E}(\sigma_x^2 + \sigma_y^2 - 2\mu\sigma_x\sigma_y) + \frac{1}{2G} \tau_{xy}^2\right] dx. \tag{4.7}$$

The integral along the entire depth in the X-direction can be evaluated by summation of the energy of small segments in the X-direction or by integration of the energy function in X-direction. As the stress information is available in numerical form it will be convenient to evaluate the energy by a graphical method. For this purpose  $\sigma_y^2$ ,  $\sigma_x^2$ ,  $\tau_{xy}^2$ were plotted, and the summation of the area between each curve and X-axis was carried out with a Planimeter. Figure 4.5 shows, for example, the curves of  $\sigma_v^2$  at sections #3, #1, #2, #3 and the areas obtained. With the application Of this area information to the Formula 4.7 the energy can be evaluated. The results of the computation are shown in Table 4.10. The value of Poisson's ratio m is used as 0.30 throughout the text. The effect of M on equivalent depth Will be discussed later. Knowing the energy the equivalent depth can be calculated.

Equivalent depth. The equivalent depth at any section is defined as the one which, when used in the evaluation of the energy by the conventional beam theory formula will give

the actual energy. This can be illustrated in the following manner.

In the conventional energy formula, if the segment of the structure is under pure bending moment M, then the energy of the segment per unit length is given by M<sup>2</sup>/2EI. The energy of the segment of rectangular cross section of unit length and of unit width and depth D will be 6M<sup>2</sup>/ED<sup>3</sup>. According to the definition of equivalent depth, the following equation can be written for any section,

$$\frac{6M^2}{Ed_e^3} = \text{true energy at any section (Table 4.10),}$$

e.g. for section #3, 
$$\frac{6M^2}{Ed_e^3} = \frac{0.403109 \text{ K}_1^2 d^3}{2E}$$
.

Note that  $d_e$  is the equivalent depth at the section while d is the half depth of the actual beam. M is the bending moment at the section. In this case M = 0.66667  $K_1d^3$  and the equation yields

$$d_e^3 = \frac{5.3333d^3}{0.493199}.$$

Let R represent the ratio of equivalent depth to actual depth,

$$R = \frac{d_e}{2d} = \frac{Equivalent depth}{Depth of beam}$$
.

For section #3, 
$$R^3 = \frac{0.66667}{0.403109} = 1.6538$$
.

The results for R at various sections are given in Table 4.11. The graphical representation of the equivalent depth is given in Figure 4.6. The results indicate that there is a gradual increase in equivalent depth or moment of inertia and at the face the fillet is not fully effective as far as the energy evaluation by conventional beam theory is concerned. The equivalent depth, from Section #4 onwards, approaches 1.0 as expected.

### B. Equivalent Depth Related to Ratio of d/b of Cross Shape

As mentioned earlier the ratio of the beam depth to the column width will affect the interaction of the column and the beam. In other words, the equivalent depth diagram will be affected by the ratio d/b. This can be viewed from two angles: (1) the effect of the ratio on the stress distribution curve at the face of the column, and (2) the effect of the ratio on the stress distribution inside the column even though the stress distribution on the face of the column is the same. The stress distribution on the face of the column will affect the equivalent depth at the face and also inside the column where the stress distribution is not that of the conventional theory even though the stress distribution on the face is linear. At this Stage the primary interest will be in studying the effect Of the ratio on the equivalent depth at the face of the Column. How the stress distribution curve on the face of

the column will affect the equivalent depth inside the column will be discussed later. The stress distribution on the face depends upon the intensity of stress concentration near the corner. The effect of dimension changes on the stress concentration has been studied by several investigators and will be referred to below. The second effect will be studied in Chapter V under the reasonable assumption that for a given applied moment and beam depth the variations in the other dimensions which do not change the stress concentration factor also leave unchanged the stress distribution on the face of the column.

Stress concentration. In the neighborhood of the joint the stress concentration will be a function of the radius of the fillet, the clear height of the column, the clear span length of the beam, the depth of the beam, and the column width. According to the photoelasticity study in Chapter III, the stress distribution in the beam at a distance from the face of the column greater than half the width of the column coincides with the elementary beam theory distribution. This indicates that the same stress distribution in and around the joint would be obtained for any clear span length of the beam greater than half the column width. Hence, it is concluded that the stress concentration factor will be independent of the clear span length when the ratio of clear span length to half the

column width exceeds one, which covers all practical cases. It has been shown that with a given ratio of beam depth to column width, when the ratio of radius of fillet to the depth of the beam is greater than 0.10, i.e. r/d > 0.20, the stress concentration factor is independent of the ratio of clear height of the column to the radius of the fillet. 17 This covers the case analyzed in the previous pages and also all practical cases. Hence, for practical purposes it can be concluded that the stress concentration factor is independent of the clear height of the column and the ratio of the height of the column to the radius of the fillet. So for a given r/d ratio the only parameter affecting the stress concentration factor is the ratio, d/b, of the depth of the beam to column width. The following paragraph will show that the stress concentration factor is independent of d/b when this ratio is less than about 0.30 for r/d = 1/3. In most cases of frame structures with short beams, this condition is not satisfied and it is necessary to study the effect of varying d/b.

The ratio d/b is equal to  $d/h \cdot h/b$  where 2h is the total height of the column. In the range where the stress concentration factor is independent of d/h and h/b, it will

York: D. Van Nostrand Co., Inc., 1956), p. 327.

be independent of d/b. It has been shown that for d/h = 1/2 and h/b smaller than 1/2, the stress concentration is independent of h/b for values of r/d ranging from 0.30 to 2.0. The same investigation showed that the stress concentration factor is almost independent of d/h (within 6%) when this ratio is smaller than 3/5 and h/b is smaller than 1/2 with r/d varying from 0.3 to 2.0. Hence, for d/h equal to or smaller than 3/5 and h/b equal to or smaller than 1/2, the stress concentration factor is independent of d/b. Since in all cases of practical interest d/h is equal to or smaller than 3/5, the stress concentration factor is independent of d/b when d/b is smaller than 3/10.

For r/d = 1/3 and d/h = 3/7, the stress concentration factors for d/b = 1.0, 1.5 and 2.0 are 1.54, 1.50 and 1.47, respectively.<sup>20</sup> The equivalent depth analysis for the case of d/b = 1.0 is given in part IA. To show how the stress concentration factor affects the equivalent depth, another case is analyzed with d/b = 1.5.

<sup>18</sup> J. B. Hartman and M. M. Leven, "Factors of stress concentration for the bending case of fillets in flat bars and shafts with central enlarged section," Proceedings of the Society for Experimental Stress Analysis, IX, No. 1 (1951), p. 57.

<sup>&</sup>lt;sup>19</sup>Ibid., p. 58.

<sup>&</sup>lt;sup>20</sup>R. E. Peterson, <u>Stress Concentration Design Factors</u> (New York: John Wiley and Sons, Inc., 1955), p. 71.

Cross shape having the ratio L/b = 2.5, h/b = 3.5, d/b = 1.5, and r/d = 1/3. The cross shape shown in Figure 4.7 was analyzed. The boundary conditions are the same as of the case shown in Figure 4.3. The same procedure was followed for the analysis. The resulting stress functions and stresses have been summarized in Tables 4.12 and 4.13. By the application of the numerical procedure explained before, the energy at various sections is calculated. Computations are given in Table 4.14. The equivalent depth information is in Table 4.15 and is presented graphically in Figure 4.8. Comparing the ratio at the face of the column of Table 4.15 (Section #2) to the one of Table 4.11 (Section #3), it is found that R has decreased from 1.1826 to 1.1388. It indicates that as d/b increases the R-value decreases. Interpretation of this fact will be discussed in Part III of this chapter.

Also a comparison of Figure 4.8 with Figure 4.6 indicates that the equivalent depth increases more slowly inside the column for the case of d/b = 1.5 than the case of d/b = 1.0. It means that the ratio of d/b affects the shape of the curve inside the column, i.e. even for the same d and the same mode of stress distribution on the face of the column, the alteration in the width of column will change the mode of distribution inside the column. This is the second effect as mentioned earlier in Part IB of this

chapter. The effect of various d/b ratios will be discussed in Chapter V.

# C. Cross Shape Having L/b = 1.333, h/b = 2.333, d/b = 1.0, and r/d = 0

To study the effect of the removal of the fillet, an analysis was made of the cross shape as shown in Figure 4.3 with the fillet replaced by a corner. From the similarity of the boundary conditions it could be noted that the equations set up for the cross shape with fillet shown in Figure 4.3 can be used for the cross shape with a square corner. Due to elimination of the fillet, the  $\emptyset$  values of the nodes 34,3; 3,3; and 3,34 are known now. Also the expression for 34,34 in terms of internal nodes will be changed as the boundary conditions which relate 34,34 are changed. Hence, after making these alterations the equations were solved. The results for the stress functions are given in Table 4.16. The resulting stresses, energy, and equivalent depth information are given in Tables 4.17, 4.18, and 4.19, respectively. The equivalent depth is presented graphically in Figure 4.9.

Calculation of the equivalent depth was carried out only as far as section #4 because Figure 4.6 indicates that, from section #4 on, the equivalent depth does not differ significantly from the actual depth. Comparison of results for equivalent depth from Table 4.19 with Table 4.11

indicates that the equivalent depth at the face has decreased. The reason is that in the case of a square corner the contact area at the face is smaller than the contact area in the case of fillet. Hence, for the same external moment at the section, the area between the graph of  $\sigma_v^2$ and the X-axis will be greater, which will yield more energy and consequently less equivalent depth. The stress distribution of  $\sigma_y$  on the face of the column in the case with a fillet is flatter than in the case without a fillet, and this effect will be carried inside the column. The flatter the curve of the stress  $\sigma_v$  is, the less will be the energy. Hence, the energy due to  $\sigma_{v}$  at any section in the case of the fillet is less compared with the energy at the corresponding section in the case of the square corner. This indicates why the equivalent depth in the case of the fillet is greater for any section than it is at the same section in the square corner case.

## D. Effect of Poisson's Ratio on Equivalent Depth

Poisson's ratio depends upon the kind of material. For steel it is between 1/2 and 1/3. For concrete it lies between 0.10 and 0.30. The most common value for concrete is between 0.15 to 0.20. As the elastic energy depends upon Poisson's ratio, another analysis is made with the value of Poisson's ratio of 0.15. The calculations are carried out with the information from Table 4.10. The

results are tabulated in Table 4.20. Comparison of equivalent depth of Table 4.20 with that of Table 4.11 indicates that the equivalent depth has increased inside the column by decreasing the value of Poisson's ratio. But this change is not significant compared with the value of the equivalent depth. Hence, for the pure bending case it is concluded that the equivalent depth is not sensitive to variations in Poisson's ratio.

# II. VARIABLE BENDING MOMENT CONDITION (SHEAR-LOADING CASE)

# A. Cross Shape Having L/b = 1.333, h/b = 2,333, d/b = 1.0 and r/d = 1/3

The cross shape shown in Figure 4.3 is taken for this analysis. As it was concluded that the grading shown in Figure 4.3 gives good results, the same grading is used in this case. According to the conclusion regarding the extent of the interaction zone drawn from the photoelasticity study, the conventional beam theory stress distributions will act on the boundaries of the cross shape shown in Figure 4.3. The boundary forces are shown in Figure 4.10.

Boundary conditions. Because of the loading conditions, the Airy's stress function  $\emptyset$  in the cross shape is anti-symmetrical about the Y-axis and symmetrical about the X-axis. Therefore, only one-quarter of the region

shown in Figure 4.10 has been analyzed. All grading and notations are as in Figure 4.3b. As all the boundary forces will be distributed in the conventional beam theory form, the boundary condition can be summarized as follows:

On AB, 
$$T_{xy} = -K_2 (d^2 - x^2);$$
  $\sigma_y = 0$ 

On BCDE, Normal and shear stresses are zero.

On EF, 
$$\sigma_{x} = 2K_{2}d^{2}/_{3}$$
;  $\tau_{xy} = 0$ 

On OA, 
$$\sigma_{V} = 0$$

On OF, 
$$\boldsymbol{Z}_{XV} = 0$$

where  $K_2$  is a constant. These boundary conditions can be expressed in terms of Airy's stress function as follows:

On AB, 
$$\emptyset = 0$$
;  $\frac{\partial \phi}{\partial x} = K_2 (d^2 x - x^3/3)$ .

On BC, 
$$\emptyset = 2/3(K_2d^3y) - 14/9(K_2d^4); \frac{\partial \phi}{\partial x} = 0.$$

On CD, 
$$\emptyset = -2/9 (K_2 d^4) Sin (x,r) - 2/9 (K_2 d^4);$$

$$\frac{\partial \phi}{\partial x} = 0; \qquad \frac{\partial \phi}{\partial y} = 2/3 \, (K_2 d^3).$$

On DE, 
$$\emptyset = -8/9 (K_2 d^4)$$
;  $\frac{3\phi}{3y} = 2/3 (K_2 d^3)$ .

On EF, 
$$\emptyset = 1/3 (K_2 d^2 y^2) - 11/9 (K_2 d^4);$$

where the angle (x,r) is the angle of inclination of the fillet radius drawn to the point in question measured from the X direction. All these boundary conditions are transformed into the finite difference form by the same method as in the case of pure bending moment with graded net.

Stress function \$\mathcal{1}\$ and stresses. The finite difference equation of the biharmonic differential equation was set up for all interior nodes, and by use of the above boundary conditions the equations were transformed to contain only unknowns at interior nodes. These equations were solved by the L2 Program in the MISTIC computer. The results are given in Table 4.21. From the  $\emptyset$  values the stresses  $\sigma_v$ ,  $\sigma_x$ ,  $\tau_{xy}$  are calculated by using the finite difference forms. Results are recorded in Table 4.22. From the stress values, resisting moments and forces  $\mathbf{M}_{\mathbf{y}}\text{, }\mathbf{V}_{\mathbf{x}}\text{, and }\mathbf{N}_{\mathbf{x}}\text{ were }$ calculated graphically at various sections; they are compared in Table 4.23 with the values of  $M_{\rm W}$ ,  $V_{\rm X}$ , and  $N_{\rm X}$  calculated by statics from the applied loads. The comparison shows that results are in fair agreement except for  $\mathbf{V}_{\mathbf{X}}$  at section #4. This discrepancy may be due to an incorrect value of stress  $\mathbf{Z}_{xy}$  at 3,4, since the value given in Table 4.22 is inconsistent with the boundary conditions. But the error in  $\boldsymbol{\mathcal{T}}_{xy}$  at node 3,4 and other evident errors  $\boldsymbol{\tau_y}$  and  $\boldsymbol{\tau_{xy}}$  at 4,3 will not significantly affect the accuracy of the energy study inside the joint. The errors in maximum stress values at any section or errors in boundary stress values will not introduce significant errors into the energy calculation, because when the square of the stress is plotted as in Figure 4.5 the area change caused by the error in the stresses is very small compared with the total area between the curve and X-axis.

Energy and equivalent depth. The energy at various sections has been calculated from the results of the stress distribution by the formula and the method discussed before. The results are tabulated in Table 4.24. In the case of shear-loading also, the equivalent depth is defined as before, i.e. the one which if used in the conventional beam theory energy formula will give the true energy at the section. For a beam of uniform section subjected to variable moment the energy per unit length is written as,

$$M^2/2EI + 1.2 V^2/2GA$$
.

where M and V are bending moment and shear force at the section, I and A are moment of inertia and area of the cross section, and G is the shear modulus. According to the definition of equivalent depth, for a rectangular cross section,

 $6M^2/\text{Ed}_e^3$  + 1.2  $V^2/2\text{Gd}_e$  = True energy at the section, e.g. for section 3,

$$6M^2/Ed_e^3 + 1.2 V^2/2Gd_e = 5.809534 K_2^2 d^5/2E$$
 (from Table 4.24)

From the known M and V at any section, the ratio of equivalent depth d<sub>e</sub> to the depth 2d of the beam has been calculated and recorded in Table 4.25 and presented graphically in Figure 4.11. Comparison of Figure 4.11 with Figure 4.6 indicates that equivalent depth at the face is smaller in

the shear-loading case than in the pure bending moment case, but that the equivalent depth increases more rapidly with distance inside the column than it does in the pure bending case so that the maximum attained is greater in the shear-loading case by about 15%. Hence, it can be concluded that the shear energy due to shear force is dissipated more rapidly than the bending energy. As the bending energy in the shear-loading case depends upon the span length of the beam, the equivalent depth will be affected by it. This phase will be discussed in Part III and Chapter V.

# B. Cross Shape Having I/b = 1.333, h/b = 2.333, d/b = 1.0, and r/d = 0

The fillet was removed to study the effect of the fillet on the equivalent depth. The boundary conditions in this case are identical to those of Figure 4.10. Following the same approach, of functions at all interior nodes have been evaluated and are given in Table 4.26. Stresses, energy, and equivalent depth are given in Tables 4.27, 4.28, and 4.29. The equivalent depth has been plotted in Figure 4.12. Comparison of results of Table 4.29 with 4.25 indicates that the equivalent depth at a section is smaller in case of a square corner than in the case with a fillet. This can be explained with the same reasoning as in the case of pure bending moment (Part I, C).

### C. Effect of Poisson's Ratio on Equivalent Depth

It was concluded in the case of the pure bending moment that variations in Poisson's ratio do not affect greatly the equivalent depth. This was due to the fact that in that case elastic energy was principally contributed by bending stresses. In the case of shear-loading, the shear energy will be a significant part of the total energy. Hence, it was decided to analyze the case of shearloading for equivalent depth with Poisson's ratio as 0.15. The calculations are carried out with the information of Table 4.24. The results of the equivalent depth are recorded in Table 4.30. Comparison of Table 4.30 with Table 4.25 indicates that the noticable differences are at beam sections #4, #3, #2, and #1. But these differences are not significant compared with the equivalent depth. The change in Poisson's ratio also affects, in approximately the same degree, the evaluation of the energy by the conventional beam formula. Hence, it is concluded that for all practical purposes the exact value of Poisson's ratio is unimportant for calculation of the equivalent depth in the case of shear-loading also.

#### III. INTERPRETATION OF RESULTS

# A. Equivalent Depth Ratio R at the Face of the Column

Pure bending case. It was concluded in Part I--B that the stress concentration factor depends on d/b when d/b is

greater than 0.30 for ratio r/d = 1/3 and h/d greater than 5/3. For investigation of the effect of different stress concentration factors on R (the ratio of equivalent depth to the depth of beam at the face of column) at the face, two cases of d/b were analyzed in Part I. The value of R at the face of the column with r/d = 1/3 and d/b = 1.0was found to be 1.1826 (Table 4.11) compared with 1.1388 (Table 4.15) for d/b equal to 1.5. This decrease in R at the face can be attributed directly to the stress concentration factor which is decreased as mentioned earlier. Looking at the computation of energy in Tables 4.10 and 4.14 for section #3 and section #2 (vertical sections at the face) or #4 and #3, it can be concluded that the energy due to the bending stress  $\sigma_y$  is most of the total energy. So for analysis of the stress concentration effect, it can be considered that the equivalent depth ratio R is a function of the stress  $\sigma_y$  alone. With this in mind, the  $\sigma_{v}$  stresses are examined in both cases. The stress concentration factor at section #3 for d/b = 1.5 is 1.3804 (Table 4.13) compared with 1.4933 at section #4 for d/b =1.0 (Table 4.7). The effect of stress concentration on the equivalent depth may be seen from the following consideration. The effect of different stress concentration factors on the distribution of the stress  $\sigma_{v}$  with the same resultant moment at the section is shown qualitatively in Figure 4.13. It can be shown that the area between the

 $\sigma_y^2$  curve and the X-axis decreases as the stress concentration factor increases. Since the equivalent depth is a function primarily of the energy due to  $\sigma_y$ , the equivalent depth ratio R will increase as the stress concentration factor is increased. Hence, if d/b is increased, the ratio R will decrease.

Two different values of d/b have been considered here giving values of R equal to 1.1826 and 1.1388. It is recommended that for all values of d/b less than 2.0, and r/d equal to 1/3, the value of R be taken as 1.16.

In the case of the cross-shaped joint without fillets, i.e., r/d=0, theoretically there will be stresses of infinite magnitude at the re-entrant angle. This fact has not been observed in the calculated results because of the use of the finite difference method. But this will not make any significant error in the application of the results inasmuch as the practical limit for  $\sigma_y$  is determined by the strength of the structural material and this strength is far from infinite. For the case r/d=0, no calculations have been made except for d/b=1. It seems reasonable to assume that the dependence of R on d/b is no greater in the case of r/d=0 than it was for r/d=1/3, namely, a variation of about 4% for d/b less than 2.0.

Summarizing the results of R for the two cases, one With r/d = 0 and another with r/d = 1/3, it is concluded

that the value of R for any value of d/b smaller than 2.0 and r/d between 0 and 1/3 will lie between about 1.10 and 1.16.

Variable bending moment case. In the case of shearloading the ratio R at the face of the column for the joint with the fillet is 1.0689 (Table 4.25) compared with 1.1826 (Table 4.11) for the case of pure bending. As the span of the beam increases conditions at the joint approach the pure bending state as far as the total energy evaluation is concerned. That is, the shear energy due to shear force becomes less and less important compared with the bending energy. The same effect will be observed inside the joint, which will be studied in Chapter V. If one desires to obtain the ratio R at the face for different span lengths of the beam, i. e. I/d greater than 1.3333 with available calculation information it can be done by superimposing the results. In the cross shape of Figure 4.14, I/d is greater than 1.3333 and the height of the column is such that h/d is 2.3333. The stresses in the shaded area can be determined by analyzing the shaded cross shape. This can be done by superimposing the stress system due to Moment M = VL3 (calculated with the use of pure bending moment stress information) on the stress system due to shear force on section AB. After superposition of the stresses, the energy can be evaluated and hence the ratio

R at the face. A similar approach could be followed for the joint without fillets and the ratio R which will vary from 0.9242 (Table 4.29) to 1.1010 (Table 4.19) for various span lengths can be determined.

In practice there will not be any cases of pure bending moment. Of course, the joint with a very long beam will approximate the pure bending moment case. But the determination of equivalent depth is important only for short spans inasmuch as the contribution of the joint to the total behavior of the beam becomes less important as spans increase. Hence, one will be interested in the equivalent depth information for the shear case. In this study actual values of R at the face of column for various values of L/d are not determined.

Also when d/b is greater than 1.0, the value of R will decrease due to reasons discussed for the pure bending moment case. In the case of pure bending moment this decrease was about 5%. With the thinking that the decrease in the shear case will not be too far from 5%, an analysis was not made in the shear case for d/b = 1.5. Summarizing the results of two cases of shear loading, one with r/d = 0 and another with r/d = 1/3, the value of R for 1/d = 1.3333 and 1/d between 0 and 1/3 will lie between 0.9242 and 1.0689.

### B. Contribution of Shear Stresses to the Total Energy

In most problems the shear energy is neglected. This cannot be done when the spans are small. From Table 4.24 it can be seen that at the face of the column the shear energy is even greater than the bending energy, and also inside the joint the contribution is significant. The same fact is observed in the results of Table 4.28. In short beams the assumption of infinite moment of inertia implies zero bending energy, which is not true as can be seen from the results. By taking infinite moment of inertia in the joint and also neglecting the shear energy two errors will be introduced, which do not compensate in any way. In the case of the joint subjected to pure bending moment there are shear stresses. The energy due to these shear stresses inside the joint is in some cases as high as 25% of the corresponding bending energy. In beam theory there is no way to find these shear stresses. In this case it was included because it was significant.

# C. Stresses on the Face of the Column

The bending stress at the face of a column at a joint with square corners subjected to pure bending moment (beam Section #3 in Table 4.17) is plotted in Figure 4.15. The stress concentration factor is obviously not correct, since it should be infinity. But in studying the general mode of stress distribution, it is to be noted that the stress

distribution is fairly linear in almost 3/4 of the depth. The effect of such distribution on the energy can be observed with the help of Figure 4.13. Also the magnitude of shear energy on the face of the column is small compared with the total energy. Hence, it can be considered that as far as total energy evaluation is concerned, the actual stress distribution on the face of the column which includes

 $\sigma_y$  and  $\tau_{xy}$  can be replaced by a linear distribution of  $\sigma_y$  attaining the maximum value  $FK_1d$  shown as dotted in Figure 4.15. The correction factor F is to be selected in such a way that energy due to the linear distribution with maximum value  $FK_1d$  on the face will be equal to true total energy. This suggests that for the study of energy variations inside the joint subjected to pure bending moment M, the stresses on the column face can be replaced by linear stress distribution of  $\sigma_{v}$  attaining maximum FK<sub>1</sub>d. In Chapter V the stresses inside the column for such an assumed linear distribution on the face are calculated by series method. Comparison of results presented in that chapter Shows that if the correction factor is selected to make the two equivalent depths agree at the face of the column, then the equivalent depth diagrams agree closely inside the Column. The value of F in the case of a cross shape with Square corner comes to 0.87. It is to be noted that the above modification of stress distribution is only for energy evaluations to calculate equivalent depth. When this

equivalent depth is used in the conventional beam theory formula, the moment used should be M and not FM. This is an arbitrary way to determine the mode of energy distribution inside the joint by the linear distribution of stress on the boundary.

The shear stress distribution on the face of the column also will be different from the conventional parabolic distribution. Even in the case of pure bending moment the shear stresses were found. Hence, in the case of the joint subjected to shear force, to find the distribution of the shear stress due to shear force V. it will be necessary to separate the effect of the corresponding moment from the total shear stress. Applying the principle of superposition, the separation can be done by using the results of the pure bending case. The shear stresses corresponding to the bending moment are evaluated at the face of the column. This shear stress is subtracted from the total shear stress obtained when the joint was sub-Jected to external shear force. The remaining shear stress distribution is plotted in Figure 4.16. Again, as far as the magnitude is concerned, the net shear stress might not be correct at least in the stress concentration zone; the magnitude of the shear stress is certainly not correct at the re-entrant point in the case of a joint without fillets. But in general it appears that in almost 2/3 of the beam depth the shear stress is approximately a uniform

distribution. This fact has been observed by Neuber. 21 He analyzed a bar which has a deep notch subjected to shear force. On the section passing through the notch the shearing stress approaches uniformity except near the notch where there is stress concentration effect. Neglecting the effect of the area of the curve in the zone near the notch, with little error in the energy, the shearing stress distribution on the face of the column can be assumed as uniform. The uniform shear stress assumption will be considerably better than a parabolic distribution would be.

N. Neuber, Theory of Notch Stresses (Ann Arbor, Michigan: J. W. Edwards, 1946), p. 44.

TABLE 4.1

% VALUES FOR THE CROSS SHAPE HAVING L/b = 2.0, h/b = 3.0, d/b = 1.0, AND r/d = 1/3 SUBJECTED TO PURE BENDING MOMENT

Following values are to be multiplied by  $-K_1d^3/81$ .

Node	Ø
1,765432108765432103210210210210210210 1,11111222222223333334445556667777888	12.912334 12.812339 12.685156 12.432035 11.898325 11.032010 10.163045 9.556025 9.341692 22.870239 22.7646023 22.875402 21.680103 20.235799 18.761616 17.734676 17.374676 17.374676 17.374692 25.899469 24.518384 23.492986 23.125730 26.968565 26.509573 26.968565 26.509573 27.473239 27.473239 27.478157 27.297142 27.54326 27.35881 27.15456 27.35881 27.404686 27.144863

TABLE 4.2

BENDING STRESS y FOR THE CROSS SHAPE HAVING d/b = 1.0AND r/d = 1/3 SUBJECTED TO PURE BENDING MOMENT

Following values are to be multiplied by  $K_1d$ .

Node	<b>o</b> y	Node	<b>-</b>
1,888777776655544433332222222222	0.32826 0.64758 0.91775 0.31775 0.631775 0.635727 0.635299 0.62257 0.62257 0.96770069 1.0235770 0.35570 0.35570 0.362825 0.3625148 0.36740 0.3	1,1 234,1 1,1 1,1 1,1 1,1 1,1 1,1 1,1 1,1 1,1	0.15304 0.26893 0.30463 0.22810 0.09930 0.03131 -0.03138 -0.037574 0.28543 0.14557 0.28543 0.14557 0.28543 0.1285 0.01609

TABLE 4.3

COMPARISON OF RESISTING AND APPLIED MOMENTS M, FOR THE CROSS SHAPE HAVING d/b = 1.3 and r/d = 1/3

SUBJECTED TO PURE BENDING MOMENT

Moments are to be multiplied by  $K_1d^3$ .

Beam-Section	Resisting $\mathtt{M}_{\mathtt{y}}$	Applied M <sub>y</sub>	Percentage Error
#8* #76 #5 #4 #32 #1	0.6160 0.6340 0.6340 0.6520 0.5660 0.5772 0.6856 0.7094 0.6864	0.6667 0.6667 0.6667 0.6667 0.6667 0.6667 0.6667	- 7.60 - 4.90 - 4.90 - 2.20 -15.10 -13.42 + 2.83 + 6.40 + 2.95

\*Note: The beam section #8 identifies the cross section parallel to X-axis and located at Y=8 mesh units, which means beam section #3 passes through the X-axis. The same notation is used throughout the text.

TABLE 4.4

Following values are to be multiplied by  $-K_1d^3/81$ .

TABLE 4.5

BENDING STRESS  $\sqrt{y}$  FOR THE CROSS SHAPE HAVING d/b = 1.0 AND r/d = 1/3 SUBJECTED TO PURE BENDING MOMENT (GRADED NET)

Following values are to be multiplied by  $K_1d$ .

Node	<b>√</b> y
1,77,666,5,5,5,4,4,4,3,3,3,3,3,3,2,2,2,2,2,2,1,1,1,1,1,1,1,1	0.3333 0.6666 0.8888 0.6477 0.9200 0.3016 0.92570 0.3016 0.92570 0.3200 0.2570 0.3200 0.4500 0.5883 0.5830 0.5883 0.3883 0.3883 0.3883 0.3889 0.3889 0.3889 0.3889 0.3889 0.3889 0.3889 0.3889 0.3889 0.3889 0.39880 0.3889 0.39880 0.3889 0.39880 0.3889 0.39880 0.3889 0.39880 0.3889 0.39880 0.3889 0.39880

<sup>\*</sup>The value should be zero according to boundary conditions.

TABLE 4.6 COMPARISON OF RESISTING AND APPLIED MOMENTS  $M_y$  FOR A CROSS SHAPE HAVING d/b = 1.0 AND r/d = 1/3 SUBJECTED TO PURE BENDING MOMENT (GRADED NET)

Moments are to be multiplied by  $K_1d^3$ .

Beam-Section	Resisting My	Applied M <sub>y</sub>	Percentage Error
#7 #65 #43 #2 #1	0.6322 0.6332 0.6500 0.6340 0.7196 0.6426 0.6810 0.6496	0.6667 0.6667 0.6667 0.6667 0.6667 0.6667 0.6667	- 5.17 - 5.02 - 2.50 - 4.90 + 7.93 - 3.61 + 2.56

TABLE 4.7

BENDING STRESS  $\sigma_v$  FOR A CROSS SHAPE HAVING d/b = 1.3 AND r/d = 1/3 SUBJECTED TO PURE BENDING MOMENT (HIGHER ORDER DIFFERENCE FORMULA, GRADED NET)

Following values are to be multiplied by  $K_1d$ .

Node	€y	Node	σy	Node	<b>√</b> y
1,7 2,7,7 1,6,6,5 1,5,5,4,4 23,4 23,4	0.3333 0.6574 0.9259 0.3247 0.6519 0.9654 0.2995 0.6284 1.0150 0.2533 0.5706 1.4933	1,3 2,3 3,3 34,3 1,2 2,2 3,2 4,2 5,2 6,2 7,2	0.2218 0.4389 0.5992 0.4513 0.1942 0.3559 0.4105 0.1627 0.0489 0.0112 -0.0172 0.1710	2,1 3,1 4,1 5,1 7,1 2,0 3,0 56,0 7,0	0.2973 0.3209 0.1897 0.3865 0.3265 -0.3228 0.1619 0.2766 0.2946 0.1968 0.0993 0.0321 -0.0224

TABLE 4.8

COMPARISON OF RESISTING AND APPLIED MOMENTS My FOR A CROSS SHAPE HAVING d/b = 1.3 AND r/d = 1/3 SUBJECTED TO PURE BENDING MOMENT (HIGHER ORDER DIFFERENCE FORMULA, GRADED NET)

Moments are to be multiplied by  $K_1d^3$ .

Beam-Section	Resisting M <sub>y</sub>	Applied M <sub>y</sub>	Percentage Error
#7 #6 #5 #3 #1 #1	0.6392 0.6482 0.6498 0.6366 0.7184 0.6682 0.6702 0.6698	0.6667 0.6667 0.6667 0.6667 0.6667 0.6667 0.6667	- 4.12 - 2.77 - 2.53 - 4.51 + 7.75 + 3.23 + 3.52 + 3.46

TABLE 4.9

Following values are to be multiplied by  $K_1d$ .

Node	<b>♂</b> <sub>X</sub>	Node	<b>て</b> xy
12121212331233333333333333333333333333	0.02431 0.03113 0.03148 0.03948 0.02463 0.02463 0.02463 0.02473 0.02473 0.02473 0.02473 0.02473 0.02473 0.02473 0.02473 0.02463 0.02847 0.03474 0.03474 0.03474 0.03212 -0.03212 -0.03212 -0.03212 -0.03218 -0.05318 -0.05318 -0.053154 -0.05839 -0.05839 -0.05839 -0.05837 -0.05837 -0.0116	6665554444433333332222221111111 0120123301234401234560123456	-0.01689 -0.00845 -0.03395 -0.01738 -0.01697 -0.07364 -0.05877 -0.09877 -0.09877 -0.09656 -0.16558 -0.16558 -0.168844 -0.05437 -0.05437 -0.0313 -0.05579 -0.04261 -0.02506 -0.00506

<sup>\*</sup>The value should be zero according to boundary conditions.

TABLE 4.10

COMPUTATION OF THE ENERGY FOR THE CROSS SHAPE HAVING d/b = 1.0 AND r/d = 1/3 SUBJECTED TO PURE BENDING MOMENT (POISSON'S RATIO = 0.30)

Following values are to be multiplied by  $K_1^2 d^3/2E$ .

Beam Section	∫ <sub>h</sub> σ <sub>γ</sub> .dx	h fox dx	-2/M fox. oy. dx	$2(1+M).$ $\left(\int_{h}^{h} C_{XY} \cdot dx\right)$	Energy = 1+2+3+4
#76543213	0.621860 0.595200 0.595200 0.653400 0.354140 0.237220 0.177066 0.160000	0.001237 0.000149 0.001088 0.014507 0.016043 0.022237 0.014421 0.019029	-0.012544 -0.002432 -0.011200 -0.046208 -0.032192 \0.039296 0.029824 0.032256	0.00000 0.000583 0.002108 0.034667 0.065118 0.042987 0.040546	0.610553 0.593500 0.587196 0.646365 0.403109 0.341740 0.261857 0.211285

TABLE 4.11

RATIO R, THE EQUIVALENT DEPTH  $d_e$  TO THE DEPTH 2d OF THE BEAM, FOR THE CROSS SHAPE HAVING L/b = 1.333, h/b = 2.333, d/b = 1.3 AND r/d = 1/3 SUBJECTED TO PURE BENDING MOMENT (POISSON'S RATIO = 0.33)

Beam Section	Ratio R = $d_e/2d$
#7 #6 #5 #4 #3 #1 #1	1.0298 1.0395 1.0432 1.0104 1.1826 1.2495 1.3654 1.4667

TABLE, 4.12

 $\not$  VALUES FOR THE CROSS SHAPE HAVING L/b = 2.5, h/b = 3.5, d/b = 1.5 AND r/d = 1/3 SUBJECTED TO PURE BENDING MOMENT

Following values are to be multiplied by  $-\kappa_1 d^3/81$ .

Node	ø
1,6 1,3 1,3 1,0 1,3 1,0 1,0 1,0 1,0 1,0 1,0 1,0 1,0 1,0 1,0	12.91553 12.816863 12.673738 12.8294 11.557676 10.827834 10.541963 17.257483 22.775483 22.775483 22.653435 19.182924 25.534736 25.534736 25.534738 26.667933 26.667933 26.616489 27.081935 27.092927

TABLE 4.13 STRESS VALUES FOR THE CROSS SHAPE HAVING d/b = 1.5 AND r/d = 1/3 SUBJECTED TO PURE BENDING MOMENT

Following values are to be multiplied by  $K_1d$ .

Node	<b>♂</b> y	Node	<b>♂</b> x	Node	<b>て</b> xy
1,666,555,444,333322222221111111000000000000000000000	0.32850 0.64833 0.961542 0.645096 0.645096 0.623451 0.623451 0.623451 0.5659594 0.7383857 0.588051 -0.588051 -0.588051 -0.588051 -0.53334 0.135471 0.435471 0.37451 0.37451 0.37451 0.37451 0.37451 0.37451 0.37451 0.37451 0.37451 0.37451 0.37451 0.37451 0.37451 0.37451 0.37451 0.37451 0.37451	12121212331222222211111100000 23312334456123456123456	. 0.0158 -0.0289 0.00527 0.00287 0.02236 0.02746 0.02544 0.10256 0.12044 0.12999** -0.03397 0.03588 -0.01892 -0.01393 -0.01393 -0.01887 0.01580 -0.01580 -0.01580 -0.01580 -0.01580 -0.01580 0.00559 -0.01673 -0.02634 0.00673	012012012012330123340123456	0.01017 0.00624 -0.00509 0.01360 0.02680 0.02742 0.01380 -0.01371 0.06183 0.04630 -0.01270 -0.24794** 0.08308 0.07208 0.01253 -0.09600 -0.14773 -0.06780** 0.05643 0.05643 0.05001 0.05643 0.05001 0.03936 -0.03936 -0.0310

<sup>\*</sup>Calculated by the application of standard difference formulas.

<sup>\*\*</sup>The value should be zero according to boundary conditions.

TABLE 4.14

COMPUTATION OF THE ENERGY FOR THE CROSS SHAPE HAVING d/b = 1.5 AND r/d = 1/3 SUBJECTED TO PURE BENDING MOMENT (POISSON'S RATIO = 0.30)

Following values are to be multiplied by  $K_1^2 d^3/2E$ .

Beam Section	Jhoy.dx	∫h e dx	-2M∫σx.σy.d) 2 3	2(1+/n). ( ( t xy.dx) 4	Energy = 1+2+3+4
#6 #43 #13 #13	0.621866 0.628266 0.612266 0.654934 0.417280 0.276054 0.238934	0.000000 0.000000 0.001003 0.011264 0.008086 0.012907 0.019712	0.00000 -0.001600 -0.010560 -0.041344 -0.019328 0.037200 0.040832	0.000211 0.000316 0.001425 0.024688 0.045372 0.016196	0.622077 0.626982 0.604134 0.649542 0.451409 0.342336 0.299478

### **TABLE 4.15**

RATIO R, THE EQUIVALENT DEPTH  $d_e$  TO THE DEPTH 2d OF THE BEAM FOR THE CROSS SHAPE HAVING L/b = 2.5, h/b = 3.5, d/b = 1.5 and r/d = 1/3 SUBJECTED TO PURE BENDING MOMENT (POISSON'S RATIO = 0.30)

Beam Section	Ratio R = $d_e/2d$
#5 #5 #4 #3 #1	1.0233 1.0207 1.0334 1.0087 1.1388 1.2488

TABLE 4.16

 $\not$  VALUES FOR THE CROSS SHAPE HAVING L/b = 1.333, h/b = 2.333, d/b = 1.3 AND r/d = 3 SUBJECTED TO PURE BENDING MOMENT

-Following values are to be multiplied by  $-K_1d^3/81$ .

Node	Ø
1,321065432105 1,111122222222233333333344444555566633	12,894170 12.723336 12.390653 11.676058 10.709995 9.963409 9.691901 22,860477 22.698227 22.361995 21.334047 19.610856 18.304426 17.838595 25.741312 25.654421 25.459267 24.918531 26.168627 25.153184 23.339476 26.976441 27.008374 26.976441 27.008374 26.701685 26.246298 26.044825 26.94946 27.077141 27.035479 26.995728 27.107700 27.112256 23.986184

TABLE 4.17 STRESSES FOR THE CROSS SHAPE HAVING d/b = 1.0 AND r/d = 0 SUBJECTED TO PURE BENDING MOMENT

Following values are to be multiplied by  $K_1d$ .

Node	σy	Node	<b>♂</b> <sub>X</sub>	Node	T <sub>xy</sub>
1,44,4333332222221111111000000000000000000000	0.26423 0.58307 0.86526* 1.25120 0.2465 0.44634 0.66488 1.020345 0.38163 0.47566 0.037766 0.037779 0.02004 0.18403 0.18409 0.18409 0.175884 0.076669 -0.07581 0.3278 0.17581 0.3278 0.17581 0.32164 0.19382 0.3334	1,444,333,333,333,332222221111110000000000000	0.04243 0.07686 0.04812 0.02794 0.07725 0.17405 0.36950 0.35809 -0.09744 -0.01714 -0.01610 -0.02439 -0.04631 -0.05279 -0.01745 0.017	0,4 4,4 3,3 3,3 3,3 1,2 2,2 2,1 1,1 1,1 1,1 1,1 1,1 1,1 1,1	0.05818 0.03789 -0.02909 0.09337 0.07642 0.00461 -0.06096 0.24780 0.09515 0.08416 0.04111 -0.06322 -0.08967 -0.02393 0.005656 0.04923 0.05656 0.04923 0.02210 -0.03098 -0.04812 -0.01935 -0.00226

<sup>\*</sup>Calculated by the application of standard difference formulas.

TABLE 4.18

COMPUTATION OF THE ENERGY FOR THE CROSS SHAPE HAVING d/b = 1.0 AND r/d = 0 SUBJECTED TO PURE BENDING MOMENT (POISSON'S RATIO = 0.30)

Following values are to be multiplied by  $K_1 d^3/2E$ .

Beam Section	Shoy?dx	_h σ <sub>x</sub> . dx	h -2 <b>/≈</b> ∫σ <sub>x</sub> .σ <sub>y</sub> .d <sub>x</sub> 3	2(1+M). (	Energy = 1+2+3+4
#4 #3 #1 #3	0.667733 0.419200 0.282453 0.212907 0.187733	0.005013 0.113707 0.004352 0.015083 0.019179	-0.028608 -0.068352 0.029028 0.032960 0.034240	0.006739 0.034944 0.043236 0.013978 0.00000	0.650877 0.499499 0.350959 0.274928 0.241152

TABLE 4.19

RATIO R, THE EQUIVALENT DEPTH  $d_e$  TO THE DEPTH 2d OF THE BEAM FOR THE CROSS SHAPE HAVING L/b = 1.333, h/b = 2.333, d/b = 1.0 AND r/d = 0 SUBJECTED TO PURE BENDING MOMENT (POISSON'S RATIO = 0.30)

Beam Section	Ratio R = $d_e/2c$		
#4 #3 #2 #1 #0	1.0080 1.1010 1.2385 1.3435 1.4055		

TABLE 4.20

RATIO R, THE EQUIVALENT DEPTH de TO THE DEPTH 2d OF THE BEAM, FOR THE CROSS SHAPE HAVING L/b = 1.333, h/b = 2.333, d/b = 1.3 AND r/d = 1/3 SUBJECTED TO PURE BENDING MOMENT (POISSON'S RATIO = 3.15)

Beam Section	Ratio R = $d_e/2d$		
#7 #6 #5 #3 #2 #1	1.0262 1.0388 1.0400 0.9956 1.1743 1.2812 1.4014 1.5061		

TABLE 4.21

% VALUES FOR THE CROSS SHAPE HAVING L/b = 1.333, h/b = 2.333, d/b = 1.0 AND r/d = 1/3 SUBJECTED TO VARIABLE BENDING MOMENT

Following values are to be multiplied by  $-K_2d^4/27$ .

				· · · · · · · · · · · · · · · · · · ·	
Node	Ø Value	Node	⊅ Value	Node	Ø Value
1,6 1,5 1,4 1,3 1,2 1,0 2,5 2,4 2,2 2,1	2.836040 5,531027 7.841399 9.130839 9.744581 9.977754 10.033637 5.067647 10.015973 14.487830 17.055711 18.298496 18.803364	2,0 23,45 23,4 23,34 23,34 23,34 3,33 3,23 3,10 34,3	18.933481 14.351914 16.858783 18.800852 20.158745 21.105676 20.477396 22.350146 23.661692 24.543491 25.502780 25.770193 23.543537	34,23 4,23 4,1 4,1 45,23 5,1 5,2 6,1 6,0	25.380255 26.324080 27.862889 29.589936 30.095707 26.707999 28.831883 31.388433 32.180314 29.034005 31.954697 32.904771

TABLE 4.22 STRESS VALUES FOR THE CROSS SHAPE HAVING d/b=1.0 AND r/d=1/3 SUBJECTED TO VARIABLE BENDING MOMENT Following values are to be multiplied by  ${\rm K_2}d^2$ .

Node	<b>o</b> y	Node	σ <sub>X</sub>	Node	<b>て</b> xy
12312312312331233333332222222111111100000000	0.19897 0.43668 0.43668 0.6229 0.837330 1.405589 1.405555 1.63765 1.63766 0.821551* 1.498257** 0.60890 0.708148 0.708148 0.708148 0.708148 0.708148 0.708148 0.708149 0.38244 0.38244 0.38324 0.46589 0.785793 0.496618 0.608361 0.766393 0.76639 0.76639 0.76639 0.76639 0.76639 0.76639 0.76639 0.76639 0.	7766554444333333333222222111111000000000000000	0.03525 0.03525 0.02898 0.04792 0.13720 0.138829 0.158829 0.69681** 0.69681** 0.69681* 0.69681* 0.441795 0.72382467 0.72382467 0.7287870 0.124591 0.750444 0.124591 0.750444 0.123070 0	7776665555444443333333322222221111111777666555544444333333322222221111111	-0.96296 -0.951852 -0.91852 -0.9218466 -0.934908 -0.934997 -0.582973 -0.582997 -0.558625806*** -0.5645907 -0.5645907 -0.317544 -0.317544 -0.31756 -0.317599866 -0.31970986 -0.31970986 -0.31970986 -0.052914 -0.113684 -0.1136

<sup>\*</sup>Calculated by the application of standard difference formulas.
\*\*The value should be zero according to boundary conditions.

TABLE 4.23

COMPARISON OF APPLIED AND RESISTING FORCES FOR THE CROSS SHAPE HAVING L/b = 1.333, h/b = 2.333, d/b = 1.0 AND r/d = 1/3 SUBJECTED TO VARIABLE BENDING MOMENT

Moment  $M_y$  and shear  $V_x$  are to be multiplied by  $K_2 d^4$  and  $K_2 d^3$  respectively.

Type of Force	Beam Section	Applied	Resisting	Difference	Percentage Error Com- pared to the applied one
Moment <sup>M</sup> y	#54 #3 #10	0.44444 0.88889 1.33333 1.77778 2.14815 2.37037 2.44444	0.41810 0.85108 1.30706 1.67638 2.14216 2.36270 2.41188	0.02634 0.03781 0.02627 0.10140 0.00599 0.00763 0.03256	5.92 4.25 1.97 5.70 0.28 0.32 1.33
Shear V <sub>X</sub>	#7654 #32 #1	1.33333 1.33333 1.33333 1.33333 1.33333 0.88889 0.44444	1.27147 1.25867 1.23307 1.16907 1.35253 0.85760 0.45653	0.06186 0.07466 0.10026 0.16426 0.01920 0.03129 0.01189	4.64 5.60 7.52 12.32 1.55 3.52 2.67

Normal force  $N_x$  is to be multiplied by  $K_2d^3$ .

Column Section	Applied	Resisting N <sub>X</sub>	Difference	Percentage Error Compared to Applied N <sub>X</sub>
#6* #5 #43 #1	1.33333 1.33333 1.33333 1.3580 0.64197	1.30987 1.34400 1.35253 1.23733 1.13067 0.61867	0.02346 0.01067 0.01920 0.09600 0.00514 0.02330	1.76 0.80 1.43 7.20 0.45 3.63

<sup>\*</sup>The column section #6 identifies the cross section parallel to Y-axis and located to at X=6 mesh units, which means that #3 passes through Y-axis.

**TABLE 4.24** 

COMPUTATION OF THE ENERGY FOR THE CROSS SHAPE HAVING d/b = 1.0 AND r/d = 1/3 SUBJECTED TO VAIRABLE BENDING MOMENT (POISSON'S RATIO = 0.30)

Following values are to be multiplied by  $K_2^2 d^5/2E$ .

Beam Section	$\int_{-h}^{h} \sigma_{y}^{2} dx$	∫h2-dx -hσx.dx	h -2,M_h	$2 (1+M)  \left( \int_{h}^{h} \zeta_{xy}^{2} \cdot dx \right)  -h $	Energy = 1+2+3+4
#76543 <b>21</b> 3	0.000000	0.00000	0.000000	2.496000	2.496000
	0.270933	0.005333	-0.014080	2.468266	2.729732
	1.134933	0.034133	-0.079360	2.268565	3.358271
	3.287958	0.531200	-0.684342	1.874773	5.009589
	1.958400	2.641106	-0.842240	2.052268	5.809534
	1.683120	1.395200	-0.587520	0.557400	3.048200
	1.529600	0.857600	-0.391680	0.177492	2.173012
	1.461334	0.716800	-0.345600	0.000000	1.832534

TABLE 4.25

RATIO R, THE EQUIVALENT DEPTH  $d_e$  TO THE DEPTH 2d OF THE BEAM, FOR THE CROSS SHAPE HAVING L/b=1.333, h/b=2.333, d/b=1.0 AND r/d=1/3 SUBJECTED TO VARIABLE BENDING MOMENT (POISSON'S RATIO = 0.30)

Beam Section	Ratio R = $d_e/2d$
#7 #6 #5 #4 #3 #1	0.9259 0.9636 1.0270 0.9962 1.0689 1.4270 1.6106 1.6974

TABLE 4.26

Values for the cross shape having l/b = 1.333, h/b = 2.333, d/b = 1.3 and r/d = 0 subjected to variable bending moment

Following values are to be multiplied by  $-K_2d^4/27$ .

Node	Ø
1,1,1,1,0,5,4,321,5,4,33222 1,1,1,1,1,2,2,2,2,2,2,3,3,3,3,4,4,4,4,5,5,5,6666,1,0,1,0,1,0,1,0,1,0,1,0,1,0,1,0,1,	2.828842 5.828842 5.946709 7.982591 9.486299 10.48624905 10.7252810 10.7252810 10.651891 18.2631331 19.981587 14.26484701 19.78444701 21.873289 21.873289 21.873289 22.3495549 21.873289 26.8392135 26.8392135 26.8392135 26.83965549 30.668689 26.839651 28.548699 31.389805 31.389805 31.946813

TABLE 4.27 STRESSES FOR THE CROSS SHAPE HAVING d/b=1.0 AND r/d=0 SUBJECTED TO VARIABLE BENDING MOMENT Following values are to be multiplied by  $K_2d^2$ .

Node	бy	Node	σ <sub>x</sub>	Node	<b>て</b> xy
12331233123456712345671234567	0.41847 1.06909 1.9668? 2.63874 0.39709 0.89600 1.71273 3.30270 0.451157 1.46353 0.45355 0.94437 0.17355 0.05712 -0.03382 0.166377 0.89641 1.166377 0.32818 0.13082 -0.47162 0.13082 0.13082 0.13082 0.13082 0.13082 0.13082 0.13082 0.16064 0.1062	1,4,4,3,3,3,3,3,3,3,2,2,2,2,1,1,1,1,1,1,1,1,1	0.22556 0.34481 0.034435 0.33822 0.75462 1.26613 2.04628 1.15700 0.96093 0.74903 0.644608 0.179436 0.32436 0.32436 0.73440 0.69854 0.17741 0.459838 0.66161 0.96032 0.12917 0.69854 0.12917 0.69854 0.12917 0.69854	23,44,4,4,333,33,32,22,2,2,2,1,1,1,1,1,1,1,1,1,1,	-0.69918 -0.68814 -0.65041 -0.52667 -0.10961** -0.41728 -0.41328 -0.45134 -0.65843 -0.65843 -0.15844 -0.14354 -0.14354 -0.14657 -0.3752 -0.03752 -0.036693 -0.05693 -0.17274 -0.11699 -0.01699

<sup>\*\*</sup> The value should be zero according to boundary conditions.

TABLE 4.28

COMPUTATION OF THE ENERGY FOR THE CROSS SHAPE HAVING d/b = 1.0 AND r/d = 0 SUBJECTED TO VARIABLE BENDING MOMENT (POISSON'S RATIO = 0.30)

Following values are to be multiplied by  $K_2^2 d^5/2E$ .

Beam Section	Jhoy.dx	-h 2 dx	h -2/M∫ox.oy.dx 3	2 (1+M). ( \int_h^2 \text{xy.dx}) 4	Energy = 1+2+3+4
#4	3.029333	0.099200	-0.168320	2.043946	5.004149
#3	2.922667	5.162667	-1.248000	1.442132	8.279466
#2	2.396667	1.448533	-0.584960	0.701653	3.961893
#1	1.911447	0.864000	-0.368000	0.166400	2.573847
#3	1.802667	0.742400	-0.309760	0.000000	2.235307

TABLE 4.29

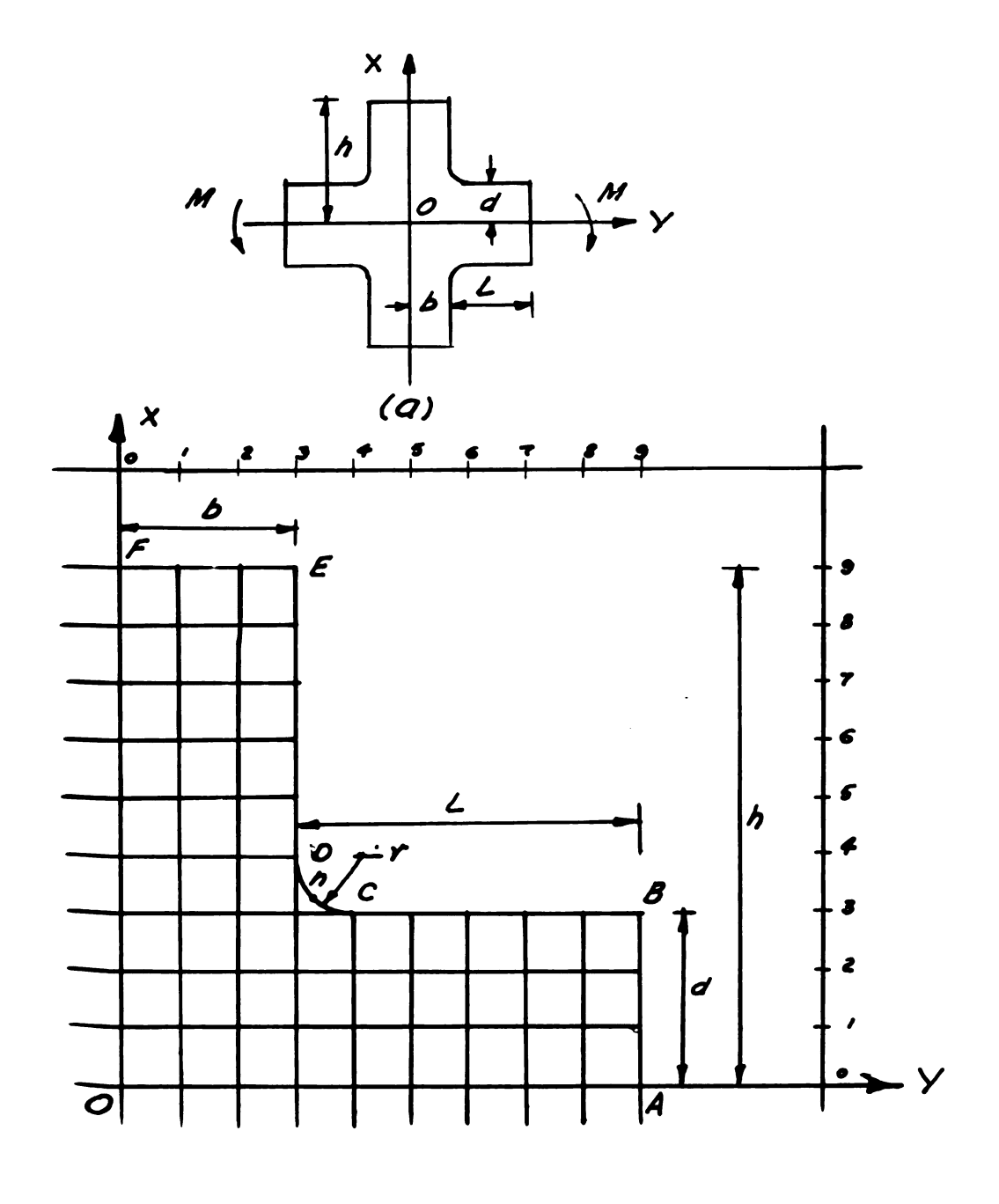
RATIO R, THE EQUIVALENT DEPTH  $d_e$  TO THE DEPTH 2d OF THE BEAM, FOR THE CROSS SHAPE HAVING L/b = 1.333, h/b = 2.333, d/b = 1.0 AND r/d = 0 SUBJECTED TO VARIABLE BENDING MOMENT (POISSON'S RATIO = 0.30)

Beam Section	Ratio R = $d_e/2d$
#4	0.9684
#3	0.9242
#2	1.2911
#1	1.5184
#0	1.5877

TABLE 4.30

RATIO R, THE EQUIVALENT DEPTH  $d_e$  TO THE DEPTH 2d OF THE BEAM, FOR THE CROSS SHAPE HAVING L/b = 1.333, h/b = 2.333, d/b = 1.3 AND r/d = 1/3 SUBJECTED TO VARIABLE BENDING MOMENT (POISSON'S RATIO = 3.15)

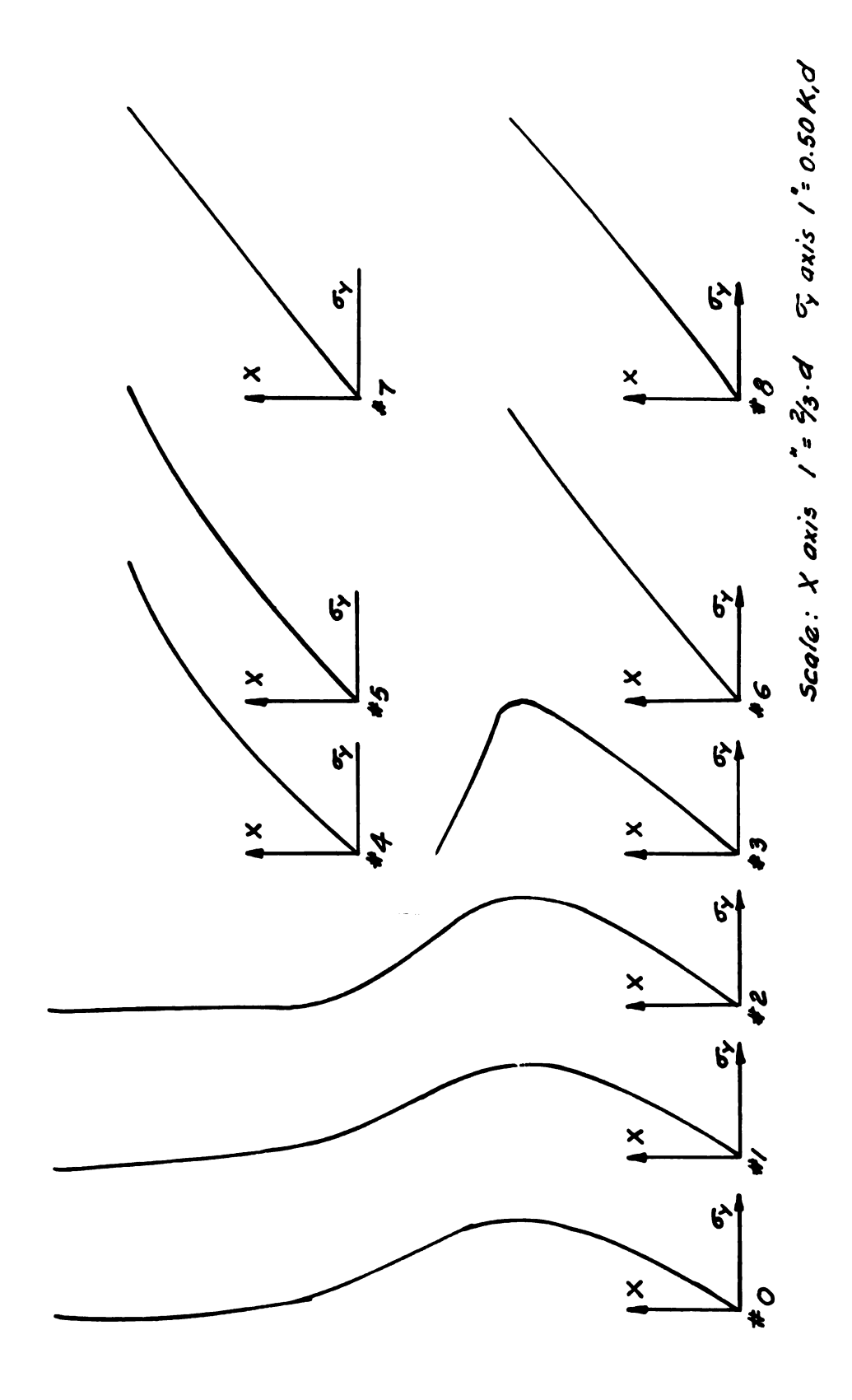
Beam Section	Ratio R = $d_e/2d$
#6 #5 #4 #2 #1 #0	0.9637 1.0265 0.9389 1.0400 1.3756 1.5632 1.7093



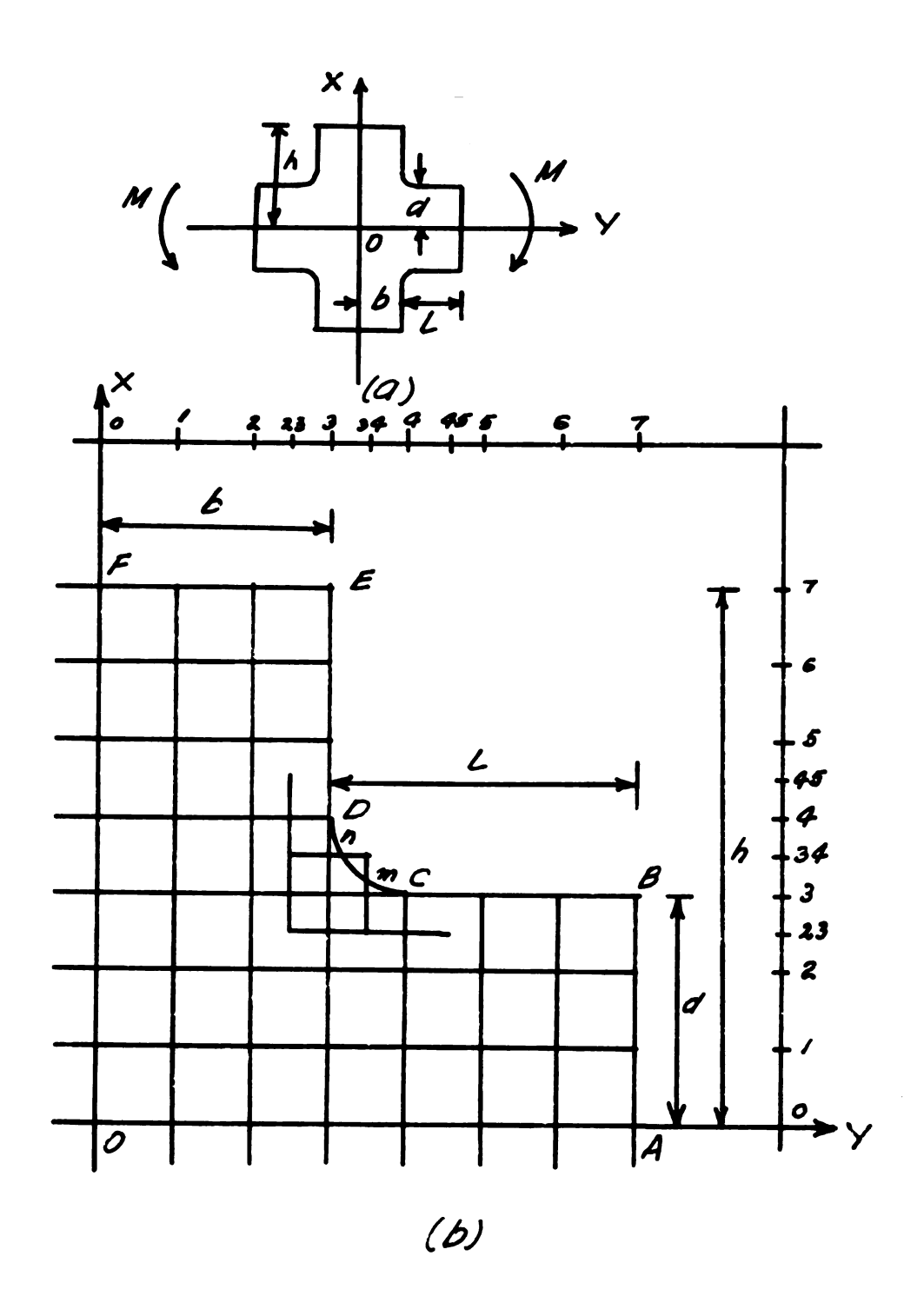
(6)

Cross Shape having  $\frac{L}{b}$ = 2.0,  $\frac{h}{d}$ = 3.0,  $\frac{d}{b}$ =1.0 and  $\frac{r}{d}$ =  $\frac{1}{3}$ 

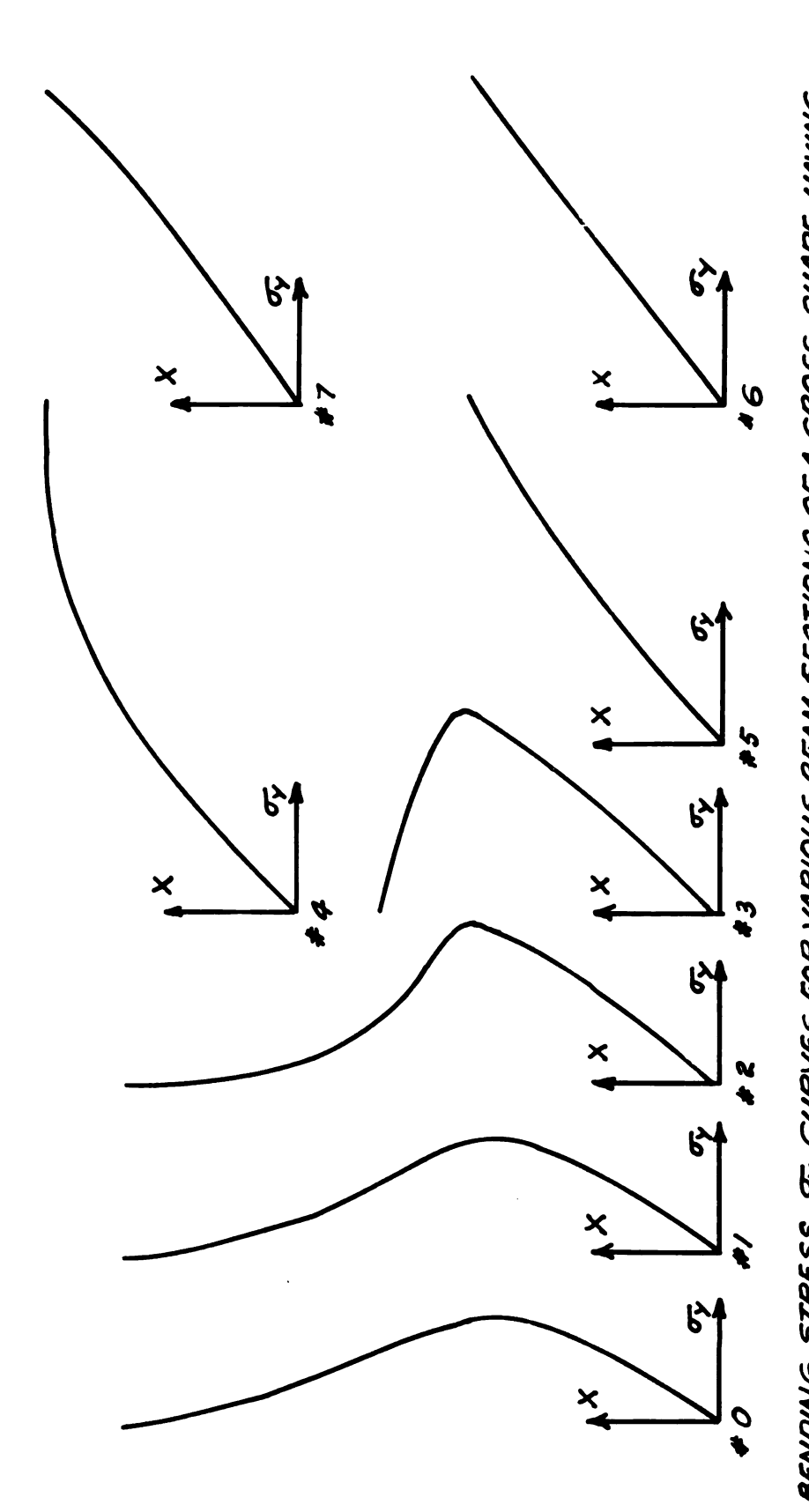
FIGURE 4.1



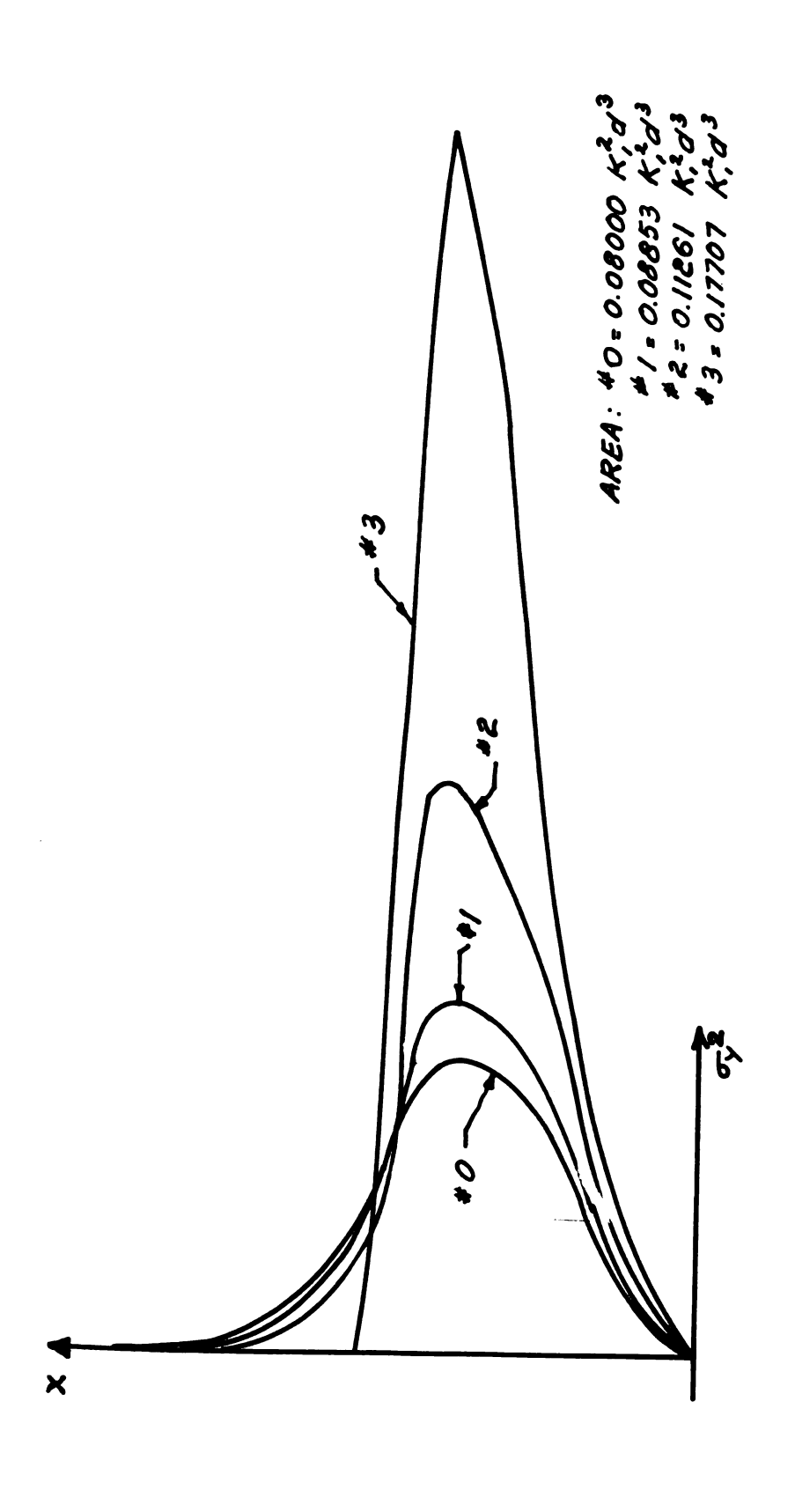
BENDING STRESS OF CURVES FOR VARIOUS BEAM SECTIONS OF THE CROSS SHAPE HAVING 6-0.0.3333A



CROSS SHAPE WITH GRADED NET HAVING  $\frac{L}{b} = 1.333, \frac{h}{b} = 2.333, \frac{d}{b} = 1.0 \text{ AND } \frac{r}{d} = \frac{1}{3}$ 

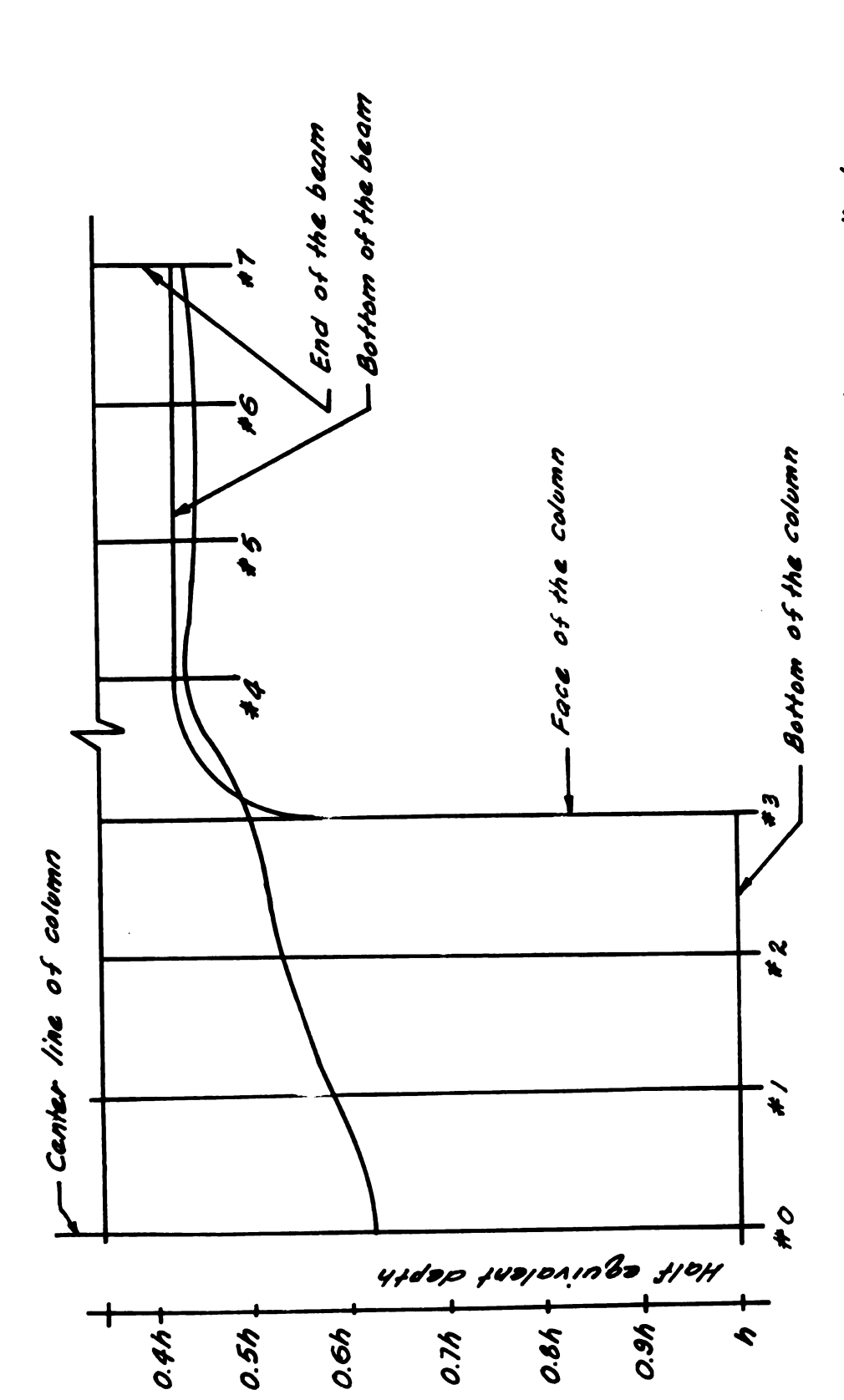


o, axis1:0.50 K.d Scole: X axis 1" 43 d. BENDING STRESS & CURVES FOR VARIOUS BEAM SECTIONS OF A CROSS SHAPE HAVING (PURE BENDING MOMENT. GRADED NET) FIGURE 4.4 b-d=0.42856h.

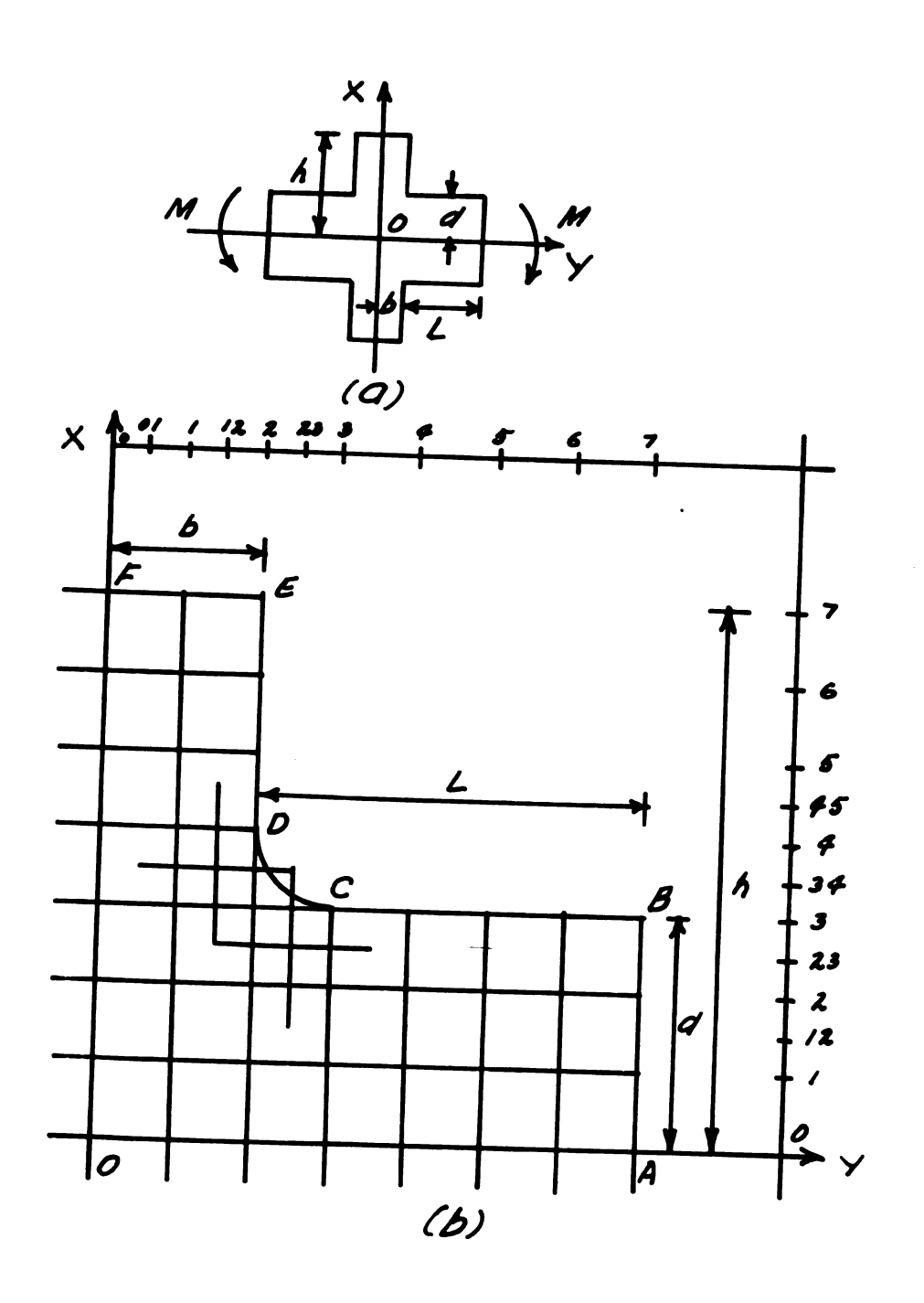


THE CURVES FOR BEAM SECTIONS FOR A CROSS SHAPE HAVING DECTO. 42856 A. (PURE BENDING MOMENT)

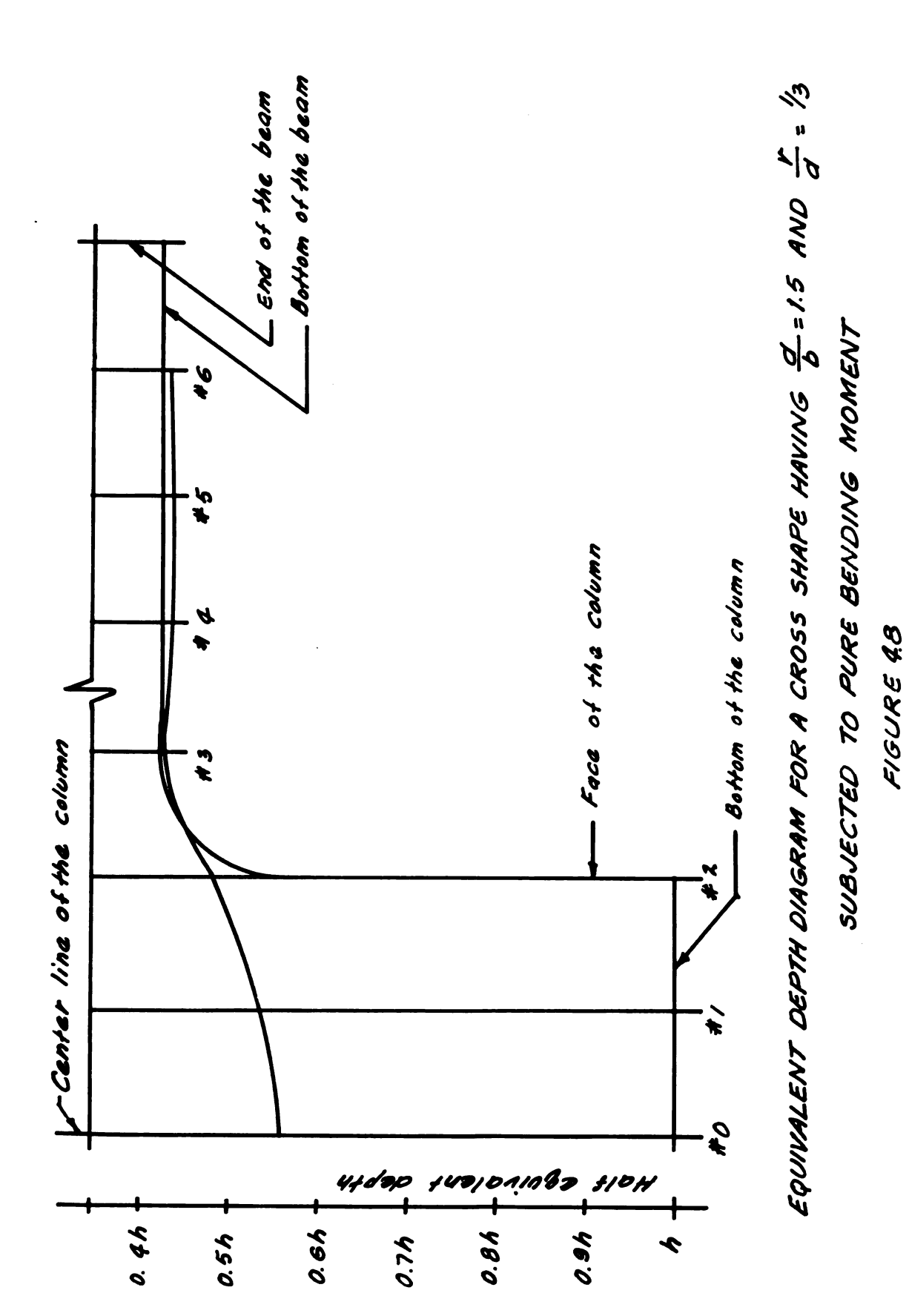
FIGURE 4.5 Scale: X axis 1"= 2 43 \sqrt{2} axis 1"= 0.05 K2 axis

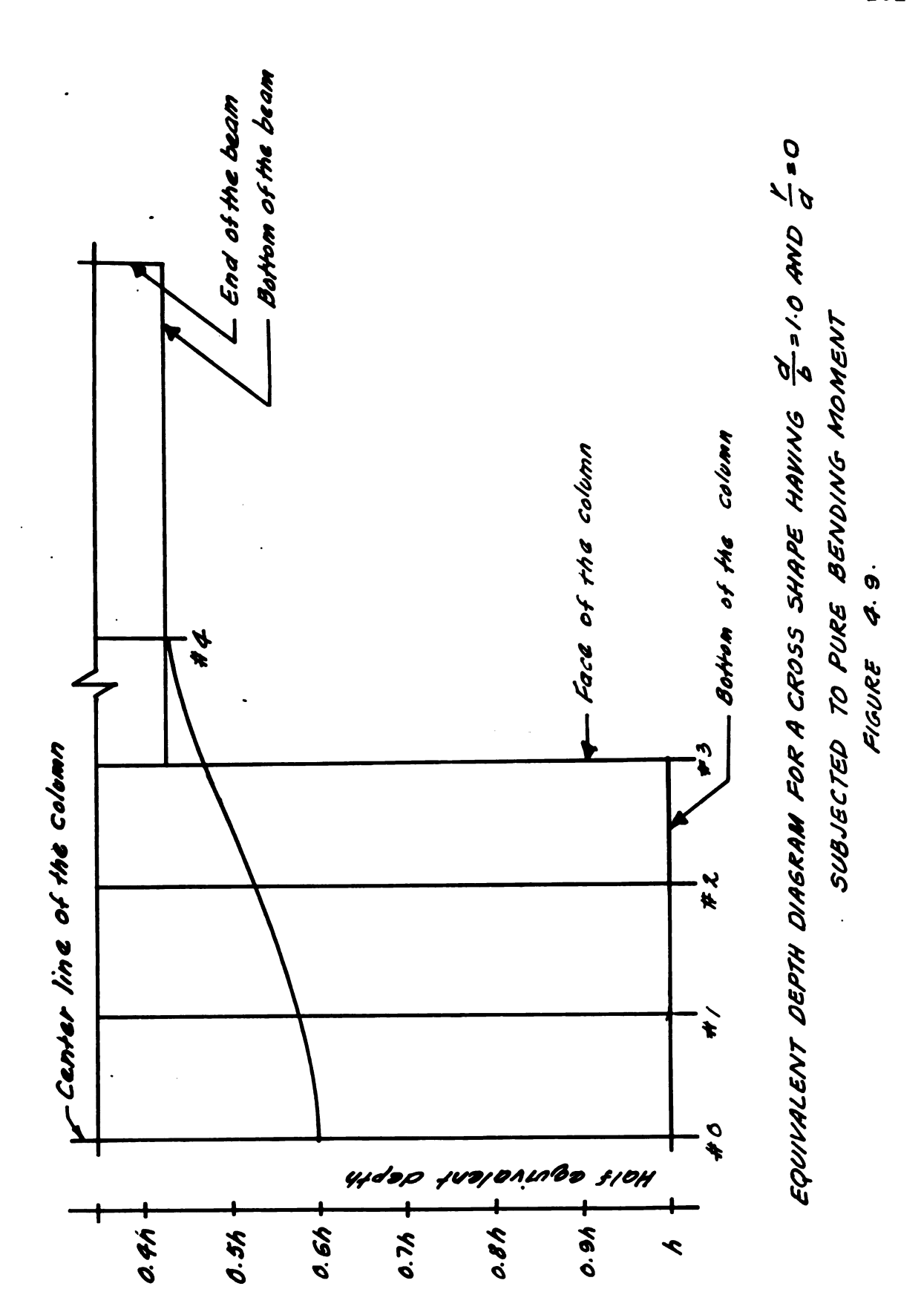


EQUIVALENT DEPTH DIAGRAM FOR A CROSS SHAPE HAVING  $\frac{d}{b}$ =1.0 AND  $\frac{l}{d}$ = $\frac{i}{3}$  SUBJECTED TO PURE BENDING MOMENT



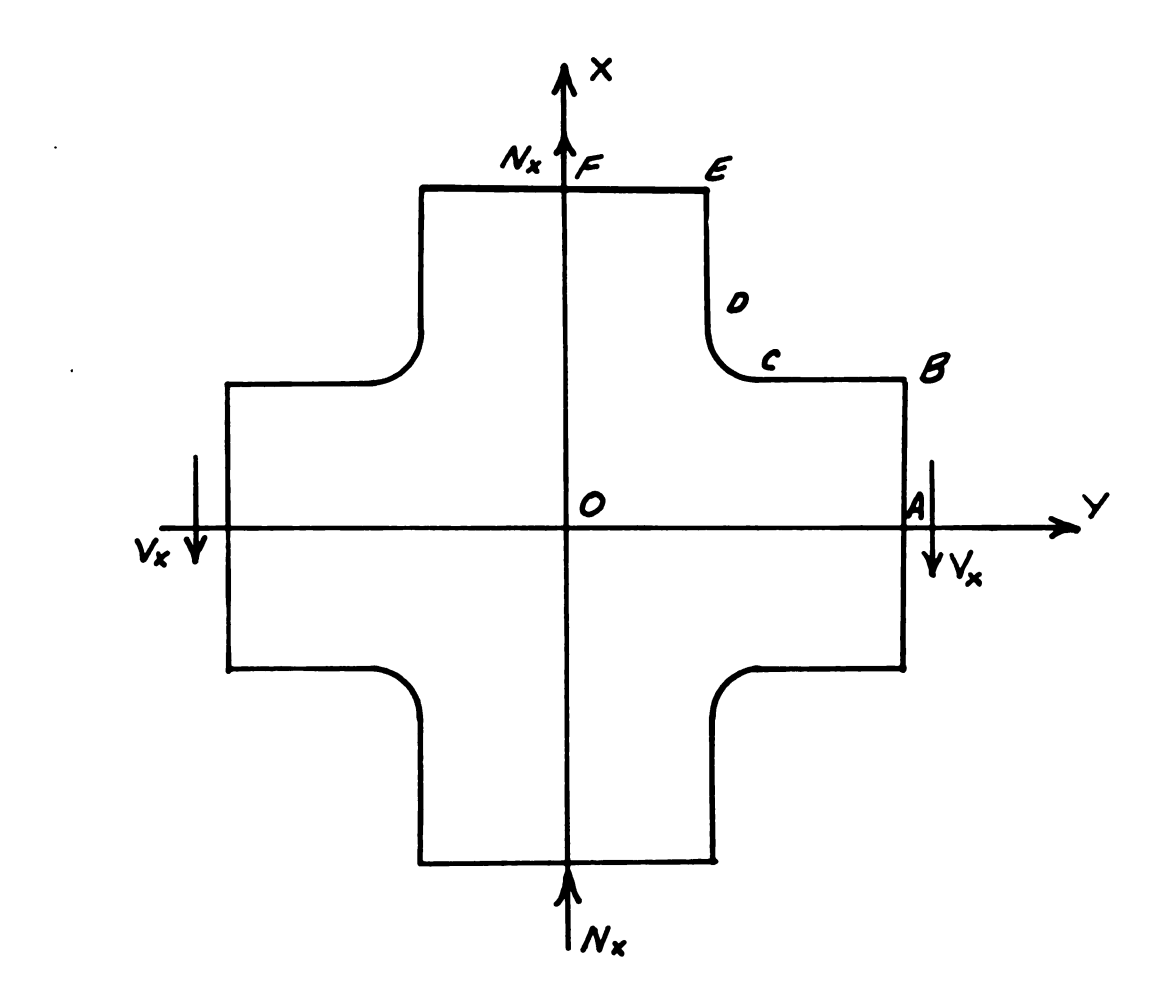
CROSS SHAPE HAVING  $\frac{L}{b} = 2.5, \frac{h}{b} = 3.5, \frac{d}{b} = 1.5$  AND  $\frac{V}{a} = \frac{1}{3}$ FIGURE 4.7





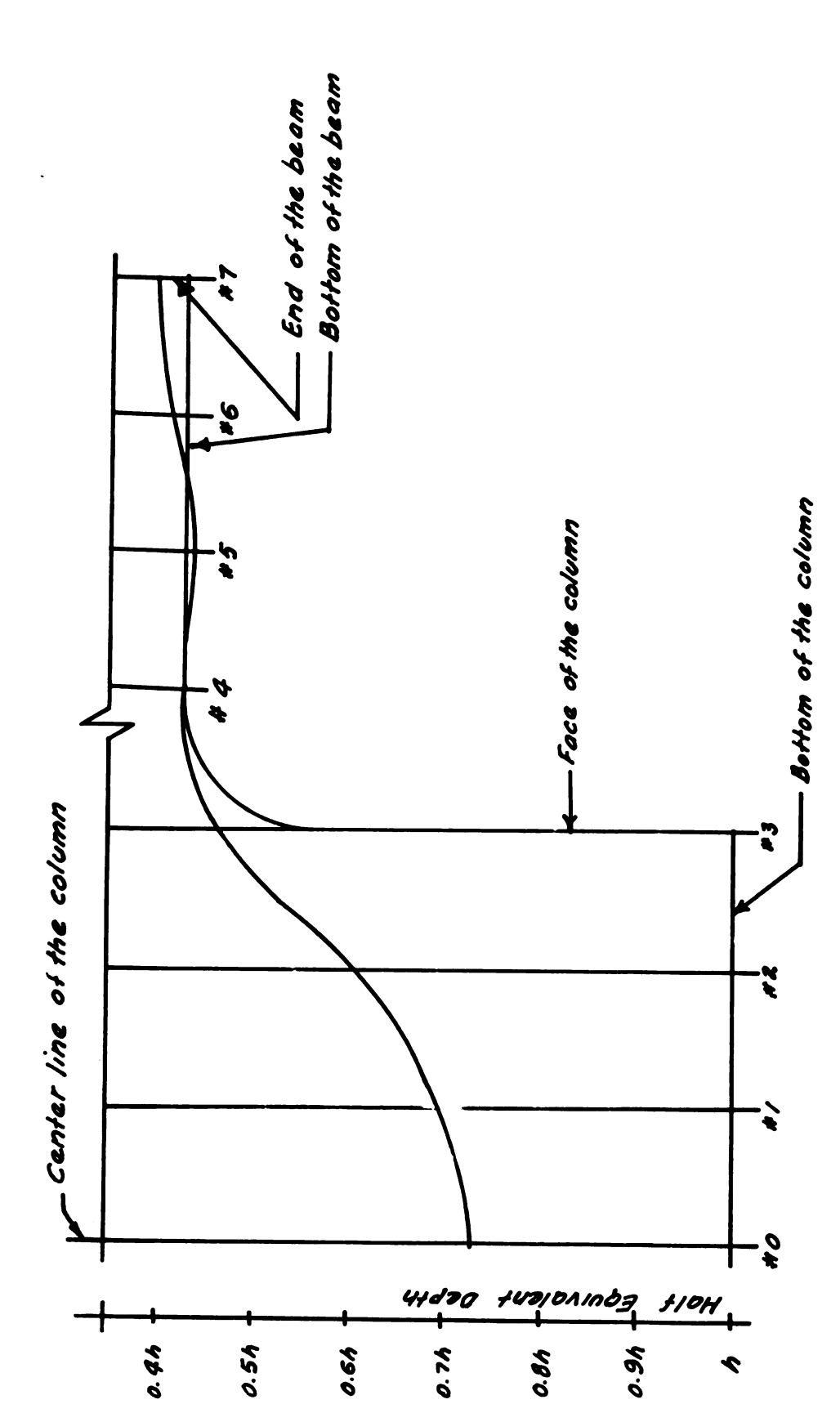
.

i

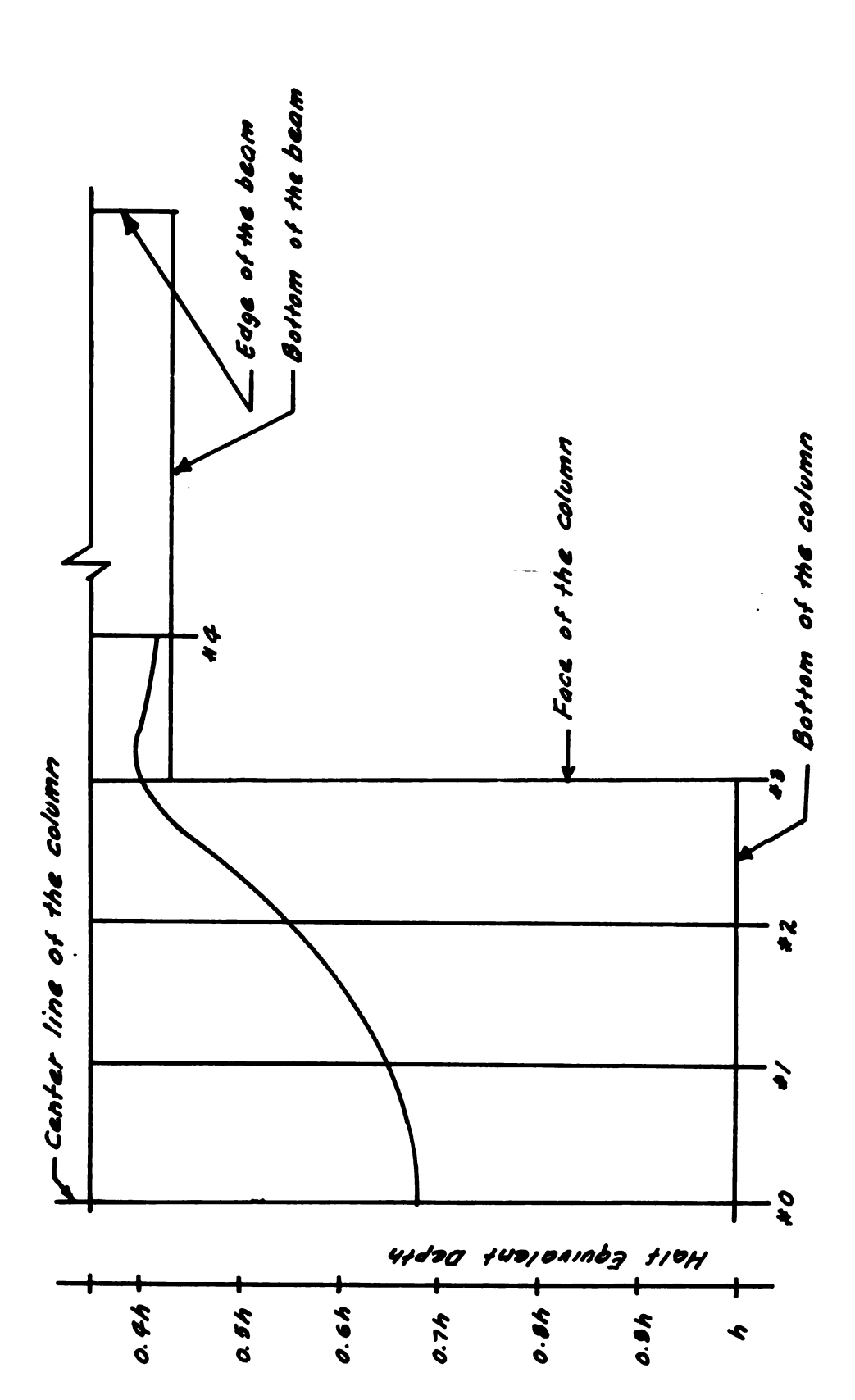


# CROSS SHAPE SUBJECTED TO VARIABLE BENDING MOMENT

FIGURE 4.10



EQUIVALENT DEPTH DIAGRAM FOR A CROSS SHAPE HAVING \(\frac{Q}{2}=1.0\) AND \(\frac{f}{a}=\frac{d}{3}\) SUBJECTED TO VARIABLE BENDING MOMENT



Equivalent depth diagram for a cross shape having  $\frac{q}{b}$ =1.0 and  $\frac{L}{a}$ =0 subjected to variable bending moment

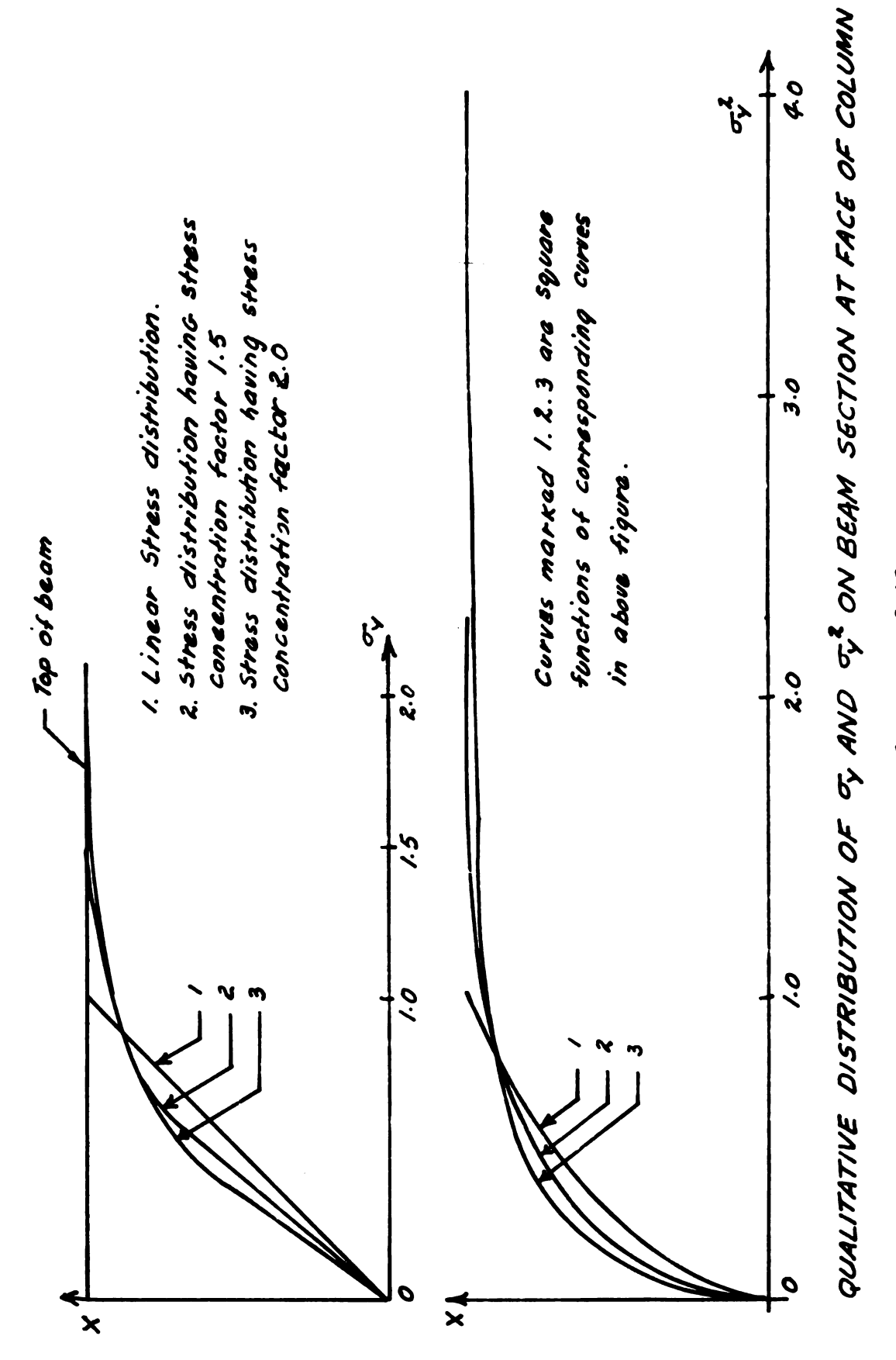
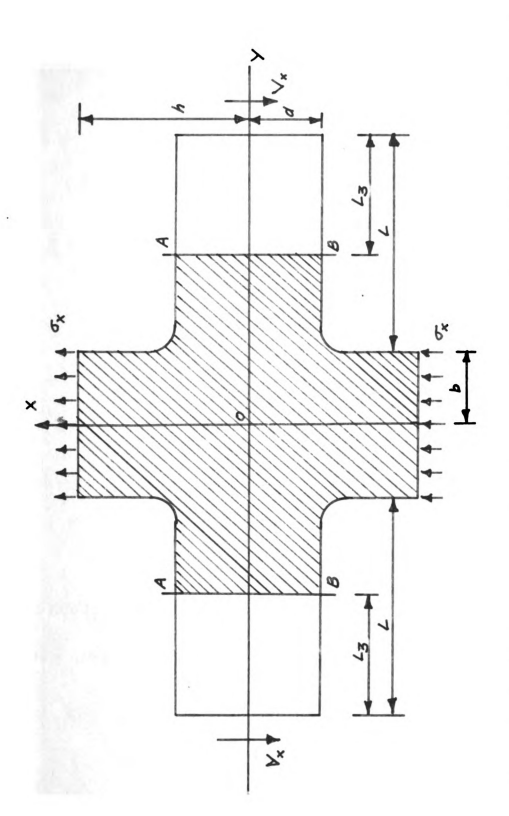
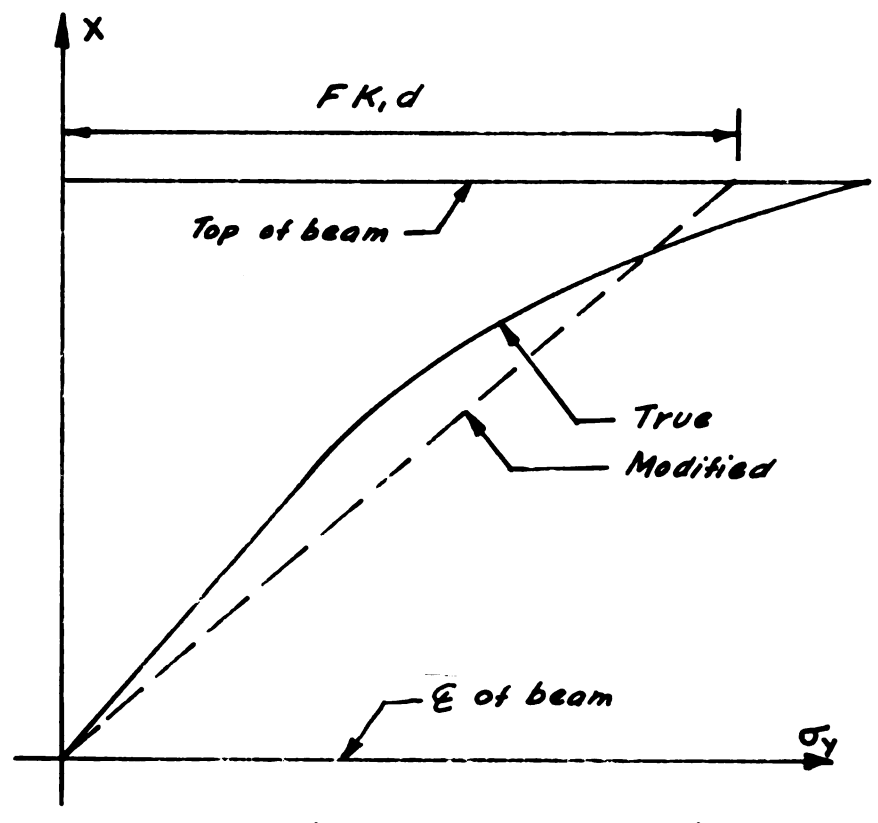


FIGURE 4.13



CROSS SHAPE HAVING  $\frac{d}{b}$ =1.0,  $\frac{1}{4}$ =2.333,  $\frac{r}{a}$ =  $\frac{s}{3}$  AND  $\frac{s}{4}$  GREATER THAN 1.333 SUBJECTED TO VARIABLE BENDING MOMENT FIGURE 4.14



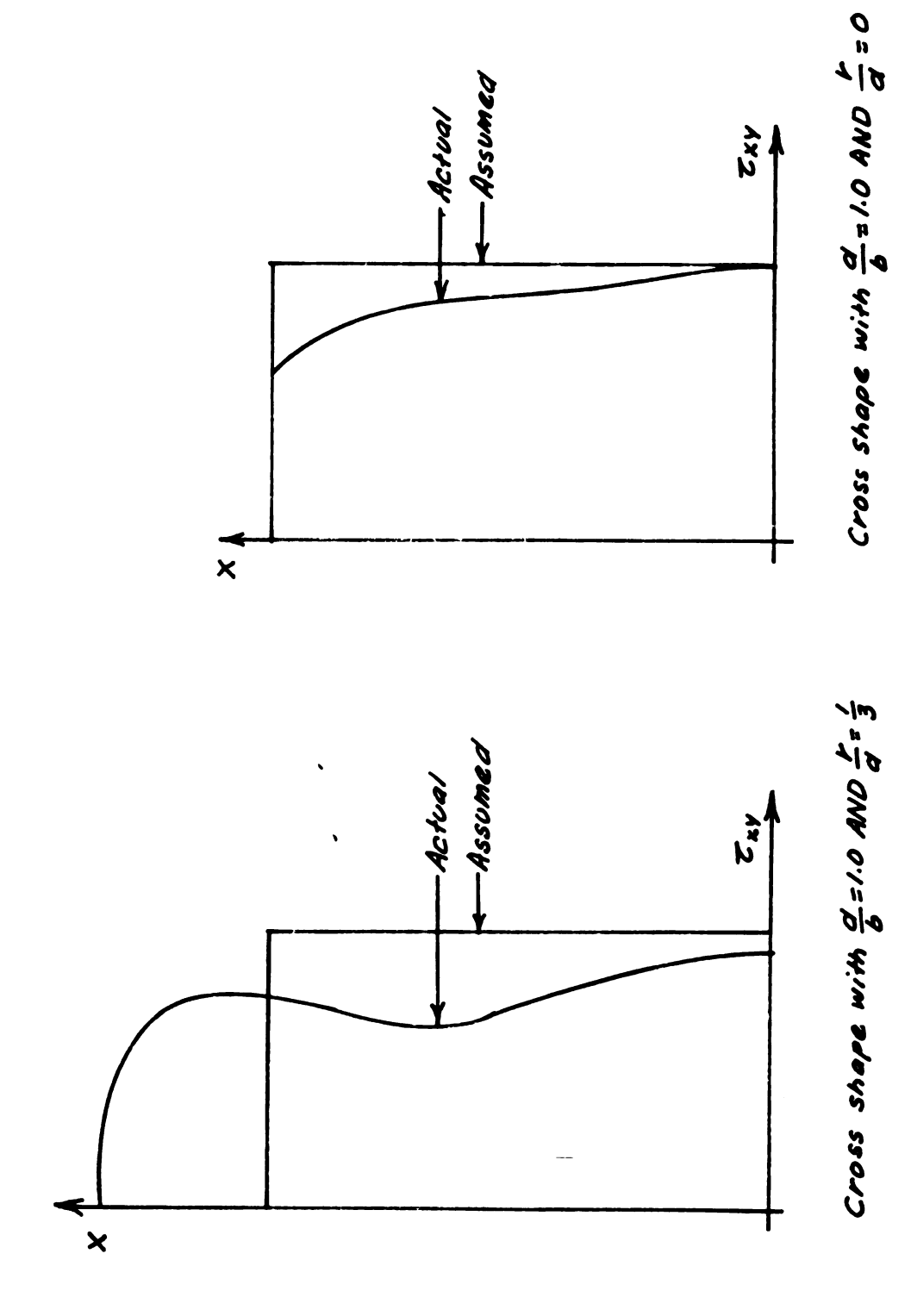
Scale: X axis, 1 = d/3 ; Ty axis, 1 = 0.25 K,d.

 $rac{a}{a}$  STRESS DISTRIBUTION FOR BEAM SECTION \*3 FOR A CROSS SHAPE HAVING b=d=0.42856h AND  $\frac{r}{d}=0$ 

(PURE BENDING MOMENT)

a			
r1 :			
~>			
		•	

.



ACTUAL AND ASSUMED SHEAR STRESS DISTRIBUTION ON THE FACE OF A COLUMN DUE TO SHEAR FORCE V

Scale: X anis. 1" = 4 Zxy anis. 1" = 0.40 Kzd k

•			
ं : : :			

#### CHAPTER V

#### SERIES SOLUTION

An analytical solution of the cross shape as a whole is cumbersome, but as the principal interest is to determine the stress distribution within the column, it will be appropriate to look for some analytical solution which can furnish the stress information in the column zone. possible to analyze the column zone separately if the stresses on the column face can be known by other means. In part I of this chapter, a general series solution is discussed for the stress function  $\emptyset$  in a column subjected to moment and shear forces due to a beam connection. formulas for energy, displacement, slope, and curvature are derived. In part II, the problem is solved for the pure bending moment case. In part III, the problem is solved for the variable bending moment case. In parts II and III the effect of different proportions of the cross shape on the equivalent depth is discussed. In part IV, the method to be used for combination of numerical method and series method results is discussed. In part V, the approximate equivalent depth curve, which is to be used for practical purposes, is discussed.

•			
<b>π</b>			
۳ <b>.</b>			

#### I. GENERAL SOLUTION

# Boundary Conditions

The loading conditions for the column are illustrated in Figure 5.1. It is assumed that the stress function  $\emptyset$ is symmetrical about the X-axis and anti-symmetrical about the Y-axis. The moment M is imposed on the boundary by some mode of stress distribution of  $\sigma_v$  on the area x = 0to  $x = \pm d$ . Also shearing stress  $Z_{xy}$  are distributed in some form with the resultant shear force V. The mode of distribution of  $\sigma_v$  and  $\tau_{xv}$  is not specified at this stage except for the assumed symmetry conditions. will be some  $\sigma_{x}$  stresses on the top and the bottom edges of the column to resist the downward forces V. If h  $\geq$  2d, as is usually the case in frame structures, it will be reasonable to assume that  $\sigma_{\rm X}$  will be distributed uniformly on the top and the bottom. This was also justified by the photoelasticity study. Also, in order to get a symmetrical problem it is assumed that the magnitudes of  $\sigma_X$  on  $x = \pm h$ are the same. It would be easy to superpose a uniform state of uniaxial  $\sigma_x$  stress on the results obtained, to get case where the two values are not equal.

# Evaluation of Stress Function $ot \emptyset$

To solve the elasticity problem for the determination of stresses in the structure, assuming a state of plane

stress to exist, one has to determine the stress function  ${\mathscr D}$  which satisfies the biharmonic differential equation

$$\nabla^{4} \emptyset = 0 \tag{5.1}$$

and the boundary conditions. As the stress is discontinuous on the boundaries  $y=\pm b$ , the stress function is assumed in the form of a trignometric series in  $x^1$ . The stress function

$$\phi = \frac{\mathbf{E} \times \mathbf{y}^2}{2} + \left[ \sum_{m=1}^{\infty} f_m(\mathbf{y}) \cdot \mathbf{S}_{in} \quad \underline{m}\pi \times \right]$$
 (5.2)

will satisfy the Equation 5.1. Here m is an integer and each  $f_m(y)$  is a function of y only. Substitution of Equation 5.2 into Equation 5.1, using the notation m  $\pi/h = 4_m$ , reduces Equation 5.1 to

$$A_{m}^{4} f_{m}(y) - 2A_{m}^{2} f_{m}^{I}(y) + f_{m}^{II}(y) = 0,$$
 (5.3)

which is to be solved for  $f_m(y)$ . The general solution of this differential equation is

$$f_m(y) = C_{1m} \cosh 4my + C_{2m} \sinh 4my + C_{3m} Y \cosh 4my + C_{4m} Y \sinh 4my.$$
 (5.4)

<sup>&</sup>lt;sup>1</sup>The series methods used in this chapter follow the procedures given in S. Timoshenko and J. N. Goodier, Theory of Elasticity (New York: McGraw-Hill Book Company, Inc., 1951), pp. 46-50.

Substituting Equation 5.4 into Equation 5.2,

$$\phi = \frac{P_0 \times y^2}{2} + \sum_{m=1}^{\infty} \left[ C_{1m} \cosh \alpha_m y + C_{2m} \sinh \alpha_m y + C_{3m} y \cosh \alpha_m y + C_{4m} y \sinh \alpha_m y \right] \sin \alpha_m x. \quad (5.5)$$

As the stress function is symmetrical about X-axis and anti-symmetrical about Y-axis,  $c_{2m}$  and  $c_{3m}$  should be zero. Hence, the stress function will be as follows:

$$\phi = \frac{P_{\text{axy}}^2}{2} + \sum_{m=1}^{\infty} \left[ C_{\text{im}} \cosh \alpha_{my} + C_{\text{4my}} \sinh \alpha_{my} \right] \sin \alpha_{mx}.$$
(5.6)

## Evaluation of Constants

In Equation 5.6, the constants  $P_0$ ,  $C_{lm}$  and  $C_{lm}$  are to be determined from boundary conditions of the structure. As the stress distribution on the boundaries  $y=\pm$  b is discontinuous, it will be convenient to express the given stress distribution in terms of Fourier series. The moments on faces  $y=\pm$  b are produced by some form of  $\sigma_y$  distribution which is anti-symmetrical about the Y-axis, and the shearing stress  $\sigma_{xy}$  are distributed symmetrically about the Y-axis in some form on the boundaries  $y=\pm$  b with the resultant shear force V. Therefore,  $\sigma_y$  and  $\sigma_{xy}$ , on the boundaries can be expressed in terms of Fourier series as follows:

$$\sigma_{y} = \sum_{m=1}^{\infty} B_{m} \cdot \sin \alpha_{m} x \tag{5.7}$$

$$T_{xy} = \pm \frac{A_2}{2} \pm \sum_{m=1}^{\infty} A_m Cos d_m x \qquad (5.8)$$

where

$$B_{m} = \frac{1}{h} \int_{h}^{h} F(x) \sin \alpha_{m} x . dx \qquad (5.9)$$

$$A_{m} = \frac{1}{h} \int_{-h}^{h} G(x) \cos x dx \qquad (5.10)$$

$$A_{o} = \frac{1}{h} \int_{h}^{h} G(x) \cdot dx \qquad (5.11)$$

F(x) and G(x) are given functions prescribing the distribution of  $\sigma_y$  and  $\tau_{xy}$ , respectively, on boundaries y=b along x=-b to y=-b. In Equation 5.8, the plus signs apply to y=+b, and minus signs to y=-b. At this stage it will be considered that  $B_m$ ,  $A_m$  and  $A_0$  are evaluated from the known stress distribution on the boundary. The stress components corresponding to the stress function, Equation 5.6, are as follows:

$$\sigma_{X} = \frac{\partial^{2} \phi}{\partial y^{2}} = P_{0} \times + \sum_{m=1}^{\infty} \left[ C_{1m} A_{m}^{2} C_{0} + A_{m} A_{m} + 2 C_{4m} A_{m} C_{0} + A_{m} A_{m}^{2} + 2 C_{4m} A_{m} C_{0} + A_{m} A_{m}^{2} + 2 C_{4m} A_{m}^{2} + 2 C_{4m}^{2} + 2 C_{4m}^{2$$

$$T_{xy} = -\frac{\partial \phi}{\partial x \cdot \partial y} = -\sum_{m=1}^{\infty} \left[ C_{1m} \, \zeta_m^2 \, Sinh \, \zeta_{my} + C_{4m} \, \zeta_{m} \, Sinh \, \zeta_{my} \right] + C_{4m} \, \zeta_{my}^2 \, Cosh \, \zeta_{my} \, Cosh \, \zeta_{my} - C_{3m} \, \zeta_{my}^2 \, Cosh \, \zeta_{my} + C_{4m} \, \zeta_{my}^2 \, Cosh \, \zeta_{my}^2 \, Cos$$

By substituting  $y = \pm b$  in Equations 5.13 and 5.14 and comparing with Equations 5.7 and 5.8,  $C_{lm}$  and  $C_{4m}$  can be evaluated as follows:

$$C_{im} = \frac{2}{\zeta_m^2} \left[ \frac{A_m b + \zeta_m S_{inh} + \zeta_m b + b + \zeta_m C_{osh} + \zeta_m b}{(2b + \zeta_m + S_{inh} + 2\zeta_m b)} \right],$$

$$C_{4m} = \frac{2}{\zeta_m} \left[ \frac{B_m Sinh \zeta_{mb} - A_m Cosh \zeta_{mb}}{(2b\zeta_m + Sinh 2\zeta_{mb})} \right],$$

$$P_0 = -\frac{A_0}{2b}.$$
(5.15)

When  $C_{1m}$ ,  $C_{4m}$  and  $P_0$  are known the stress function  $\emptyset$  is completely known. From  $\emptyset$  the stresses, energy, displacements, slope, and curvature can be evaluated.

# Evaluation of Energy, Displacement, Slope and Curvature Formulas

The energy of a small segment of Figure 5.1 per unit length in the Y direction and unit length in Z direction can be written according to Equation 2.3 as

Energy = 
$$\frac{1}{2E} \int_{-h}^{h} [(\sigma_{x}^{2} + \sigma_{y}^{2} - 2M.\sigma_{x}\sigma_{y})] + 2(1+M) T_{xy}^{2} dx.$$
 (5.16)

Substituting Equations 5.12, 5.13, and 5.14 into Equation 5.16 and simplifying after integration, will reduce Equation 5.16 to

$$Energy = \frac{1}{2E} \left[ \int \frac{2P_{0}^{2}h^{3}}{3} + h \sum_{m=1}^{\infty} (c_{1m} c_{m}^{2} \cosh c_{m} c$$

From the energy formula the equivalent depth can be evaluated. The displacement, slope, and curvature can be evaluated by expressing the displacement derivatives in terms of stresses as follows:

$$e_x = \frac{\partial u}{\partial x}$$
,  $e_y = \frac{\partial v}{\partial y}$ ,  $\gamma_{xy} = \frac{\partial u}{\partial y} + \frac{\partial v}{\partial x}$  (5.18)

$$e_{x} = \frac{1}{E} (\sigma_{x} - M \sigma_{y}), e_{y} = \frac{1}{E} (\sigma_{y} - M \sigma_{x}), \gamma_{xy} = \frac{2(1+M)}{E} \tau_{xy}.$$
 (5.19)

After substitution of Equations 5.12, 5.13, and 5.14 into Equation 5.19, proper integrations are carried out to evaluate u and v. The results are written as,

$$U = \frac{1}{E} \left[ \frac{e_{x}^{2}}{2} - \sum_{m=1}^{\infty} (c_{im} \prec_{m} Cosh \prec_{my} + 2c_{4m} Cosh \prec_{my}) + c_{4m} \prec_{my} Sinh \prec_{my}) Cos \prec_{mx} \right]$$

$$+ C_{4m} \prec_{my} Sinh \prec_{my}) Cos \prec_{mx}$$

$$- \frac{\sum_{m=1}^{\infty} (c_{im} \prec_{m} Cosh \prec_{my} + c_{4m} \prec_{my} Sinh \prec_{my}) Cos \prec_{mx}}{-\frac{e_{y}^{2}}{2} (2 + M) + \alpha_{2}} ,$$

$$V = \frac{1}{E} \left[ -\sum_{m=1}^{\infty} (c_{im} \prec_{m} Sinh \prec_{my} + c_{4m} \prec_{my} Cosh \prec_{my} - c_{4m} Sinh \prec_{my} + 2c_{4m} Sinh \prec_{my}}{-M e_{xy} - M e_{xy} - M e_{xy} \sum_{m=1}^{\infty} (c_{im} \prec_{m} Sinh \prec_{my} + 2c_{4m} Sinh \prec_{my}) Sin \prec_{mx} + \alpha_{i}} \right] ,$$

$$\frac{\partial U}{\partial y} = \frac{1}{E} \left[ -\sum_{m=1}^{\infty} (c_{im} \prec_{m}^{2} Sinh \prec_{my} + 2c_{4m} \prec_{m} Sinh \prec_{my}}{-M e_{xy} \sum_{m=1}^{\infty} (c_{im} \prec_{m}^{2} Sinh \prec_{my} + 2c_{4m} \prec_{m} Sinh \prec_{my}} + c_{4m} \prec_{m}^{2} Cosh \prec_{my}) Cos \prec_{mx} - \sum_{m=1}^{\infty} (c_{im} \prec_{m}^{2} Sinh \prec_{my} + 2c_{4m} \prec_{m}^{2} Sinh \prec_{my}) \cos \prec_{mx} - \sum_{m=1}^{\infty} (c_{im} \prec_{m}^{2} Cosh \prec_{my}) \cos \prec_{mx} - \sum_{m=1}^{\infty} (c_{im} \prec_{my}^{2} Cosh \prec_{my}) \cos \prec_{mx} - \sum_{m=1}^{\infty} (c_{im} \prec_{my}^{2} Cosh \prec_{my}) \cos \prec_{mx} - \sum_{m=1}^{\infty} (c_{im} \prec_{my}^{2} Cosh \prec_{my}^{2} Cosh \prec_{my}^{2} Cosh \prec_{my}^{2} Cosh \prec_{my}^{2} Cosh \prec_{my$$

where  $a_1$  and  $a_2$  are constants. The center line deflection u, its slope  $\frac{\partial u}{\partial y}$  and curvature  $\frac{\partial u}{\partial y}$  can be evaluated from Equation 5.20 by substituting x = 0.

All results discussed above are in terms of  $C_{lm}$  and  $C_{4m}$  and  $P_0$ , which in turn depend on  $A_0$ ,  $A_m$ ,  $B_m$ , i.e. on the boundary conditions of the structure. In the following pages the problem will be discussed with specific boundary conditions. As in the previous chapter, the analysis of the column zone will be made with two sets of boundary conditions. One is the case of pure bending moment, and the second one will be of such a nature that there will be external shear forces.

#### II. PURE BENDING MOMENT CONDITION

### Boundary Conditions

as follows:

On 
$$y = \pm b$$
,  $\sigma_y = K_1 x$  from  $x = 0$  to  $x = \pm d$ , 
$$\sigma_y = 0 \quad \text{from } x = \pm d \text{ to } x = \pm h, \text{ and}$$
 
$$\sigma_{xy} = 0 \quad \text{from } x = 0 \text{ to } x = \pm h.$$

On  $x=\pm h$ ,  $\sigma_x= \tau_{xy}=0$  from y=0 to  $y=\pm b$ . Substitution of the boundary conditions of  $y=\pm b$ . into Equations 5.9, 5.10, and 5.11 for the Fourier coefficients yields the results that constants  $A_0$  and  $A_m$  are equal to zero, and

$$B_{m} = \frac{1}{h} \int_{-d}^{d} K_{1}x. \sin \kappa_{m}x. dx$$

$$= \frac{2K_{1}}{h\kappa_{m}^{2}} \left( \sin \kappa_{m}d - d\kappa_{m}\cos \kappa_{m}d \right) \qquad (5.21)$$

Now that  $A_0$ ,  $A_m$ , and  $B_m$  are known the constants of Equation 5.15 can be evaluated.  $P_0$  will be zero in this case. Equation 5.12 yields  $\sigma_{\mathbf{X}}$  equal to zero on  $\mathbf{X} = \underline{+} \mathbf{h}$ . There are shearing stresses  $\overline{\phantom{A}}_{\mathbf{X}}$  on  $\mathbf{X} = \underline{+} \mathbf{h}$ , which are numerically insignificant.

## Evaluated Results

As the stress function has been assumed in the form of an infinite series, all functions related to it will be infinite series. In practice one takes enough terms of the series to give reasonable results. With discontinuous values of  $\sigma_y$  and  $\sigma_y$  assumed, the coefficients  $\sigma_y$  and  $\sigma_y$  assumed, the coefficients  $\sigma_y$  and  $\sigma_y$  assumed. The coefficients  $\sigma_y$  and  $\sigma_y$  and  $\sigma_y$  and  $\sigma_y$  assumed. The coefficients  $\sigma_y$  and  $\sigma_y$  will be of the order  $\sigma_y$  the coefficients of the trignometric functions in the series for the stresses will be of order  $\sigma_y$ . Hence, convergence is assured for all interior points (where  $\sigma_y$  is less than b).

The convergence on the face y = b is known for the series for y and y because these series reduce to the boundary expansions, and the 50 term partial sum represents quite accurately the given boundary stress distribution, as shown by Figure 5.2. The series for the displacement components and the series for the energy are more rapidly convergent and converge also on y = b, while the series for the slope is of the same order as that for the stresses. The coefficients in the series for the curvature are of the order x = (b-|y|)x, giving slower convergence in the interior and not converging at all on the face. In view of the above discussion, all calculations in this chapter have been carried out with at most x = 50.

Due to repetition of the arithmetic process for all functions, all computations in this chapter were carried out with the MISTIC computer. Various programs were prepared in the floating decimal form. The programs were designed in such a way that the dimensions of the cross shape are variable parameters. The program for the evaluation of the energy is given in Appendix C as an example.

In the case of the pure bending moment loading, according to the conclusions in Chapter II, the stresses on the face of the column will be independent of the beam span  $L_2$  (Figure 3.3), and the height of the column for L/b and h/d greater than 1.3 and 2.0, respectively. Hence, for the analysis of the mode of the stress distribution in

the column portion of the joint the only variables are b, d, and h. Two independent dimensionless parameters can be formed from these variables, say b/h and d/b. As an example, for b = d = 0.42856h all quantities discussed above are evaluated. Stresses are recorded in Table 5.1 and bending stress  $\sigma_y$  is plotted in Figure 5.2. The energy and the equivalent depth results are given in Table 5.2. The displacement u, slope , and curvature for the beam center line (Y-axis) are recorded in Table 5.3 and presented graphically in Figure 5.3. Equivalent depth based on center line curvature is calculated by M = EI This equivalent depth is recorded in the last column of Table 5.3. The two equivalent depth curves calculated on the energy and center line curvature concepts are plotted in Figure 5.4. Figure 5.4 indicates that the equivalent depth based on the curvature is nowhere near that based on the elastic energy. Hence, an energy calculation derived from the equivalent depth based on center line curvature would be greatly in error. To study the effect of the various ratios of the b and d dimensions of the cross shape on the equivalent depth inside the column, equivalent depths are evaluated for different proportions of b and d and are presented in Table 5.4 and in Figures 5.5 and 5.6

#### Discussion of Results

The deflection u at the face of the column can be made zero by selecting the constant ap in the deflection

Equation 5.20 as 0.203703. Comparison of the deflection and the slope diagrams indicates that the deflection is fairly constant in the central half of the column. Hence, the slope in that region is almost zero compared with the slope in the vicinity of the face of the column.

The equivalent depth diagrams inside the column calculated by the numerical method of Chapter IV and one calculated by the series method of the chapter (Table 5.2) are plotted in Figure 5.7 for comparison. From a study of Figure 5.7a it is concluded that the shape of the equivalent depth diagram for the case with the fillet agrees closely with the one calculated by series application in the middle 2/3 width of the column. But the value of the equivalent depth does not agree. These two curves can be made to coincide (within 7%) by adding a constant amount to all of the ordinates of the series method curve, raising or lowering it enough to make the two curves agree at one point. This suggests that the shape of the stress distribution in that region at various sections is not altered by replacing the true stress distribution on the face of the column of the cross shape by a linear stress distribution  $\sigma_{v}$  on the face of the column. The equivalent depth diagram in the outer 1/3 portion of the column does not agree because in the case of the cross shape with the fillet the stress is distributed over more than the depth of the beam. Hence, the contact area for transferring the

stresses from the beam to the column is not the same in two cases. Also in Figure 5.7b there is agreement in the shapes of the curves in the middle half of the column. Comparison of the results of Figures 5.7a and 5.7b indicates that the portion of the column in which there is disagreement is the same in both cases. Hence, it is concluded that even though the R value (the ratio of the equivalent depth de to the actual depth 2d of the beam), is different at the face of the column in the two cases of Figures 5.7a and 5.7b due to difference in stress concentration, the stress concentration factor does not disturb the mode of stress distribution inside the column away from the face of the column. In otherwords, the local stress concentration effect does not extend to the entire width of the column.

The suggested identity of stress distributions, based on the agreement in the shape of the equivalent depth diagrams in the middle 2/3 portion of the column can be checked by comparing the stress distributions in that region calculated by the numerical method and by the series method. As the stress contributes most of the energy, only stresses are compared. Comparison of Figure 4.4 with Figure 5.2 shows the agreement of the mode of stress distribution in the middle 2/3 of the column.

The shape of the equivalent depth diagram calculated by the numerical method for a cross shape without fillets

agrees closely with that calculated by the series method throughout the column width as can be seen from Figure 5.7. This again supports the argument presented in Chapter IV that the true stress distribution existing at the face of the column of the cross shape subjected to pure bending moment loading condition can be replaced by a linear stress distribution without altering the mode of stress distribution throughout the width of the column. The application of series results in combination with the numerical method will be discussed in Part IV.

Comparison of results in Table 5.4 for b = d = 0.42856h with those for b = d = 0.2h indicates that when the ratio d/b remains constant, the height of the column does not have any effect upon R. Indirectly this supports the conclusion of interaction limit in the column given in Chapter III. Of course, this lack of dependence on the height of the column has some limitation. This can be seen by taking d = h. The ratio R at all sections inside the column will be 1.0 as is shown by the conventional beam theory and not the one calculated in Table 5.4. With the help of the conclusion in Chapter III, about the interaction limit in the column it can be concluded that when d is greater than 0.5h, then the equivalent depth information in Table 5.4 cannot be used. The lack of dependence of R on the height of the column can be observed by comparing

the results of b = 0.42856h, d = 0.3h (d/b = 0.70) with the results for b = 0.3h, d = 0.2h (d/b = 0.667). Of course, the results for the ratio R in the two cases do not agree closely because d/b ratios are a little different in the two cases, but the trend is apparent. Here also there will be a limit to the lack of dependence on the height. In general for any d/b ratio if d exceeds 0.5h, then the ratio R will no longer be independent of the height. As d varies from 0.5h to d the ratio R will approach the value 1.0.

In Figure 5.5 the depth d of the beams is kept constant and equal to 0.2h and the column width is varied. As the width of the column is increased the equivalent depth curve becomes steeper attaining different maximum equivalent depths. This is due to the fact that as the column becomes wider there is more transition zone available and consequently the stress distribution curve at any particular beam section becomes flatter. It is to be noted that all the curves coincide near the face of the column. They spread out as they approach the center line of the column. In Figure 5.6 the width of the column is kept constant and the depth of the beam is decreased. The same characteristics are observed as in Figure 5.5.

# III. VARIABLE BENDING MOMENT CONDITION (SHEAR-LOADING CASE)

A cross shape subjected to shear loading by a shear force V having a parabolic distribution on the ends of the beam and a uniform normal stress distribution on the top and the bottom ends of the column as shown in Figure 4.14 will be replaced by a column acted upon by the shear force V on the face of the column and the bending moment M = VLas shown in Figure 5.1, where I is the span length of the Since it was concluded in Chapter IV that on the face of the column the assumption of uniform shear stress distribution due to shear force V will be better than the assumption of a parabolic distribution, a uniform stress distribution is assumed in the following analysis. bending stress distribution is assumed to be linear. assumption will not alter significantly the mode of stress distribution inside the column. The analysis of this case can be done by the application of results derived in Part I. For this the constants  $A_{\mathcal{I}}$ ,  $A_{m}$ , and  $B_{m}$  are to be evaluated by using the boundary conditions.

## Boundary Conditions

If the shear stress  $\mathbf{Z}_{xy}$  is given by  $-K_2(d^2 - x^2)$  on the end of the beam, then the moment M acting on the face of the column is equal to (4/3)  $K_2d^3L$ . The boundary conditions are summarized as follows:

On 
$$y = \pm b$$
,  $\sigma_y = 2K_2Lx$  from  $x = 0$  to  $x = \pm d$  and  $\sigma_y = 0$  from  $x = + d$  to  $x = + h$ .

$$\mathbf{z}_{xy} = (2/3) \ \text{K}_2 \text{d}^2 \ \text{from} \ x = 0 \ \text{to} \ x = \pm \ \text{d} \ \text{and}$$

$$\mathbf{z}_{xy} = 0 \ \text{from} \ x = \pm \ \text{d} \ \text{to} \ x = \pm \ \text{h}.$$
On  $x = + \ \text{h}$ ,  $\mathbf{z}_{xy} = 0 \ \text{and}$   $\mathbf{z}_{xy} = (2/3) \ \text{K}_2 \text{d}^3 / \text{b} \ \text{from} \ y = 0 \ \text{to}$ 

$$y = \pm \ \text{b}.$$
On  $x = - \ \text{h}$ ,  $\mathbf{z}_{xy} = 0 \ \text{and}$   $\mathbf{z}_{xy} = (2/3) \ \text{K}_2 \text{d}^3 / \text{b} \ \text{from} \ y = 0 \ \text{to}$ 

y = + b.

By using these boundary conditions in the Formulas 5.9, 5.10 and 5.11 for Fourier coefficients,  $A_{\rm O}$ ,  $A_{\rm m}$ , and  $B_{\rm m}$  are evaluated. Hence, the constants  $C_{\rm lm}$  and  $C_{\rm lm}$  are known, and the stress function is known.

### Evaluated Results

It is to be noted that the parameters in the stress function  $\emptyset$  will be b, d, L, and h. All these parameters will affect the energy. The equivalent depth as defined in Part III of Chapter IV is calculated with various ratios of b, d, and L to h. In Table 5.5 the results are recorded for the case in which L is kept constant at the value 0.57143h, and b and d are variables. In Table 5.6 the results are recorded for the case in which b and d are kept constant at 0.42856h and L is a variable. In Figure 5.8 the equivalent depth calculated for the case of b = d = 0.42856h and L = 0.57143h is plotted. Also in this figure

are plotted the results of equivalent depth calculated by the numerical method for shear-loaded joints both with and without fillets. In Figures 5.9 and 5.10 part of the results from Table 5.5 are plotted. Figure 5.11 represents the results of Table 5.6.

### Discussion of Results

Figure 5.8 indicates that for joints with fillets the shape of the equivalent depth curve as calculated by the series method agrees closely in the middle 2/3 of the column with that determined by the numerical method. Hence, the true mode of stress distribution at various sections inside the column is not altered by replacing the true stress distribution at the face of the column by the linear distribution of  $\sigma_y$  and uniform distribution of  $\tau_{xy}$ . The difference due to contact area on the face of the column brings out the disagreement near the face.

In the case of the joint without fillets the shape of the equivalent-depth curve as calculated by the numerical method agrees only in the middle half of the column width with that calculated by the series method. The agreement in the shear loading case is not as good as in the case of pure bending. This means that in the case without fillets the shear stress distribution due to shear force V is different from the assumed uniform one.

Figure 5.9 shows the curves of equivalent depth in which d and L of the cross shape are kept the same and b is varied. The behavior is the same as in the case of the pure bending moment. The reasoning given for this behavior in the case of pure bending moment applies here too. Figure 5.10 shows the curves in which b and I are kept constant and d is varied. The effect is the same as in Figure 5.9. Comparison of Figures 5.5 and 5.9 indicates that for b = d = 0.2h the curves for the pure bending moment case and the shear loading case are almost the same, and the variation with b/d is similar in the two cases. Although the agreement is not so close for larger values of b/d as it is for b/d = 1.0. Figures 5.6 and 5.10 indicate that for b = d = 0.42856h, the curves are not the same for the two cases of loading. The curve in the shear-loading case is steeper, and it is expected that the disagreement would even be greater for larger values of b/d. Concluding, as d increases with respect to h, the pure bending moment and shear-loading case curves spread apart. This conclusion can also be drawn from Tables 5.4 and 5.5. The agreement of the equivalent depth curves in the case of pure bending moment and the case of shear loading for d = 0.2h can be explained as follows: The relatively high loss of energy in the case of shear loading is offset by the energy due to uniform normal stress  $\sigma_{\mathbf{x}}$  existing in the column. For long columns (small d/h) this energy in the column due to

will be a significant part of the total whereas it will not be so significant for short columns.

The equivalent depth de is found by solving the equation  $M^2/2EI + 1.2 V^2/2GA = Elastic energy, in which I$ and A are expressed in terms of de. In the case of shear loading the bending moment on a section is a linear function of the beam span length. As the beam span length becomes larger, the effect of shear becomes smaller and the equivalent depth as calculated in the shear case will approach the one for the case of pure bending moment. This fact is observed by noticing the trend of the equivalent-depth curve as L increases, Figure 5.11. Comparing the results of the equivalent depth for the case of b = d = 0.42856hand L = 9.14288h from Table 5.6 with the one of the pure bending moment case with b = d = 0.42856h shows that the equivalent depth values for these two cases differ by less than 2.0%. Similar behavior is to be expected also for other ratios of b/h and d/h, so that the results given in Table 5.5 approach those in Table 5.4 as L increases. It was shown previously that for d = 0.2h the equivalent depth curves in pure bending and shear loading case are almost the same. Hence, for that particular d/h ratio, L is not important, but as d/h increases, L will be significant as far as agreement between pure bending and shear loading is concerned.

# IV. INTERPRETATION OF RESULTS OF SERIES METHOD AND NUMERICAL METHOD

#### A. Pure Bending Moment

It was noted in Part III of Chapter IV that the true stress distribution on the face of the column can be replaced by a linear stress distribution having a maximum stress  $FK_1d$ , where F is a correction factor. It was also noted that the series-method solution with assumed linear distribution having maximum  $\sigma_v$  stress equal to  $\kappa_1 d$  results in a shape of the equivalent depth diagram similar to that obtained from the numerical solution in most of the column. Hence, the value of the correction factor F is to be selected in such a way that equivalent depths at the column face as calculated by the numerical method and the series method are the same. Concluding, as far as the shape of the equivalent depth curve is concerned the equivalent depth as calculated by the series method can be used for all purposes. Hence, the equivalent depth curve inside the column can be plotted by selecting the proper curve of the series method and locating this curve by raising or lowering it enough to have at the face of the column the proper value of the ratio R as calculated by the numerical method (1.16 in case of r/d = 1/3 and 1.10 in case of r/d = 0). These values of the ratio R of equivalent depth to the actual depth are discussed in Part III of Chapter IV.

### B. Variable Bending Moment (Shear-Loading Case)

As in the case of pure bending moment, the series method results in the shear case also can be used in combination with the results of the numerical method. In the shear-loading case the R value at the face of the column will depend upon the proportional contribution of the shear energy due to shear force to the total energy. According to the type of the loading, the R value will depend upon the beam span length as discussed in Chapter IV. By selecting the proper R value at the face of the column and combining it with the proper curve of the series mentod, depending upon d, b, and L values, the equivalent depth diagram can be constructed.

# V. APPROXIMATION OF RESULTS IN FORM CONVENIENT FOR USE IN DESIGN

The correct equivalent depth diagram inside the column can be constructed for any d, b, and L proportions of the joint by the approach discussed in the preceding pages. The results indicate that the equivalent depth diagram depends upon the loading condition and proportions of the joint. Hence, for precise calculations an extensive set of curves must be prepared which can be used by the designer. This can be done by constructing the various sets of curves for different proportions of the joint and

different types of loading, by the series method, and combining these results properly with the values of R at the face of the column evaluated by the numerical method. For practical purposes, however, an approximate equivalent depth diagram has been constructed as explained in the following paragraph which can be used for all proportions and any kind of loading without introducing any serious error.

First the selection of the R value at the face of the column will be considered. For pure bending-moment loading it was concluded in Chapter IV that for practical purposes the R value at the face of the column could be taken as 1.16 for d/b less than 2.3 and r/d = 1/3. In the case of the shear loading for r/d = 1/3 and d/b = 1.3, the R value was found to be 1.07. As the span becomes larger, the R value at the face of the column approaches the value for the case of the pure bending moment. r/d = 0, R at the face is 1.10 in the case of the pure bending moment and 0.9242 in the case of shear loading. In all these cases the ratio of the span length L to the beam depth 2d was 0.667. In all practical problems this ratio is greater than 2.3. Hence, for values of I/2dgreater than 2 the R value at the face of the column in the case of shear loading will be between 1.37 and 1.16 for r/d = 1/3 and between 0.9242 and 1.10 for r/d = 0. In view of the previous discussion it is suggested that if the

R value at the face of the column is taken as 1.3 for r/d = 0 and as 1.10 for r/d = 1/3, for any kind of loading and any joint proportions, it will not introduce any significant error, keeping in mind the many uncertainties in design practice.

The equivalent-depth curves calculated by the series method are approximated by dashed straight lines in Figures 5.5, 5.6, 5.9, and 5.10. The angles which these lines make with the horizontal line are noted. In the case of pure bending for d = 0.2h, as the column width b increases from 3.2h to 3.42856h the angle  $\beta$  which the approximating line makes with the horizontal line increases from 20 degrees to 31 degrees. In the case of the shear loading for d = 0.2h it varies from 22 degrees to 35 degrees. In Figures 5.5 and 5.9 the ratio of the beam span length L to the beam depth 2d is 1.428. Almost all practical problems will have this ratio greater than 2.0. As the ratio L/2d increases the approximate equivalent depth lines in the case of the shear loading will approach to the pure bending moment case. This behavior has been discussed before. In view of the results of Figures 5.5 and 5.9 it can be generalized that for any kind of loading and beam span length the approximate equivalent depth line will be at an angle 3 varying from 20 to 35 degrees for the ratio of d/b = 1.0 to d/b = 0.4667.

For b = d = 0.42856h, which might be the most extreme case, angle paries from 20 degrees for the pure bending moment case to 30 degrees for the shear-loading case. In reality b will not be greater than 0.42856h. It can be inferred from Figures 5.5 and 5.9 that for b smaller than 0.42856h and d = 0.42856h, will be smaller than 20 degrees for the pure bending case and smaller than 30 degrees for the shear loading case. Concluding, it is suggested that the angle be taken as 30 degrees for any kind of loading and practical proportions of the cross-shaped joint of the frame structure.

The error involved in the suggested approximate equivalent depth line is examined by comparing the total energy inside the joint, which is evaluated by the true and approximated equivalent depth curves for the cross shape having b = d = 0.42856h. (The true energy is evaluated from the results of Chapter IV.) For the pure bending moment case these errors are 10.8% and 5.6% for the case of r/d = 1/3 and r/d = 0, respectively. For the shearloading case these are 8.75% and 5.32%, respectively. It is of interest to contrast this small error introduced by the approximation with much larger error introduced by the two assumptions in common practice. As was pointed out in Chapter I, the two assumptions that have been made are either (1) that the effective depth in the column is equal to the depth at the face of the joint or (2) that

the moment of inertia is infinite in the column zone. For b=d=0.42856h and r/d=0, the true total energy inside the joint is  $0.333\,K_1^2\,d^4/2E$  or  $3.75\,K_2^2\,d^6/2E$  for pure bending moment or shear-loading cases, respectively. The total energy, calculated by assuming that the equivalent depth at any section inside the joint is the same as that at the face, is  $0.6667\,K_1^2\,d^4/2E$  or  $8.12\,K_2^2\,d^6/2E$ , for pure bending moment or shear-loading cases, respectively. The total energy calculated by assuming infinite moment of inertia inside the joint is zero in both cases. The error involved in either of the present practices is about 100%. It is to be noted again that this error will be significant for frame structures only when the spans of the beams are small.

TABLE 5.1

STRESSES FOR A COLUMN HAVING b = d = 0.42856h

SUBJECTED TO PURE BENDING MOMENT

Stress values are to be multiplied by  $K_1h$ .

<u>у</u> Б	<u>x</u> d	<b>o</b> y	$\sigma_{\rm x}$	<b>て</b> xy
Э	0 2/8 4/8 6/8 7/8 1 10/8 12/8 14/8 16/8 7/3	0.00000 0.08626 0.14975 0.17138 0.16442 0.14770 0.09925 0.05374 0.02408 0.02879	0.00000 -0.02962 -0.05052 -0.05392 -0.04789 -0.013784 -0.01372 0.00372 0.00984 0.00791 0.00000	0.0000 0.0000 0.0000 0.0000 0.0000 0.0000 0.0000 0.0000
2/8	0 2/8 4/8 6/8 7/8 1 10/8 12/8 14/8 16/8	0.00000 0.09034 0.15862 0.18203 0.17283 0.15188 0.09501 0.04770 0.02021 0.00000	0.00000 -0.02640 -0.04646 -0.05060 -0.04427 -0.03329 -0.00816 0.00689 0.01026 0.00733	0.02981 0.02609 0.01357 0.00711 -0.01708 -0.02362 -0.0235 -0.01057 -0.0057 -0.0064 0.00450
4/8	0 2/8 4/8 6/8 7/8 1 10/8 12/8 14/8 16/8	0.00000 0.09987 0.18272 0.21677 0.20135 0.16434 0.07786 0.02995 0.01068 0.00329 0.00000	0.00000 -0.01263 -0.02713 -0.03577 -0.03041 -0.01710 0.00847 0.01216 0.00791 0.000000	0.05081 0.04629 0.02793 -0.01252 -0.03618 -0.05147 -0.04134 -0.01411 0.00201 0.00877 0.01100

TABLE 5.1 (Continued)

<u>x</u> b	<u>x</u> d	σy	σ <sub>x</sub>	τ <sub>xy</sub>
6/8	0 2/8 4/8 6/8 7/8 1 10/8 12/8 14/8 16/8	0.00000 0.10694 0.20860 0.28096 0.26874 0.18499 0.03471 0.00761 0.00205 0.00000	0.00000 0.02131 0.03291 0.01963 0.00958 0.02094 0.02438 0.00055 -0.00687 -0.00580 0.00000	0.04739 0.04621 0.03754 -0.00310 -0.04955 -0.08767 -0.03852 -0.00414 0.00636 0.00950 0.01029
7/8	0 2/8 4/8 6/8 7/8 1 10/8 12/8 14/8 16/8 7/3	0.00000 0.10748 0.21401 0.31301 0.33381 0.19847 0.00822 0.00131 0.00030 0.00002	0.00000 0.04669 0.08807 0.10026 0.07197 0.05768 0.00352 -0.02189 -0.02113 -0.01325 0.00000	0.03077 0.03046 0.02949 0.01235 -0.03123 -0.11015 -0.01587 0.00187 0.00560 0.00645 0.00654
1	2/8 4/8 6/8 7/8 1 10/8 12/8 14/8 16/8	0.00000 0.10326 0.21787 0.32533 0.38284 0.21141 -0.00356 -0.00280 0.00237 -0.0058 0.00000	0.00000 0.07025 0.15851 0.25084 0.30553 0.13424 -0.07304 -0.05739 -0.03629 -0.02219 0.00000	0.00000 0.00000 0.00000 0.00000 0.00000 0.00000 0.00000 0.00000

TABLE 5.2

ENERGY AND RATIO R FOR A COLUMN HAVING b = d = 0.42856h SUBJECTED TO PURE BENDING MOMENT

<u>у</u> Б	Energy	Ratio R = $d_e/2d$
0.0	0.025299	1.2756
0.1	0.025689	1.2687
0.2	0.026852	1.2513
0.33333	0.029535	1.2117
0.4	0.031403	1.1867
0.5	0.034345	1.1517
0.6	0.037616	1.1172
0.6	0.039762	1.0969
0.6667	0.043730	1.0627
0.8	0.047361	1.0347
0.9	0.061145	0.9503

TABLE 5.3

CENTER LINE DEFLECTION u, SLOPE CURVATURE
; AND RATIO R BASED ON CURVATURE\*

<u>у</u> b	Deflection	Slope <u>ðu</u>	Curvature	Ratio R Based on Curvature
0.0	0.029031	0.00000	-0.175401	1.7855
0.1	0.028868	-0.007766	-0.193022	1.7303
0.2	0.028342	-0.017082	-0.247946	1.5917
0.33333	0.026898	-0.047328	-0.387464	1.3716
0.4	0.025731	-0.047328	-0.490688	1.2679
0.5	0.023195	-0.107267	-0.694452	1.1292
0.6	0.019373	-0.138319	-0.963117	1.0127
0.6667	0.015872	-0.219948	-1.179628	0.9464
0.8	0.005776	-0.301710	-1.693661	0.8389
0.9	-0.005336	-0.410173	-2.123542	0.7780

<sup>\*</sup>Deflection, slope, and curvature are to be multiplied by  $\rm K_1h^2/E$  ,  $\rm K_1h/E$  , and  $\rm K_1/E$  , respectively.

TABLE 5.4

VALUES OF RATIO R FOR VARIOUS b, d, AND h. PURE BENDING MOMENT CONDITION

ئم						
on b=0 6h d=0	o.3h	b=0.42856h d=0.2h	b=0.28556h .d=0.42856h	b=0.3h d=0.2h	b=0.2h d=0.2h	b=0.1h d=0.2h
	.545	1 %	.127	.595	.278	
	.529	.041	.125	.578	.272	.077
	. 485	.952	.124	.530	.252	.075
	.395	.770	901.	.429	.212	.069
	1.3438	1.6679	1,0091	1.3735	1.1890	1.0659
	.264	.538	.086	. 285	.152	.059
	.189	.355	.073	.203	.117	.053
	.145	.264	.065	.155	.097	.048
	.078	.120	67C.	.081	.062	.039
	.037	.050	.033	.038	.033	.032
03	.873	.912	.980	.926	.954	.973

TABLE 5.5

VALUES OF RATIO R FOR VARIOUS b, d, and h KEEPING L CONSTANT, SHEAR LOADING CONDITION

L = 0.57143h for all following cases

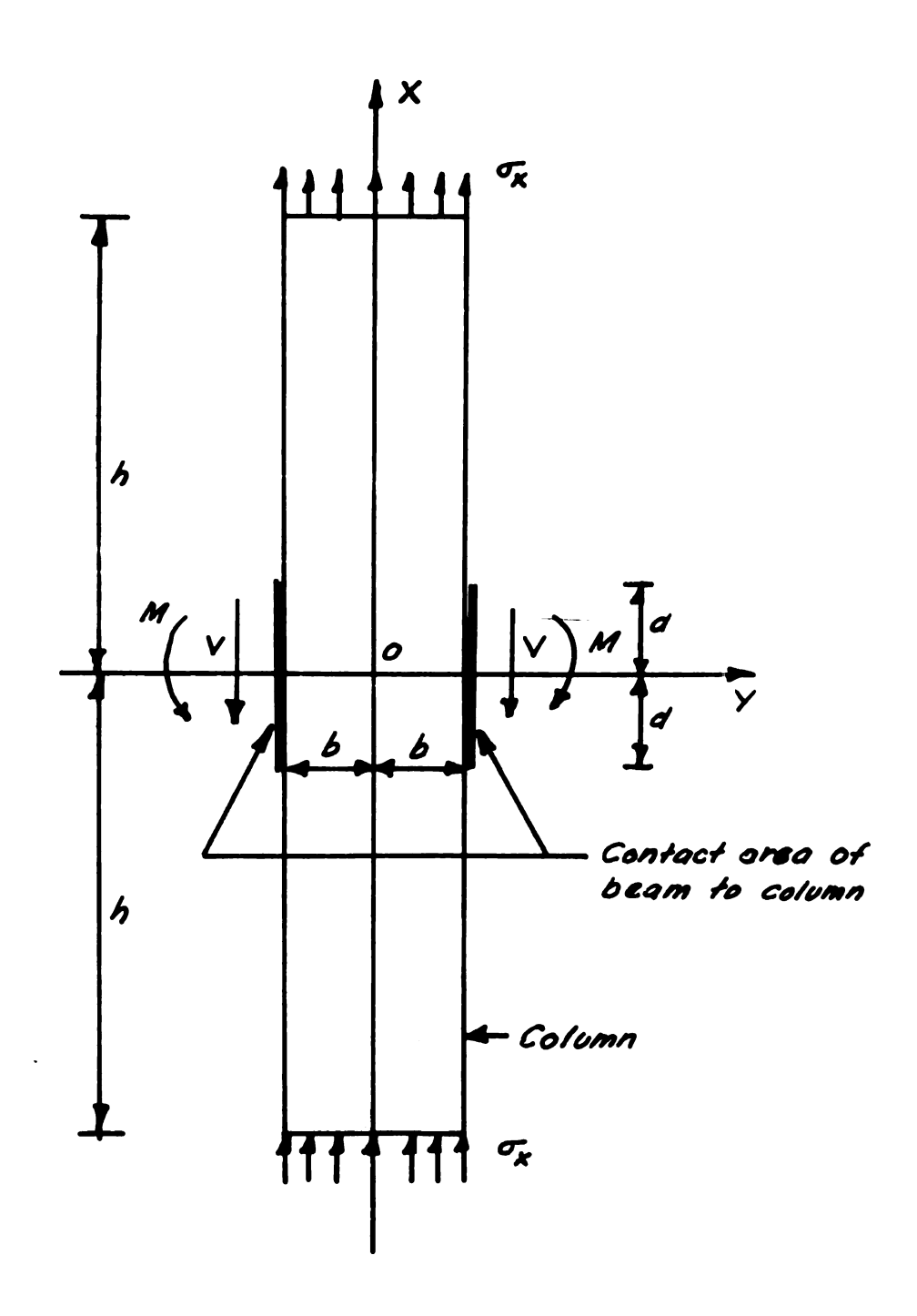
م <b>ا</b> د	b=0.42856h d=0.42856h	b=0.42856h d=0.3h	b=0.42856h d=0.2h	b=0.2h d=0.2h	b=0.1h d=0.2h
0.0 0.1 0.3333 0.5 0.6667 1.0	1.3878 1.3807 1.3600 1.2852 1.2358 1.1411 0.9576 0.8048	1.6852 1.6702 1.6271 1.5356 1.4799 1.3004 1.2420 1.1269 1.0213	2.2620 2.2313 2.1438 1.9597 1.6735 1.1991 1.0731 0.8437	1.2835 1.2749 1.2587 1.2836 1.1663 1.1284 0.9949 0.8831	0.9454 0.9446 0.9446 0.9481 0.9364 0.9385 0.9385 0.8943 0.8943

TABLE 5.6

VALUES OF RATIO R FOR DIFFERENT SPAN LENGTHS L, KEEPING b, d, and h CONSTANT, SHEAR LOADING CONDITION

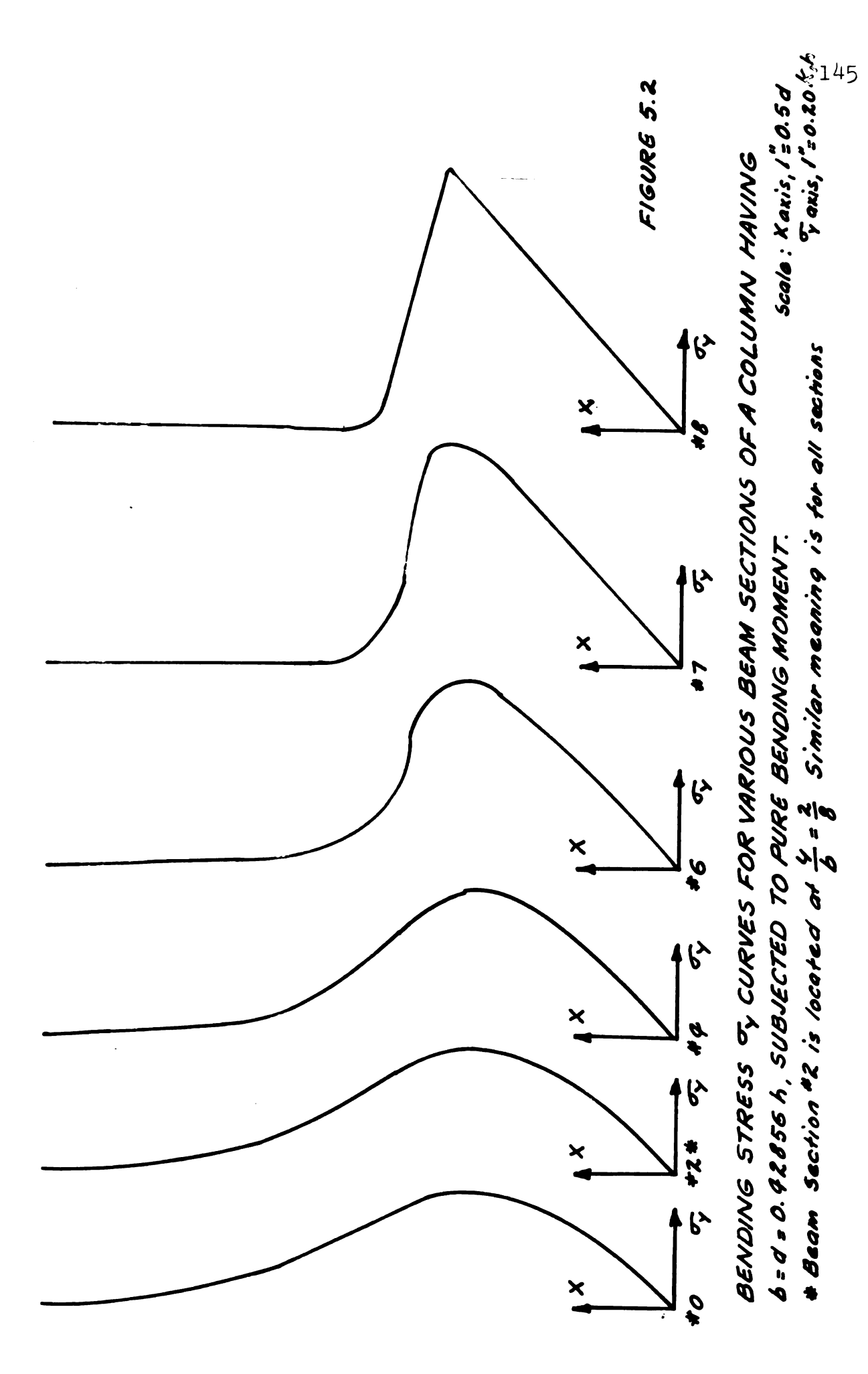
b = d = 0.42856h for all following cases

$\frac{V}{C}$	L=0.57143h	L=1.14286h	L=2.28572h	L=4.57144h	L=9.14288h
0.0 0.0 0.3333 0.5 0.6667 0.9	3878 3807 3143 2858 1858 1411 8576 9576	1.3742 1.3673 1.3461 1.8731 1.1502 1.0819	1.3376 1.3335 1.3335 1.2671 1.1987 1.1326 1.0832 0.9287	1.3029 1.8029 1.2833 1.2419 1.1781 1.0781 1.0388	1.2933 1.2867 1.2867 1.2031 1.1055 1.0696 1.0374 0.0374

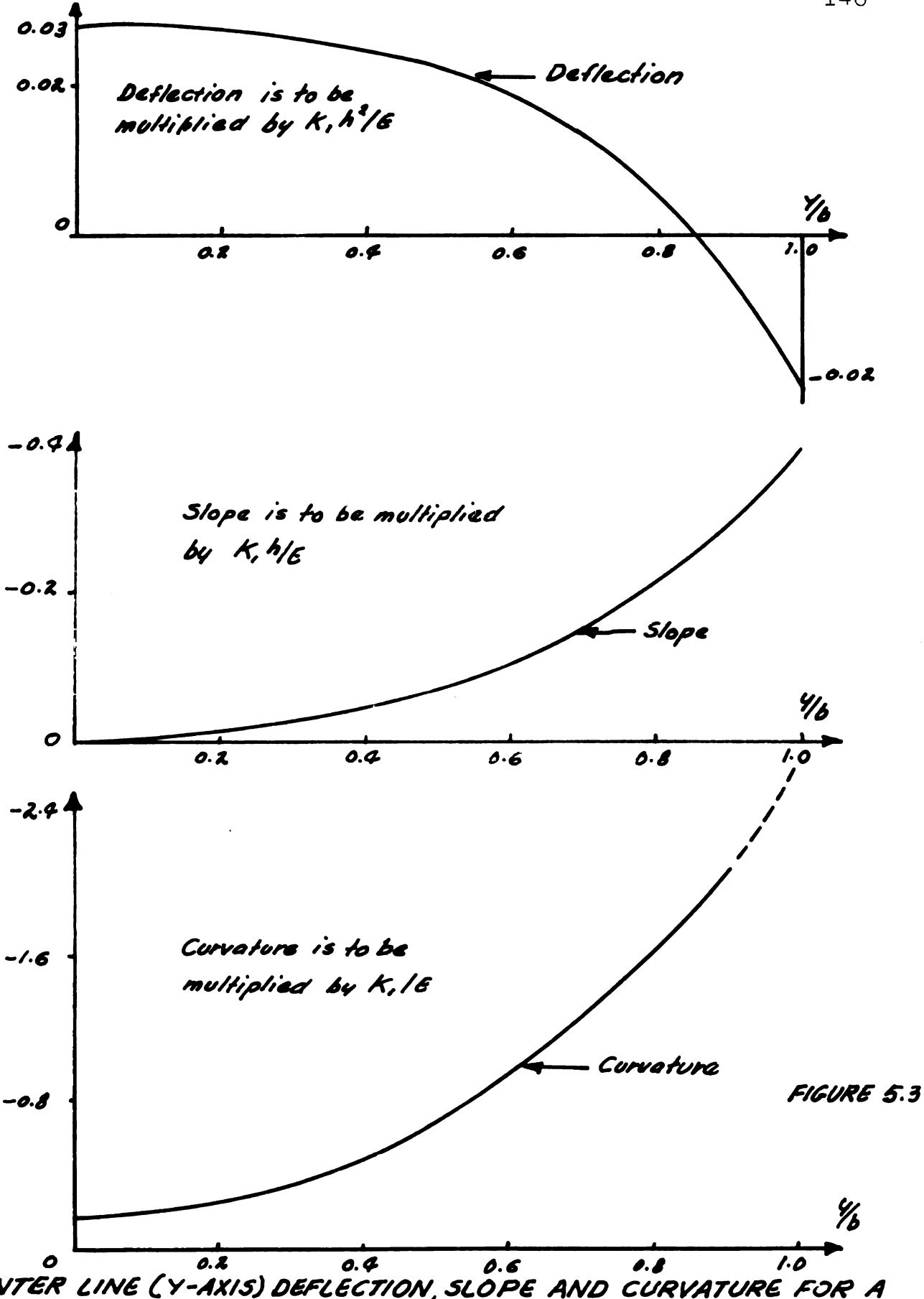


BOUNDARY FORCES ON THE COLUMN

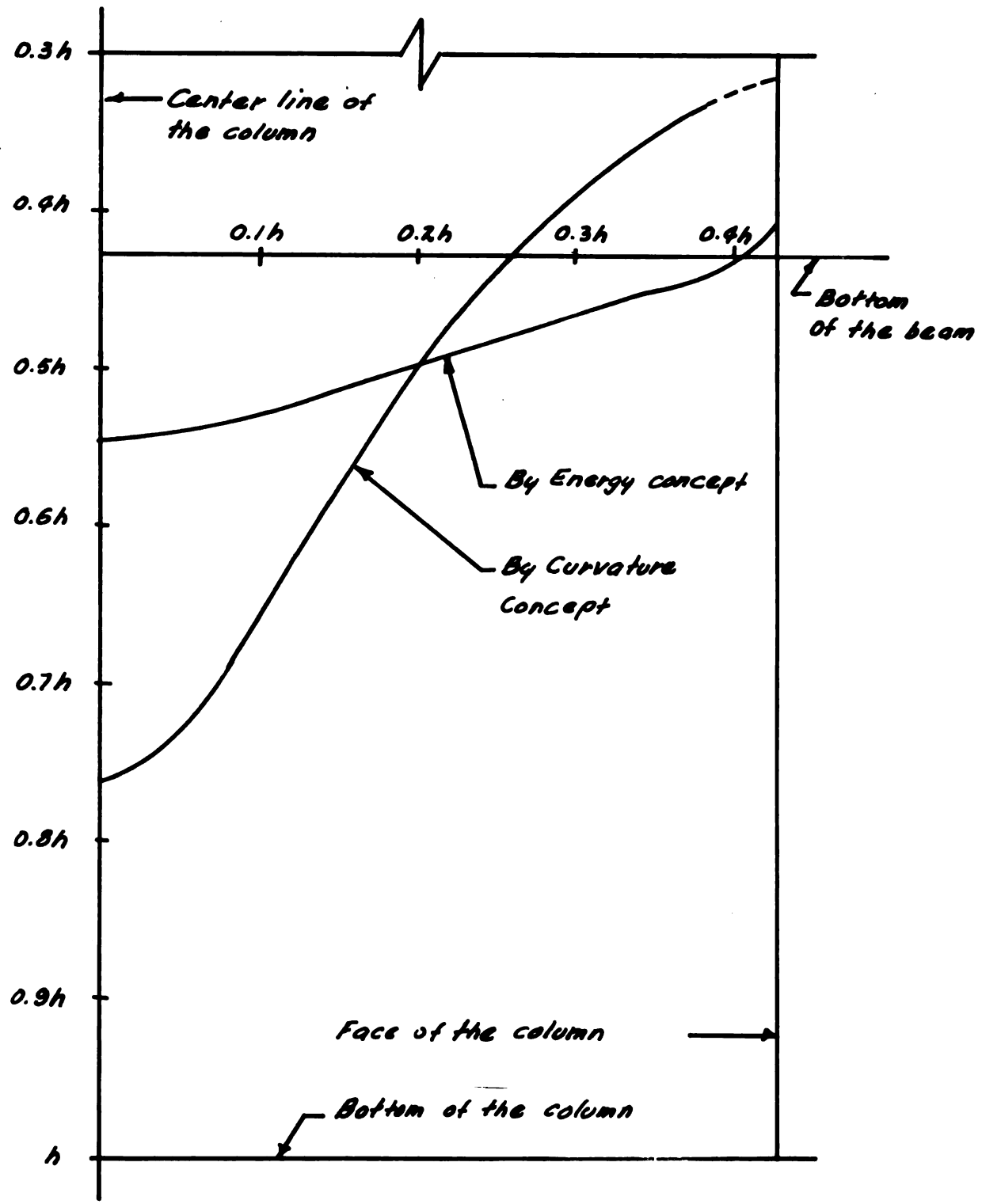
FIGURE 5.1







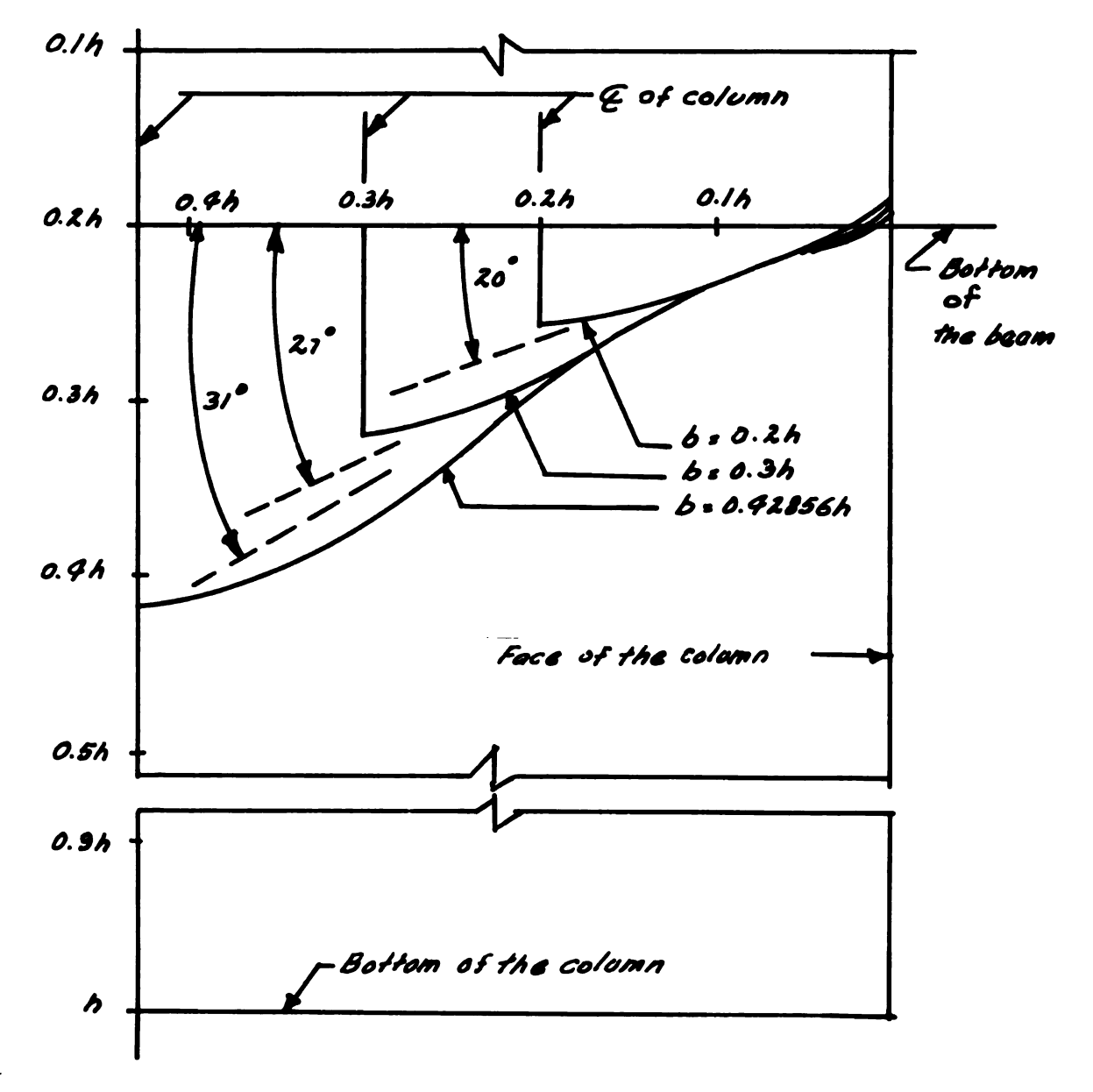
CENTER LINE (Y-AXIS) DEFLECTION, SLOPE AND CURVATURE FOR A
COLUMN HAVING 6:4:0.428564 SUBJECTED TO PURE BENDING MOMENT



EQUIVALENT DEPTH AS CALCULATED BY ENERGY AND CURVATURE

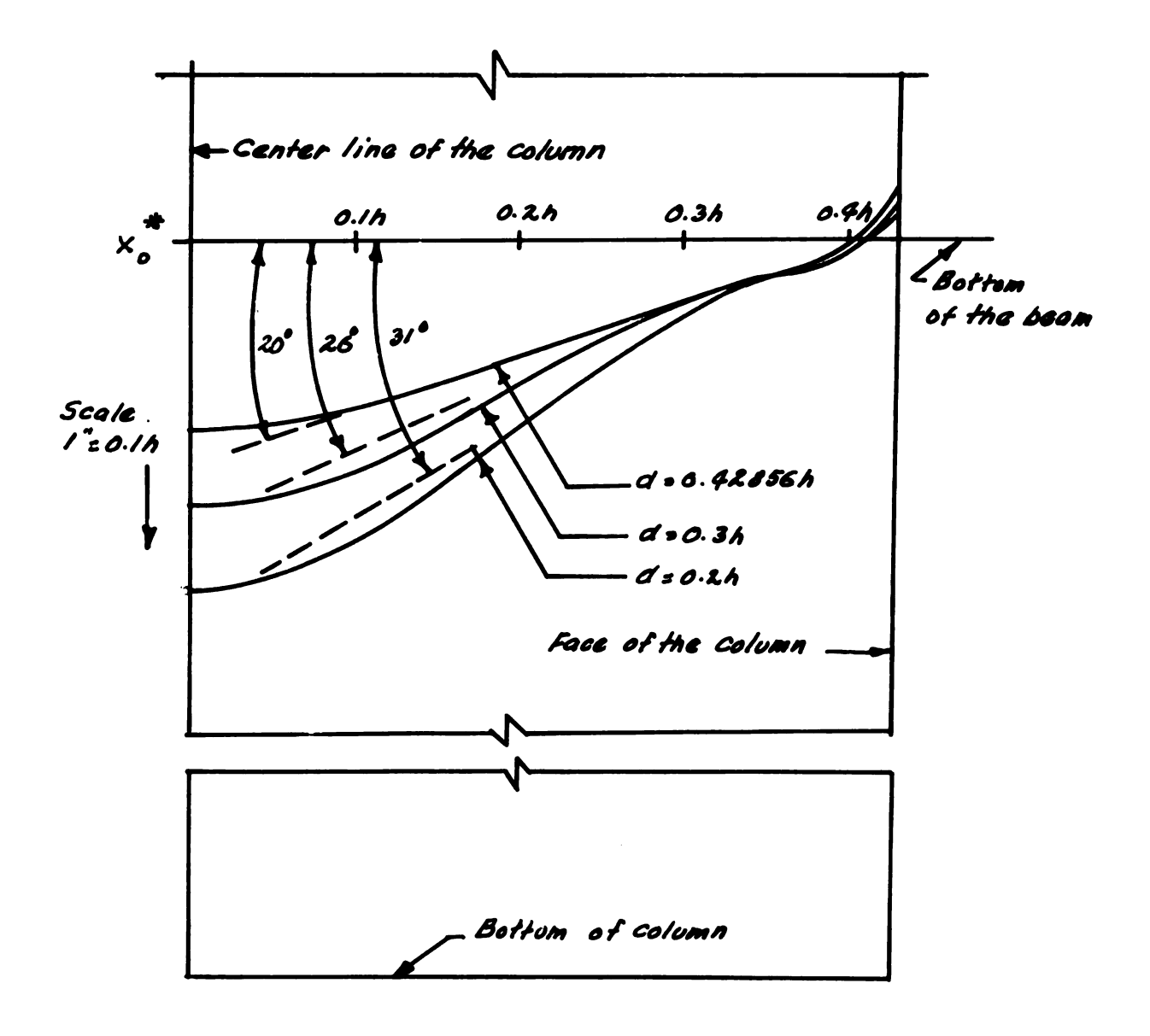
CONCEPTS FOR b=d=0.42856 h. (PURE BENDING MOMENT)

FIGURE 5.4



NOTATION: --- TRUE EQUIVALENT DEPTH CURVE
---- APPROXIMATED EQUIVALENT DEPTH LINE

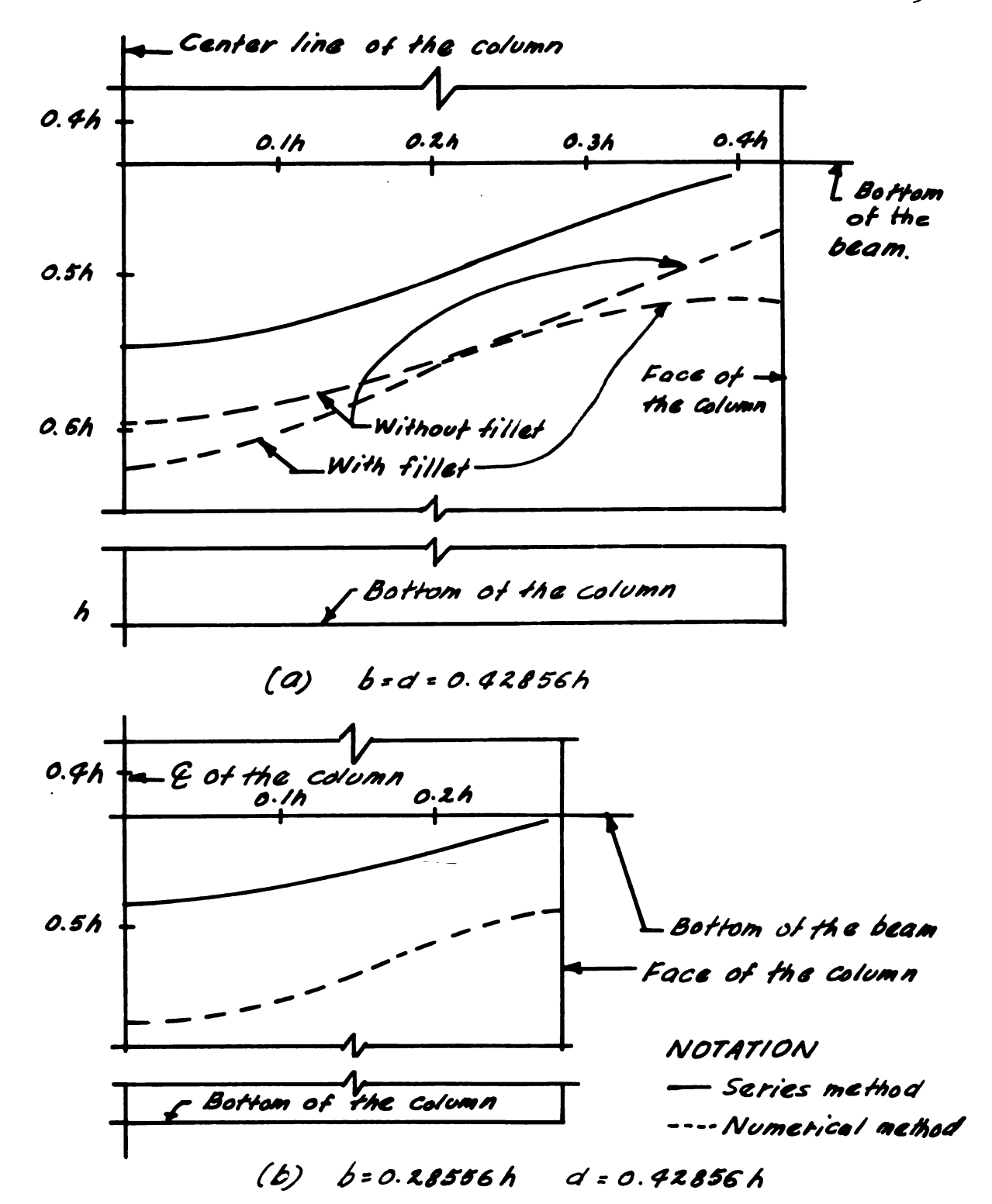
EQUIVALENT DEPTH CURVES FOR DIFFERENT COLUMN
WIDTHS WITH d=0.2h (PURE BENDING MOMENT)
FIGURE 5.5



\* X. = 0.42856 h, 0.3h AND 0.2h FOR EQUIVALENT DEPTH CURVES HAVING d=0.42856h, 0.3h AND 0.2h RESPECTIVELY.

NOTATION. --- TRUE EQUIVALENT DEPTH CURVE.
---- APPROXIMATED EQUIVALENT DEPTH LINE

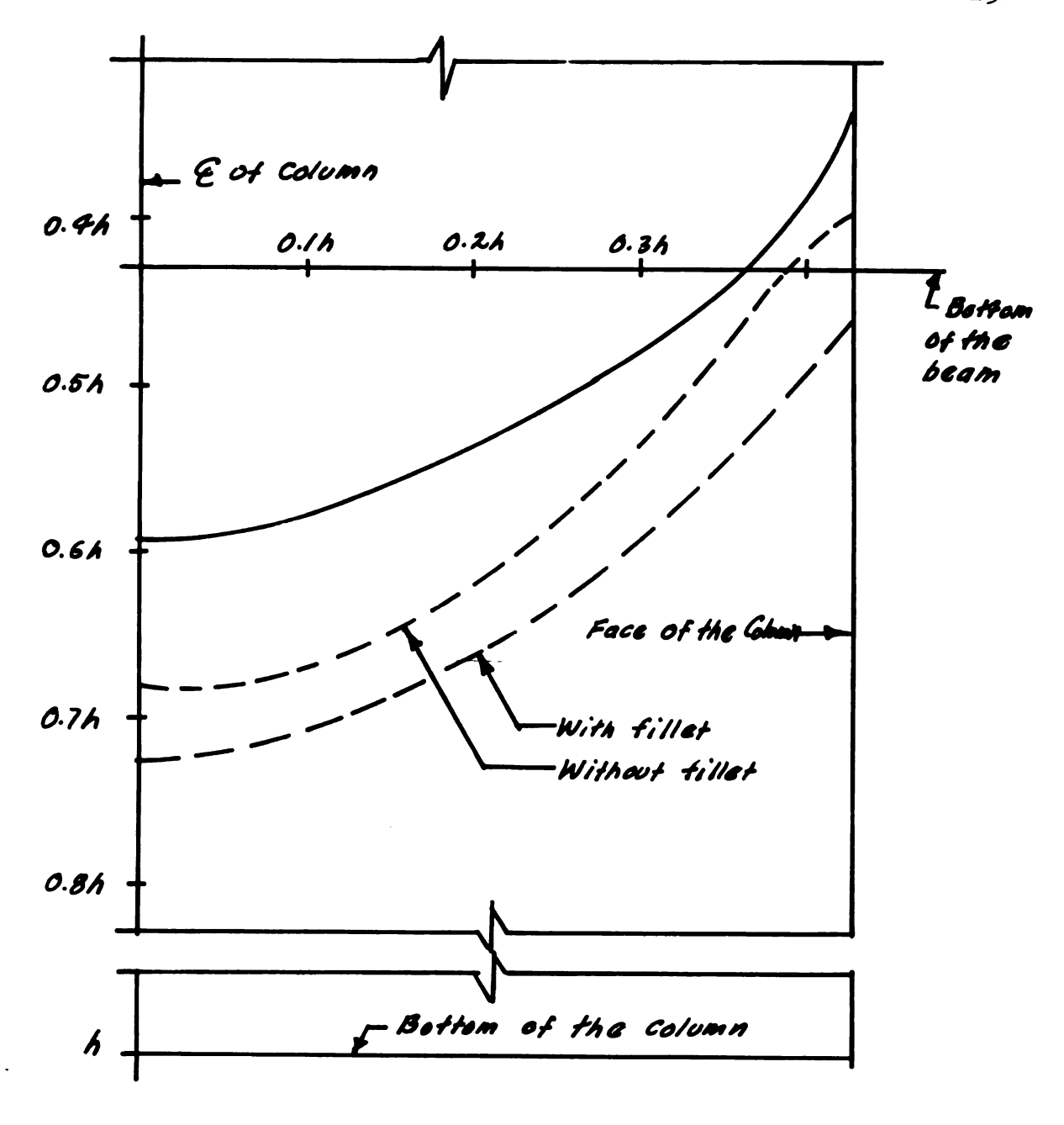
EQUIVALENT DEPTH CURVES FOR DIFFERENT BEAM DEPTHS
WITH 6.0.42856h (PURE BENDING MOMENT)
FIGURE 5.6



EQUIVALENT DEPTH CURVES AS CALCULATED BY SERIES

METHOD AND NUMERICAL METHOD (PURE BENDING MOMENT)

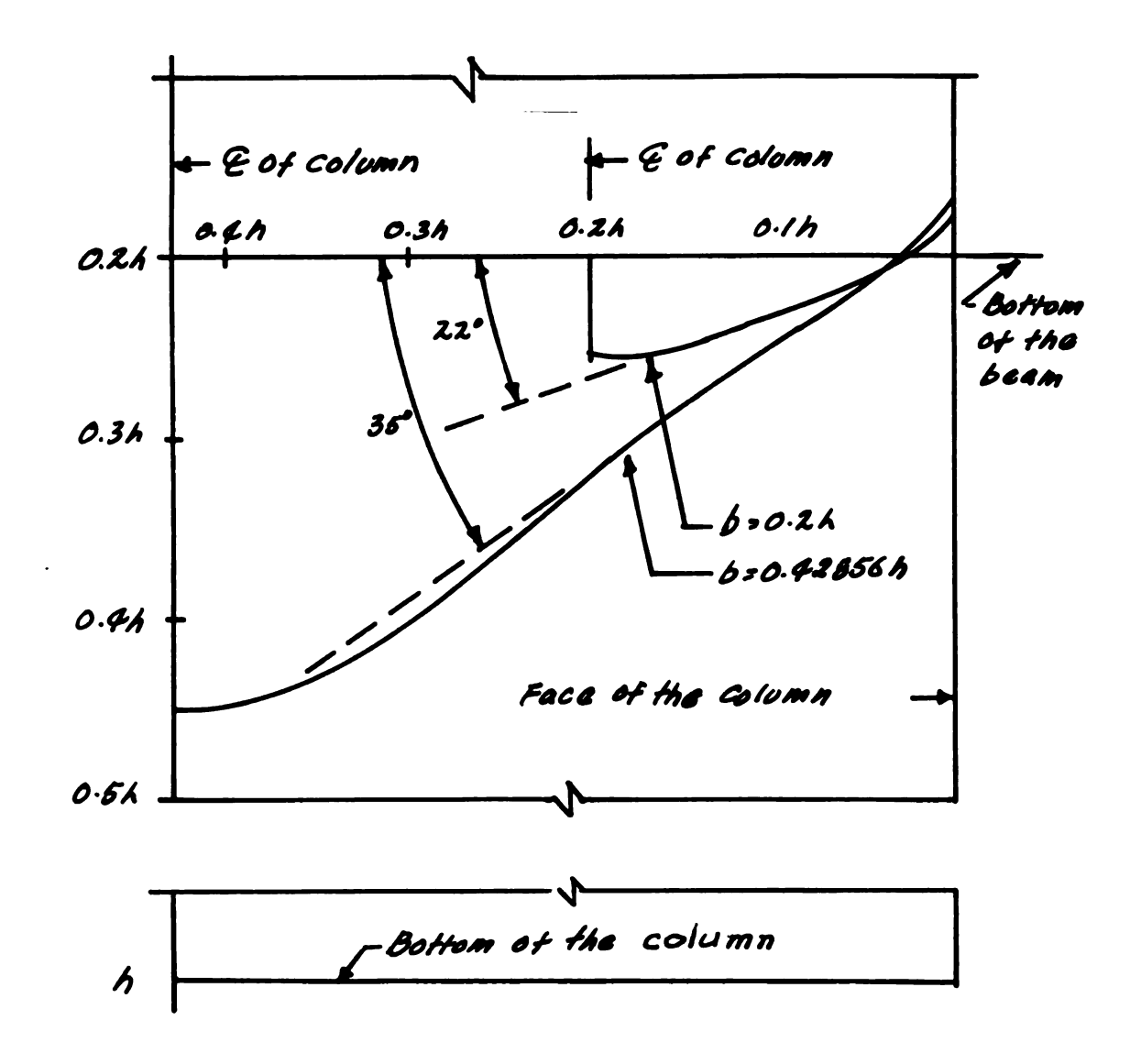
FIGURE 5.7.



NOTATION. — Series method.
--- Numerical method.

EQUIVALENT DEPTH CURVES AS CALCULATED BY SERIES METHOD AND NUMERICAL METHOD (SHEAR LOADING.)

FIGURE 5.8

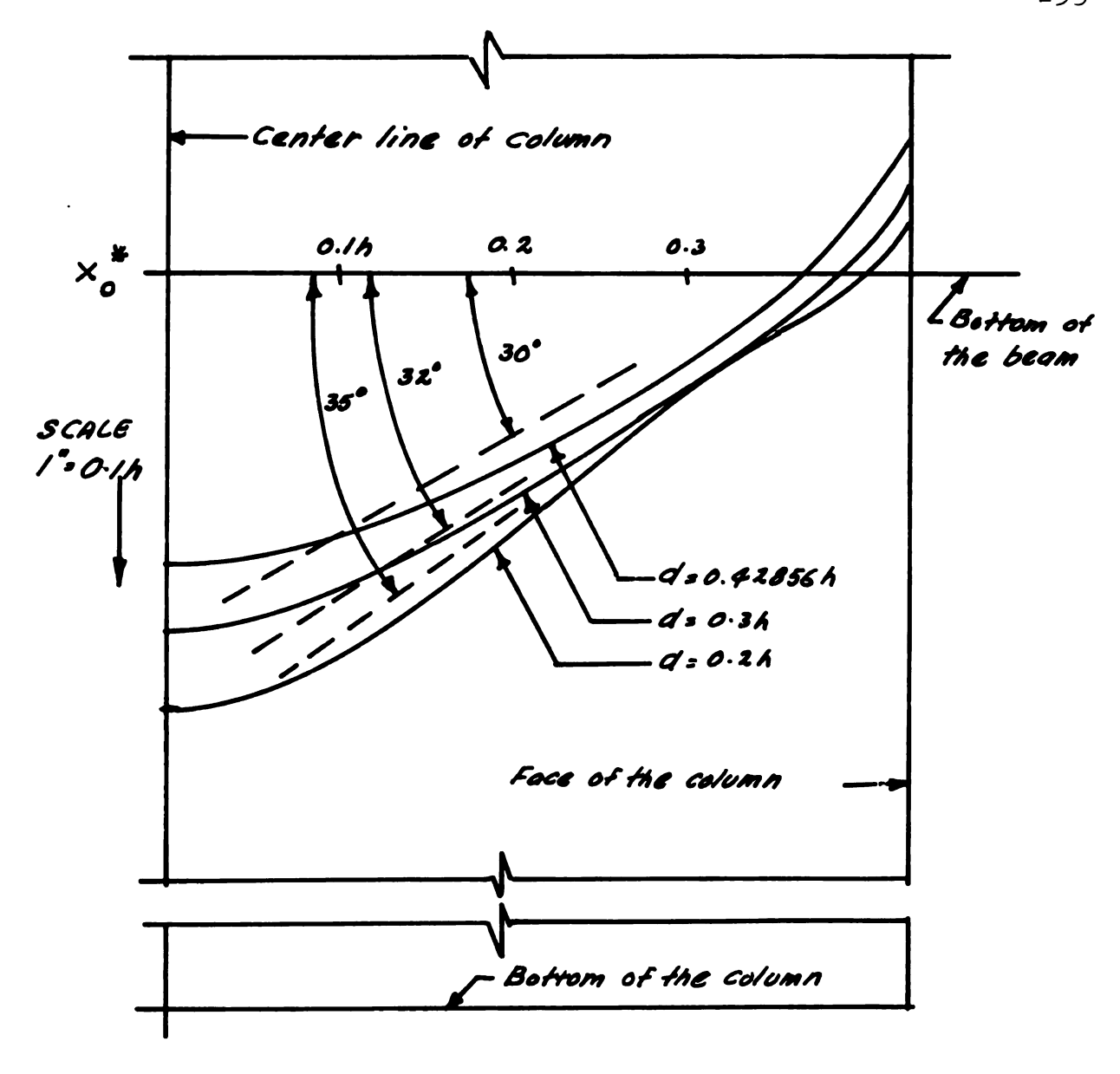


NOTATION --- True equivalent depth curve.
--- Approximated equivalent depth line.

EQUIVALENT DEPTH CURVES FOR DIFFERENT COLUMN

WIDTHS WITH d = 0.2 h AND L = 0.57143 h. (SHEAR LOADING)

FIGURE 5.9.



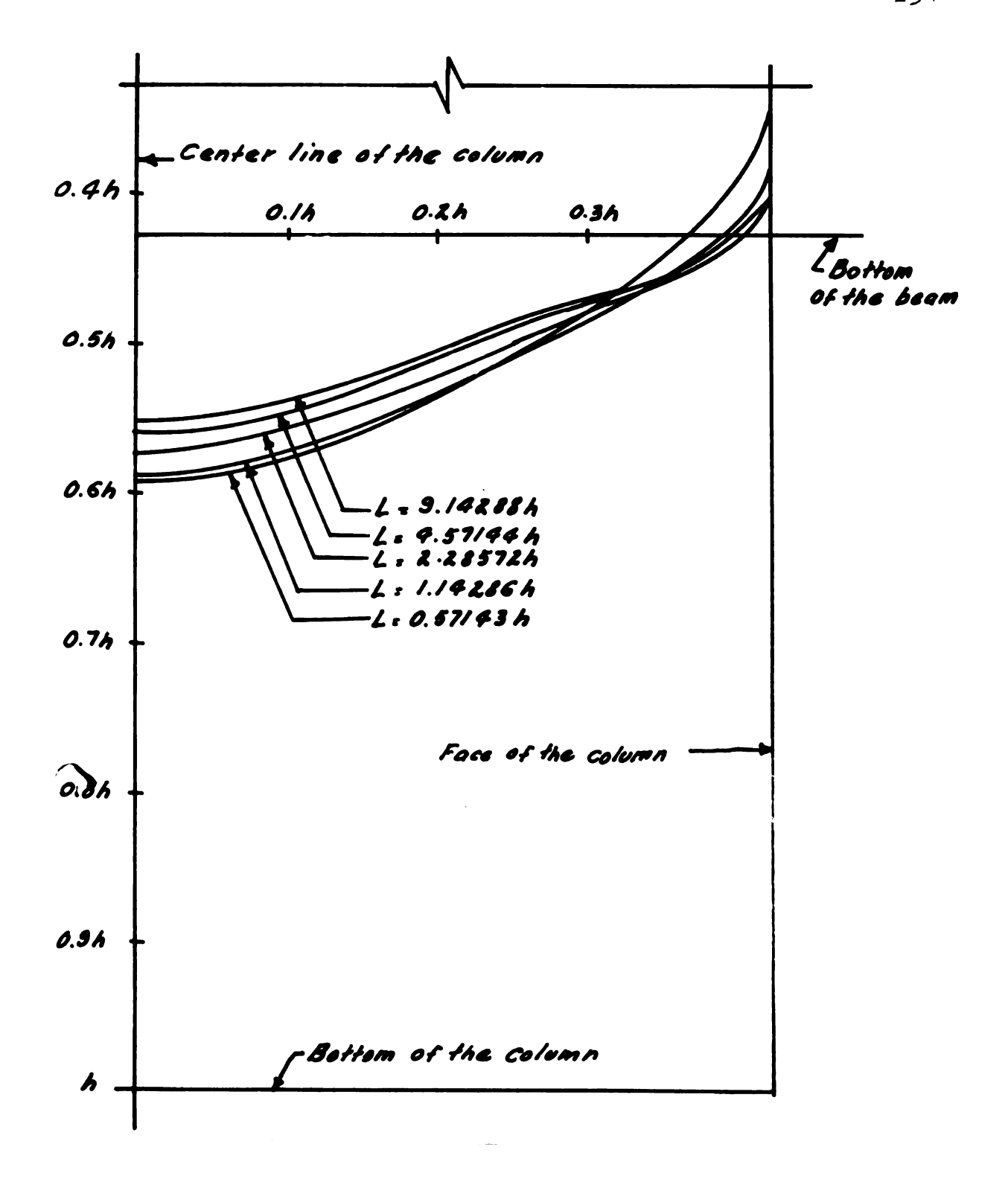
\* X<sub>0</sub> = 0.42856 h , 0.3h AND 0.2h FOR EQUIVALENT DEPTH

CURVES HAVING d=0.42856 h , 0.3h , 0.2h RESPECTIVELY

NOTATION. -- True equivalent depth curve

EQUIVALENT DEPTH CURVES FOR DIFFERENT BEAM DEPTHS
WITH b=0.42856h (SHEAR COADING).

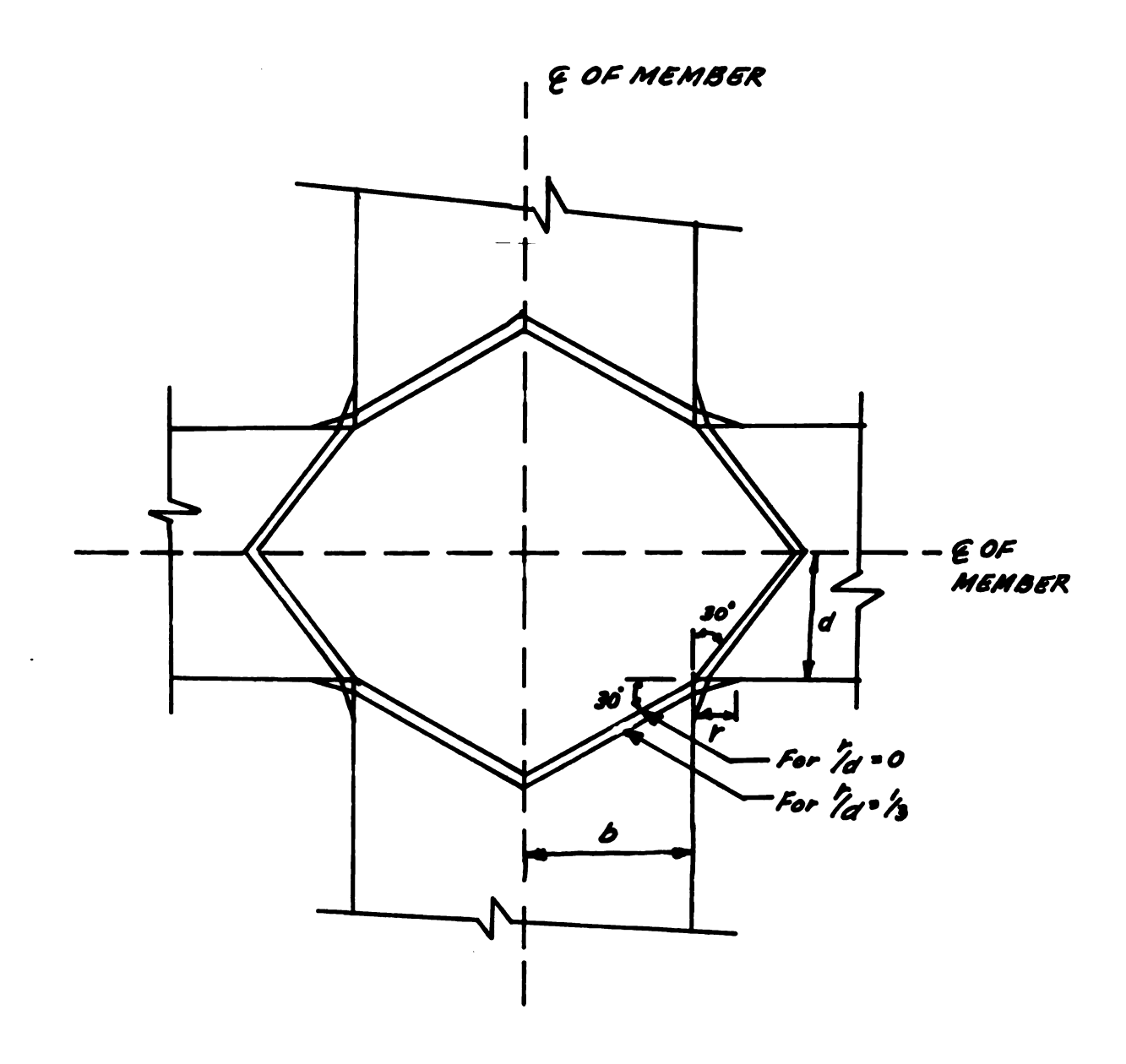
FIGURE 5.10



EQUIVALENT DEPTH CURVES FOR DIFFERENT BEAM SPAN

LENGTHS WITH b.d.o. 42856 h. (SHEAR LOADING)

FIGURE 5.11



APPROXIMATED EQUIVALENT DEPTH DIAGRAM FOR RECTANGULAR
FLEXURAL MEMBERS INTERSECTING AT A RIGID JOINT

FIGURE 5.12

### CHAPTER VI

### SUMMARY AND CONCLUSION

For the analysis of indeterminate frame structures in which the flexural deformation is the primary one, the energy variation in the beam including the joint subjected to flexural action is the essential information required to be known. Basically this reduces the problem to the determination of the stress distribution. Except in and around the joint the stress distribution is that of the conventional beam theory. Inside the joint the stress distribution can be determined by analytical or experimental methods. Photoelasticity investigations of the cross shape subjected to flexural action were carried out to determine the limits beyond which the stress distribution is that of conventional beam theory. It was concluded that the limit extends into the beam and the column portion of the cross shape a distance equal to half the column width and half the beam depth, respectively, from the face of the joint. Using this information the stress distribution in and around the joint subjected to flexural action is determined by the numerical finite difference method. From the stress distribution information the elastic energy per unit beam span length was calculated at the various beam sections.

From this was calculated an equivalent depth, which if used in the conventional beam theory energy formula would give the true elastic energy at the section. The cross shape was analyzed with two loading conditions. In one case the joint was subjected to pure bending moment. In the second case the joint was subjected to variable bending moment (shear loading). The effect of small fillets was also studied. A series method was used to determine the effect of different proportions of the cross shape on the shape of the equivalent depth curve inside the joint. An approximate equivalent depth line was suggested, which is to be used for practical purposes.

The following conclusions can be summarized from the analysis:

- 1. The knowledge of the energy variations in and around the joint of the frame structure subjected to flexural action is required for the analysis of the frame structures in which the flexural deformation is the primary one.
- 2. Under pure bending moment condition, the equivalent depth at the face of the column or the joint depends upon the fillet radius, beam depth, column width, and column height. Under variable bending moment condition (shear loading), the equivalent depth at the face of the column depends upon these things and in addition on beam span length.

- 3. The shape of the curve inside the joint depends upon the loading conditions and the proportions of the cross shape.
- 4. For exact analysis a series of equivalent depth curves must be prepared with different loading conditions and different proportions of the cross shape.
- 5. For practical purposes, the equivalent depth is not sensitive to variations in Poisson's ratio.
- 6. For practical purposes, an approximate equivalent depth line, as suggested in Part V of Chapter V, can be used for any loading condition and any proportions of the cross shape.

The analysis was limited to the cross shape with symmetry about the beam and column center lines. The tee shaped joint in which the symmetry is about one axis and the knee joint in which there is no symmetry can be analyzed for the equivalent depth information by following the procedure of this analysis. It is to be expected that in the tee shape and the knee shape joints subjected to flexural action the equivalent depth will be smaller than the corresponding beam section in the cross shape.

### APPENDIX A

### CONFORMAL MAPPING OF A CROSS-SHAPED POLYGON

For the region bounded by rectilinear polygon of n sides, such as the cross shape, the mapping function that maps the interior of the polygon onto the unit circle has the form\*

$$Z = \omega(\zeta) = P \int_{\alpha}^{\zeta} \left[ (\zeta - \zeta_1) \cdot (\zeta - \zeta_2) \cdot \dots \cdot (\zeta - \zeta_n) \right] d\zeta + Q$$

where the  $\xi$ , are the points on the boundary of the unit circle in the  $\xi$ -plane, corresponding to the vertices of the polygon in the z-plane, and the numbers  $\pi \zeta_i$  are the interior angles at the vertices of the polygon. P and Q are constants. This formula is known as the Schwarz-Christoffel transformation. Applying the formula to the symmetrical cross shape as shown in Figure A.1 the mapping function reduces to

$$Z = P \int_{0}^{\zeta} \left[ (\zeta - a_{1})^{1/2} (\zeta - a_{2})^{1/2} (\zeta - a_{3})^{1/2} (\zeta + \overline{a}_{1})^{1/2} (\zeta + \overline{a}_{2})^{1/2} (\zeta + \overline{a}_{3})^{1/2} (\zeta + a_{1})^{1/2} (\zeta + a_{2})^{1/2} (\zeta + a_{3})^{1/2} (\zeta + a_{3})^{1/2} (\zeta - \overline{a}_{3})^{1/2} (\zeta + a_{3})^{1/2} (\zeta - \overline{a}_{3})^{1/2} (\zeta - \overline{a}_{3})^{1/2} \right] d\zeta + Q$$

The cross shape region is symmetrical about X and Y axis. Due to symmetry on the unit circle  $\overline{a}_1 = 1/a_1, \overline{a}_2 = 1/a_2$ ,

<sup>\*</sup>Sokolnikoff, op. cit., p. 57.

 $\overline{a}_3 = 1/a_3$ . Hence, the mapping function reduces to

$$Z = P_0^{\xi} \left(1 - \frac{\xi^2}{a_1^2}\right) \left(1 - \frac{\xi^2}{a_2^2}\right)^{\frac{1}{2}} \left(1 - \frac{\xi^2}{a_3^2}\right)^{\frac{1}{2}} \left(1 - \xi^2 a_1^2\right) \left(1 - \xi^2 a_2^2\right)^{\frac{1}{2}} \left(1 - \xi^2 a_3^2\right) \cdot d\xi + Q$$

The mapping function as shown is an elliptical integral. This makes it difficult to use in the stress formulas of the Muskehelishvili method.\* Each factor of the integrand can be expanded by an infinite series. These series are multiplied together and the result integrated term by term to obtain the mapping function in the form  $\mathbf{Z} = \sum_{n=1}^{\infty} c_n \, \boldsymbol{\xi}^n \qquad \text{where the } \mathbf{C}_n \text{ are the constants depending upon a}_1, \, \mathbf{a}_2, \, \mathbf{a}_3. \quad \text{To evaluate the series one must take a finite number of the terms in the series. This certain number has to be decided in such a way that the mapping function obtained by this limitation should map the region of the circle onto the desired shape with reasonable accuracy.$ 

# Computer Program

The multiplication of six binomial series is very cumbersom by long hand because of the large number of terms required. A program was therefore prepared so that the tedious computations could be done by the MISTIC computer. The program for the mapping function was prepared in the floating decimal form for use with the MISTIC digital

<sup>\*</sup>Ibid., pp. 262-280.

computer located at Michigan State University. The program was prepared in such a way that the odd coefficients for the mapping function were calculated up to the 49th power for any given set values of a1, a2, a3. This allows one to evaluate the different mapping functions for different dimensions of the cross shape with the same program. A second program was made, which calculated the value of Z corresponding to any point on the unit circle for a particular cross shape. The data necessary for the second program are the 24 values of  $\Theta$  ( $\zeta = e^{i\Theta}$ ) and the coefficients evaluated by the first program for the series of the mapping function for the particular value of a1, a2, a3. The program was made in such a way that the Z value will be calulated for the same point for powers of n up to n = 21, n = 33, or n = 49. Comparison of the three results gives some idea of the convergence of the series.

# Results

The values for the mapping function for the three different proportions are given in Table A.1. Since  $a_2 = e^{0.25i\pi}$ , the cross shape is symmetrical about the 45 degree line of the quadrant. Hence, the Z values are evaluated for various values of  $\theta$  from 0 to 45 degrees ( $\xi = e^{i\theta}$ ), which are given in Tables A.2, A.3, and A.4. The transformed shapes to 1/8th of the circle to corresponding part of the cross shapes are shown in Figure A.2, A.3, and A.4.

# Discussion of Results

From the mapped figures it appears that the corners are too far off from the actual conditions. Also the rate of the improvement in the mapped shape by taking more terms of the series is very slow. By taking more terms in the series one could hope to get a sufficiently accurate explicit solution of the mapping function in the polynomial form. But it is to be noted that in the method\* for the solution of the biharmonic equation with the help of conformal mapping one has to solve a number of simultaneous equations of the same magnitude as the degree of the polynomial of the mapping function. The capability for the solution of the simultaneous equations in a practicable time will restrict the usefulness of the method even though theoretically there is a solution by this method. MISTIC computer is limited to 39 equations at the present. Since it appeared that more than 39 equations would be needed, this approach was abandoned. It is remarked also that there is a possibility that the mapping series will not converge at all at some boundary points, although the calculations seem to show a slow convergence.

<sup>\*&</sup>lt;u>Ibid</u>., pp. 278-279.

TABLE A.1
COEFFICIENTS OF THE SERIES OF THE MAPPING FUNCTION

Power	c <sub>n</sub>	= Coefficients	of $\zeta^n$
n	Case 1	Case 2	Case 3
1 9 13 17 21 25 29 33 37 41 45	1.0000 00 0.2618 03 0.0845 86 0.0240 38 -0.0116 96 -0.0227 44 -0.0232 51 -0.0148 76 -0.0052 21 +0.0038 01 +0.0085 91 +0.0095 84 +0.0067 78	1.0000 00 0.2902 11 0.1341 44 0.0843 09 0.0492 78 0.0294 33 0.0135 60 0.0035 80 -0.0041 57 -0.0085 30 -0.0113 46 -0.0120 25 -0.0117 15	1.0000 00 0.2996 05 0.1520 11 0.1094 60 0.0807 94 0.0660 83 0.0540 57 0.0465 22 0.0398 50 0.0352 01 0.0309 07 0.0277 08 0.0246 79

Coefficients  $C_n$  in cases 1, 2, and 3 are for cross shapes defined by the following positions of  $a_1$ ,  $a_2$ ,  $a_3$ .

Case 1. 
$$a_1 = e^{0.1i\pi/2}$$
 ,  $a_2 = e^{0.5i\pi/2}$  ,  $a_3 = e^{0.90i\pi/2}$  ; Case 2.  $a_1 = e^{0.05i\pi/2}$  ,  $a_2 = e^{0.5i\pi/2}$  ,  $a_3 = e^{0.95i\pi/2}$  ; Case 3.  $a_1 = e^{0.01i\pi/2}$  ,  $a_2 = e^{0.5i\pi/2}$  ,  $a_3 = e^{0.99i\pi/2}$  .

TABLE A.2

Z-VALUES OF THE TRANSFORMED SHAPE FOR A CROSS SHAPE HAVING  $a_1=e^{\text{o-ii}\pi/2}$ ,  $a_2=e^{\text{o-5i}\pi/2}$ ,  $a_3=e^{\text{o-90i}\pi/2}$ 

	и	= 21	<b>"</b>	= 33	= u	- 49
in Degrees	Real Part of <b>Z</b>	Imaginary Part of <b>Z</b>	Real Part of <b>Z</b>	Imaginary Part of <b>Z</b>	Real Part of <b>Z</b>	Imaginary Part of <b>Z</b>
0 '	1.3359 88	$\frac{1}{2}$	1.2926 39	000	321	
CV .	.3326 7	. 9952	.3077 1	à 0090°	.3390	.0885 3
7	3200 5	.1944 9	.3341 0	.1543 4	.3065 2	.1568 1
9	.2917 6	.2975 3	.3316 6	.2859 6	.3281 0	.2597 9
ω	.2418 0	.3983 7	.2733 5	.4232 4	.2976 4	.4188 6
	.1688 5	7865 4	.16719	.5249 8	.1721 0	.5469 9
	9 9820.	.5512 5	9 2840.	.5714 1	6 7820.	.5765 3
	.9830 4	.5862 2	.9508	.5744 5	9 8546.	.5577
	.8958 8	.5928 3	.8867 7	.5623 7	5 7006.	.5577 4
	.8279 7	.5799 4	.8451 9	.5563 2	.8491 5	.5675 8
	.7831 0	.5604 7	.8097 0	.5596 1	.8010	.5627 0
	.7572 0	.5462 9	.7728 3	.5645 2	.7707 5	.5581 9
	.7408 7	.5438 2	.7372 9	.5650 4	.7415 5	.5640 3
	.7240 7	.55228	9 9202.	.5623 1	7 92c2.	.5648 2
	.7005 8	.5653 7	.6840 2	.5605 8	.6829 3	.5596 2
	.6702 4	.5752 3	6659 6	.5613 8	.6647 1	.56138
	.6380	.5766	.6423	.5628 7	.6415 9	.5651 3
	.6108 7	.5696 0	. 6229	.5631 4	.6204 3	.5618 0
	.5934 3	.55868	9 <b>2</b> 909.	.5624 6	6269.	.5599 1
	.5858 7	.5503 4	.5923 2	.5620 4	.5946	.5639 0
	.5844 3	.5492 8	.5804 2	.5620 5	.5784 8	.56388
	.5829 5	.5560 4	.5708 0	.5619 4	.5696 3	.5599 6
<b>†</b> †	.57728	.5671 1	.5646 2	.5621 7	.5666 1	.5617 7
45	.57260	.5726	.56299	. 5629 9	.5643 9	.5643 9

TABLE A.3

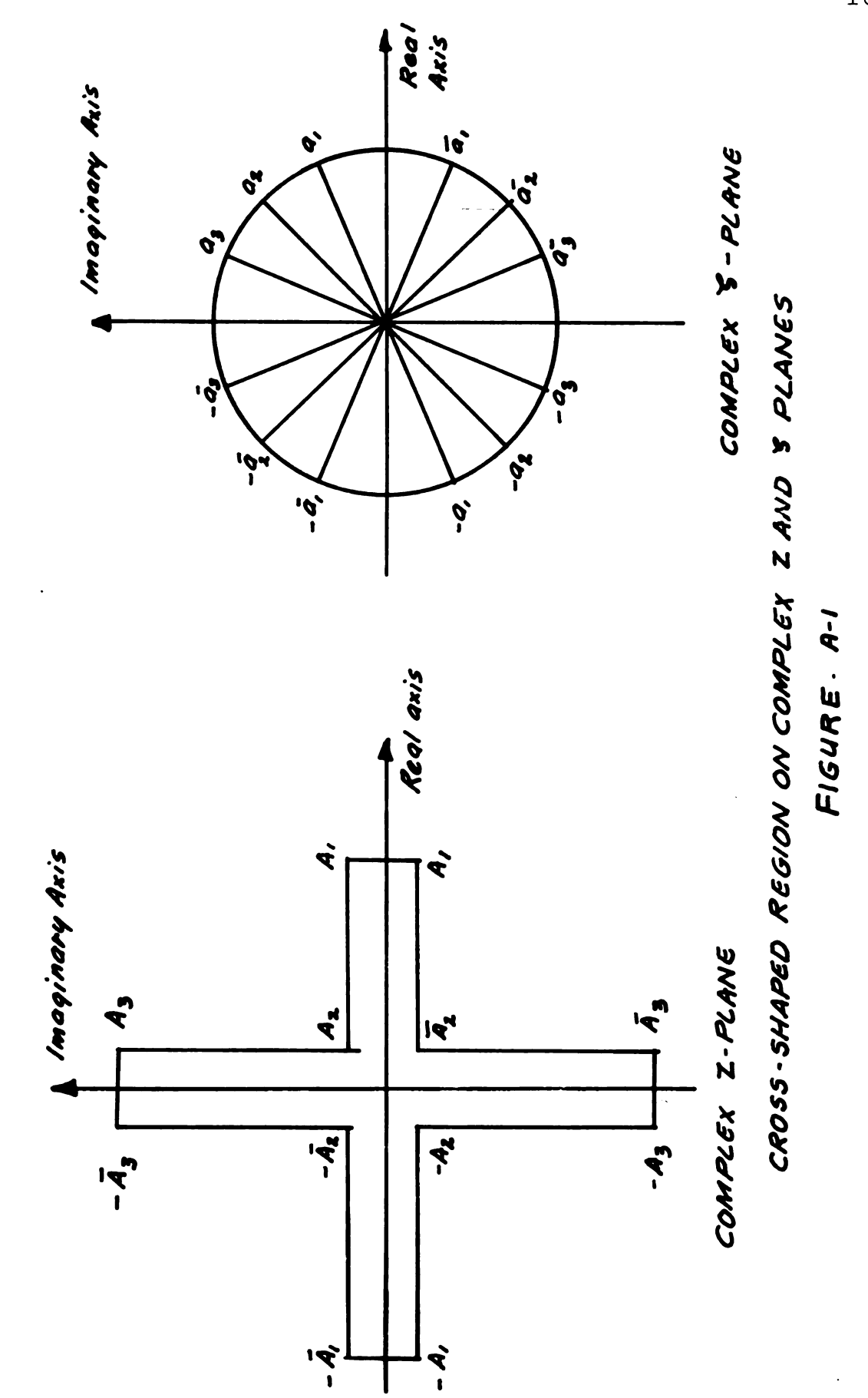
Z-VALUES OF THE TRANSFORMED SHAPE FOR A CROSS SHAPE HAVING  $a_1 = e$  ,  $a_2 = e$  . e .  $a_3 = e$  . e .

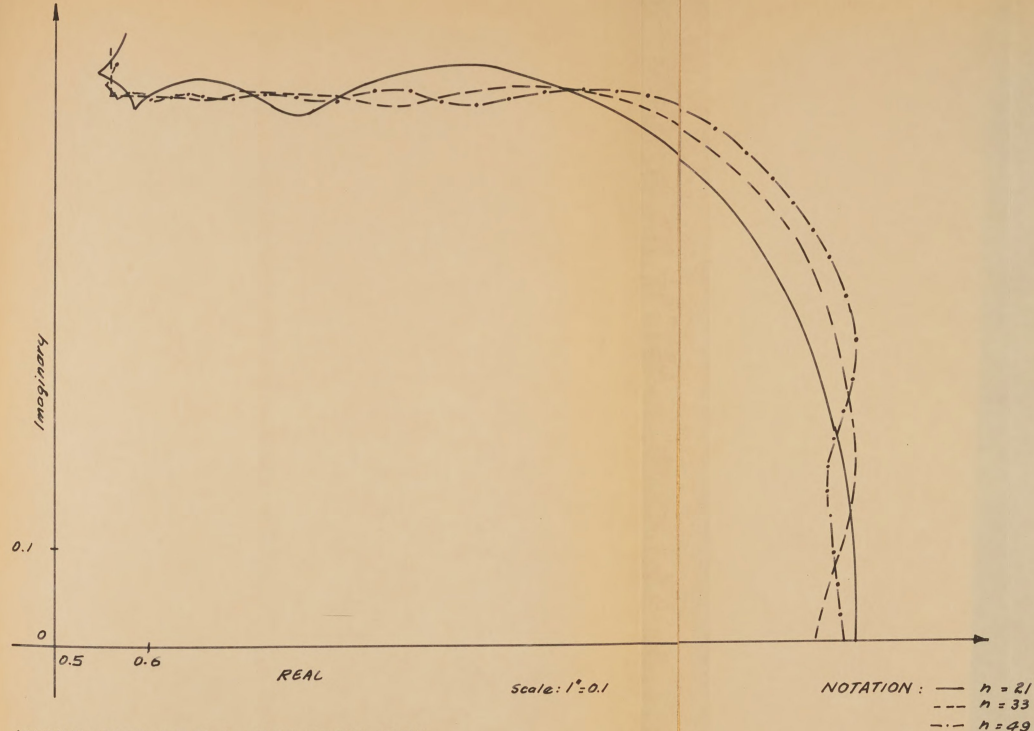
O	ш Ш	- 21	u	= 33	= u	6† :
in Degrees	Real Part of <b>Z</b>	Imaginary Part of <b>Z</b>	Real Part of <b>Z</b>	Imaginary Part of <b>Z</b>	Real Part of <b>Z</b>	Imaginary Part of <b>Z</b>
	010		1 2 3 3 7			
O 1	.5873	. 0000	5009.	00000.	.5567 4	0000.
<b>(</b> )	.5512	.2109 5	.5601 9	. 2205 x	. 5578 9	.1775 2
7 '	.4522	.3892 6	.4510 9	.4027 4	.4925 2	.3983 2
9	.3146	.5126 3	.3033 3	.5210 7	3395 2	.5598 7
ω	.1694	.5754 5	.1548 9	.5721 2	.1195 6	.5795 9
	.0431	.5885 3	.0361 2	.5745 0	9 62cc.	.5433 3
	.9506	.5730 7	.9575 8	.5581 4	.9841 5	.5499 3
	.8923	.5515 3	1 0606.	.5476	.9166	.5694 1
	.8573	.5394 8	.8708 8	.5508 1	0 6758.	.5572 0
	.8308	.5417 0	.8299 1	.5597 3	.8252 5	.5474 8
	.8015	.5534 3	.7863 2	.5634 4	.7943 4	.5608 9
22	0.765281	0.5655 32	0.7482 92	0.5591 97	0.7485 19	0.5635 18
	.7254	.5704 8	.7206 9	.5533 3	.7194 2	.5511 9
	. 6891	.5663 0	6998 5	.5527 8	.7042 1	.5538 6
	. 6619	.5567 3	.6784 0	.5573 6	.6756 5	.5636 3
	.6450	.5483 2	.6536 7	.5610 4	9 6579.	.5572 7
	. 6344	.54618	6298 6	.5595 4	.6341 0	.5509 8
	.6242	.5511 3	.6122 0	.5551 7	6209 8	.5594 3
	.6098	.5595 5	.6004 8	.5534 9	.5964 8	.5618 2
	.5909	.56588	.5896	.5564 0	.5824 1	.5528 3
	.5712	.5661 7	.5763 4	.5599 5	.5794 5	.5543 4
	.5565	.5606 0	.5632 0	.5595 8	.5667 4	.5623 2
	.5506	.5534 4	.5559 0	.5562 3	.5533 7	.5574 4
	.5511	.5511 6	.55528	.5552 8	.5535 1	.5535
					والمؤول الإسبار الأمراب المتحدد المتحدد المتحدد	

TABLE A.4

Z-VALUES OF THE TRANSFORMED SHAPE FOR A CROSS SHAPE HAVING  $a_1 = e^{-oli\pi/2}$ ,  $a_2 = e^{-si\pi/2}$ ,  $a_3 = e^{-sqi\pi/2}$ 

l	i	16 I
64 =	Imaginary Part of <b>Z</b>	0.000000000000000000000000000000000000
u	Real Part of <b>Z</b>	1.9668 79 1.3398 67 1.3398 67 1.1507 89 1.1507 89 1.0408 38 0.7598 35 0.6630 05688 57 0.5585 95 0.5586 91 0.5688 88
= 33	Imaginary Part of <b>Z</b>	0.000000000000000000000000000000000000
= u	Real Part of <b>Z</b>	1.8483 83 1.7290 97 1.17290 97 1.0339 10 1.0339 10 0.9915 23 0.78480 27 0.76784 88 0.74628 37 0.6487 89 0.6430 30 0.5682 56 0.5725 58 0.5725 58
= 21	Imaginary Part of <b>Z</b>	0.0000 0.4884 0.4884 65 0.6168 70 0.6523 99 0.5607 59 0.5137 31 0.5943 93 0.5288 73 0.5288 75 0.5830 50 0.5830 50 0.5357 444
u	Real Part of <b>Z</b>	1.7279 1.5534 88 1.5566 44 1.5566 44 0.8580 88 0.8580 88 0.7749 68 0.6538 74 0.6638 74 0.5685 80 0.5685 11 0.5685 10 0.5685 10 0.5368 92 0.5368 92
đ	in Degrees	Ω τ <b>υ</b> Ο αθ τυ Ο αθ

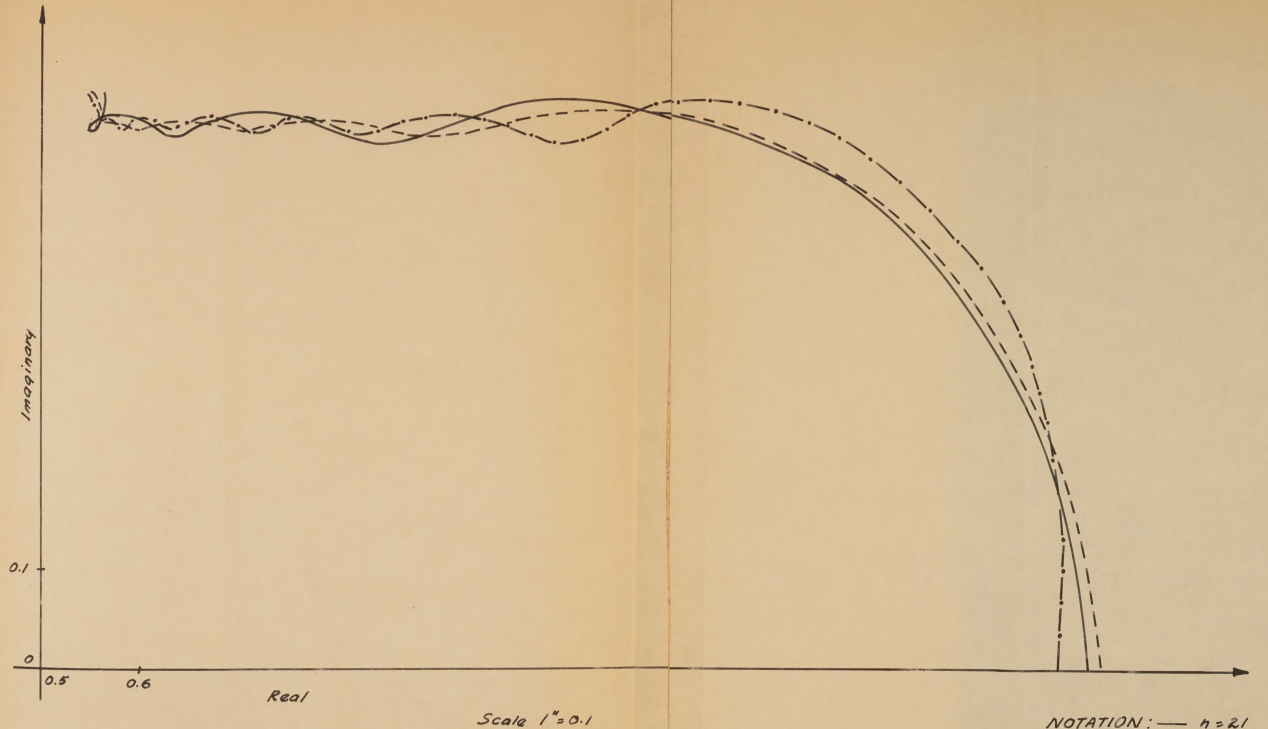




MAPPED REGION FOR A CROSS SHAPE WITH

 $Q_{i}=e^{-10i\frac{\pi}{2}}$ ,  $Q_{2}=e^{-5i\frac{\pi}{2}}$ ,  $Q_{3}=e^{-90i\frac{\pi}{2}}$  (if the region shown in figure.) FIGURE A-Z.

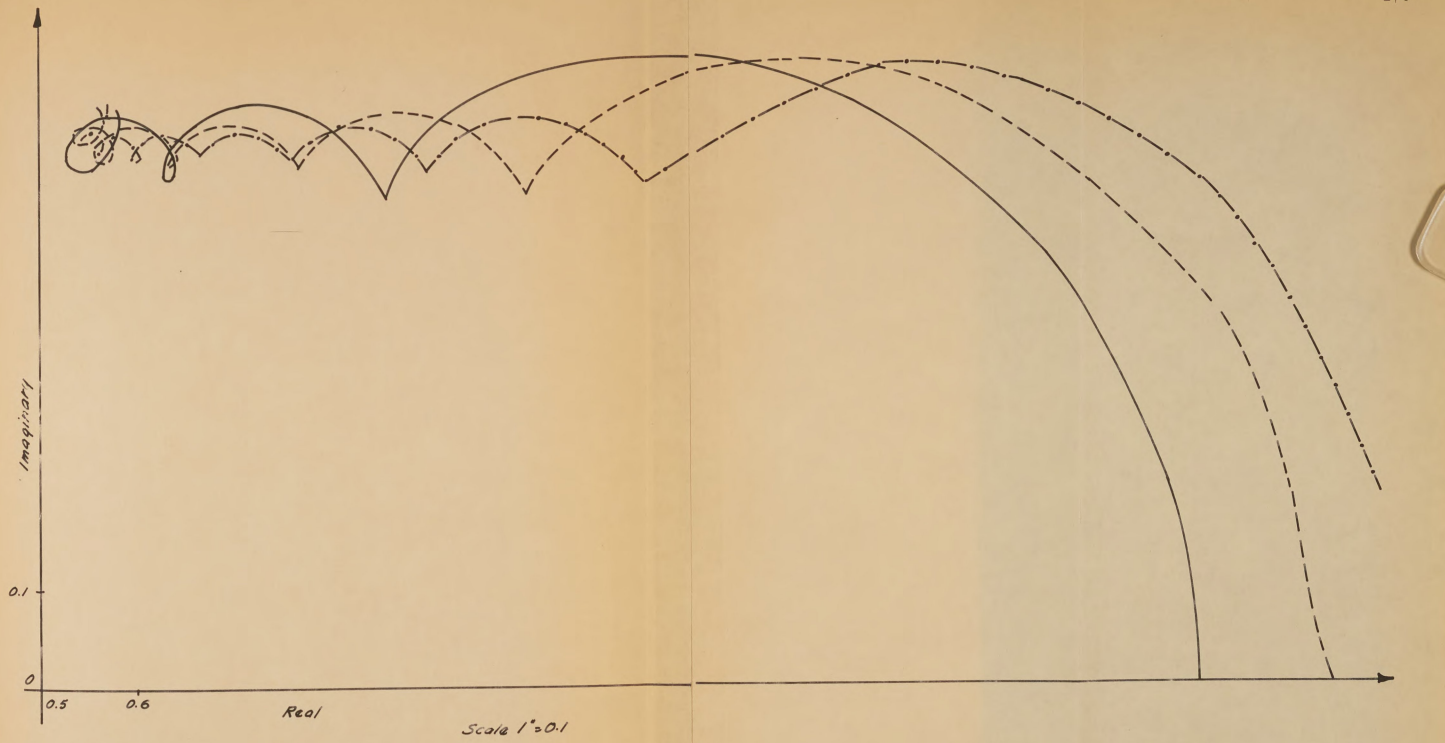
NOTATION : - n = 21



MAPPED REGION FOR A CROSS SHAPE WITH  $a_1 = e^{-(S_1 - M_2)}$   $a_3 = e^{-(S_1 - M_2)} \left( \frac{1}{16} \frac{\pi}{4} \operatorname{region shown in figure} \right)$ 

FIGURE A.3

NOTATION: - h = 21 --- h = 33



MAPPED REGION FOR A CROSS SHAPE WITH  $0_1 = e^{-01; \frac{\pi}{2}}, \quad 0_2 = e^{-5: \frac{\pi}{2}}, \quad q_3 = e^{-99: \frac{\pi}{2}} (/e^{\frac{\pi}{6}} region shown in tigure)$ FIGURE A.4

NOTATION: -- h = 21 --- h = 33 -.- h = 45

#### APPENDIX B

### FINITE DIFFERENCE EQUATIONS

# I. Finite Difference Equation for the Biharmonic Differential Equation for an Irregular Node

In finer grading of a region in which the biharmonic differential equation is to be solved by the finite difference method, a problem arises in applying the standard finite difference formula, Equation 4.2, for a node in the intermediate region such as 23,23 in Figure 4.3b. This difficulty is resolved if the procedure which was discussed and referred to in Chapter IV is followed as suggested by Allen and Dennis. This procedure is illustrated below in setting up the finite difference equation for the biharmonic differential equation for the node 23,23 of Figure 4.3b.

The biharmonic differential equation for the node 23,23 is as follows:

$$(\nabla^{4} \emptyset)_{23,23} = 0.$$

The finite difference equation can be derived as follows:

$$(\nabla^{2}) (\nabla^{2})_{23,23} = 0$$

$$(\nabla^{2}) (\emptyset_{3,3} + \emptyset_{3,2} + \emptyset_{2,2} + \emptyset_{2,3} - 4\emptyset_{23,23})/(s/\sqrt{z})^{2} = 0$$

$$(\emptyset_{34,3} + \emptyset_{3,23} + \emptyset_{23,3} + \emptyset_{3,34} - 4\emptyset_{3,3})/(s/2)^{2}$$

$$+ (\emptyset_{4,2} + \emptyset_{3,1} + \emptyset_{2,2} + \emptyset_{3,3} - 4\emptyset_{3,2})/(s)^{2}$$

$$+ (\emptyset_{3,2} + \emptyset_{2,1} + \emptyset_{1,2} + \emptyset_{2,3} - 4\emptyset_{2,2})/(s)^{2}$$

$$+ (\emptyset_{3,3} + \emptyset_{2,2} + \emptyset_{1,3} + \emptyset_{2,4} - 4\emptyset_{2,3})/(s)^{2}$$

$$-4 (\emptyset_{3,3} + \emptyset_{3,2} + \emptyset_{2,2} + \emptyset_{2,3} - 4\emptyset_{23,23})/(s)^{2}$$

$$= 0$$

where s = ungraded mesh size.

This will reduce to

$$32\emptyset_{23,23} - 22\emptyset_{3,3} - 11\emptyset_{3,2} - 10\emptyset_{2,2} - 11\emptyset_{2,3} + 4\emptyset_{34,3}$$

$$+ 4\emptyset_{3,23} + 4\emptyset_{23,3} + 4\emptyset_{33,34} + \emptyset_{4,2} + \emptyset_{3,1} + \emptyset_{2,1} + \emptyset_{1,2} + \emptyset_{2,4}$$

$$+ \emptyset_{1,3} = 0$$

It is to be noticed that the mesh size is not the same throughout the derivation. The mesh size taken at any stage of derivation is one suitable for setting up the finite difference equation for the Laplace operator at the node without introducing new intermediate points. Also net directions are chosen as suitable for the node.

# II. Approach for Evaluation of $\emptyset_{34,34}$ (Refer Figure 4.3)

The  $\emptyset$  value for the node 34,34 can be expressed in terms of  $\emptyset_{3,34}$  or in terms of  $\emptyset_{34,3}$  by evaluating the finite difference equations for the boundary conditions at m and n, respectively. In reality the singularity of  $\emptyset_{34,34}$  is to be observed. In the present analysis  $\emptyset_{34,34}$  has been taken as the average of the two values of  $\emptyset_{34,34}$  evaluated by satisfying the boundary conditions at m and n,

respectively. For that, first  $\emptyset$  is expanded in terms of Taylor series in the X or Y direction, respectively, at points m or n. In the Taylor series, the boundary conditions are substituted. Then the value of  $\emptyset_{34,34}$  can be evaluated. The discussed procedure is illustrated as follows:

Applying the Taylor series formula,

Also,

$$\emptyset_{3,34} = \emptyset_{m} + (x_{3,34} - x_{m})(\emptyset_{m}') + (1/2)(x_{3,34} - x_{m})^{2} (\emptyset_{m}'')$$

where  $\mathcal{J}_{m}^{'}$  and  $\mathcal{J}_{m}^{''}$  are first and second partial derivatives of  $\mathcal{J}$  with respect to x, evaluated at m. By substituting the values of  $\mathcal{J}_{m}^{'}$ ,  $\mathcal{J}_{m}^{''}$  and the difference of X coordinates, the required value of  $\mathcal{J}_{34,34}$  can be evaluated in terms of  $\mathcal{J}_{3,34}$  from the above relations. In a similar manner by expanding  $\mathcal{J}$  in a series in the Y direction  $\mathcal{J}_{34,34}$  can be evaluated in terms of  $\mathcal{J}_{34,3}$ . Then the average is taken of the two  $\mathcal{J}_{34,34}$  values.

### APPENDIX C

MISTIC COMPUTER PROGRAM FOR EVALUATION OF TOTAL ELASTIC ENERGY ALONG THE BEAM SECTION OF THE COLUMN SUBJECTED TO PURE BENDING MOMENT ACCORDING TO THE SERIES SOLUTION

# Problem Outline

For a column subjected to pure bending moment condition, the total energy across the beam section per unit length in the Y direction is given by the Equation 5.17 in which the constants  $P_{\text{J}}$ ,  $C_{\text{lm}}$  and  $C_{\text{4m}}$  are evaluated according to boundary conditions mentioned in Part II of Chapter V. In the formula for such a case the variable parameters are dimensions d and b; and the Poisson's ratio  $\mathcal{M}$ , m the number of terms for a series and the value of y. The variables d, b, and y are expressed as follows:

$$d = K_d h$$
,

$$b = K_b h$$
,

$$y = F_y K_b h$$
,

where  $F_y$  will vary from  $\Im$  to 1.

# Data and Answer Form

In the following program the data to be supplied is to be in the sequence of  $\mathcal{T}$ ,  $K_d$ ,  $K_b$ , and eleven values of  $F_y$ . The answers will be printed out in the sequence of  $\int_{-\infty}^{\infty} dx$ ,  $\int_{-\infty}^{\infty} dx$ ,  $\int_{-\infty}^{\infty} dx$ ,  $\int_{-\infty}^{\infty} dx$ ,

and total energy (in terms of 2E where E is modulus of elasticity) for each value of  $F_y$ . Eleven sets of such values will be printed out in the order in which  $F_y$  values are fed in the machine. This program manipulates the numbers in the floating decimal form,\* i.e. the numbers represented in the form of  $A(10)^p$ , where  $1 \ge A \ge 1/10$  and  $64 > p \ge -64$ . Hence, the numbers to be fed in the data should be in the floating decimal form. The answers will be printed out in the floating decimal form.

### Master Program

The master program, i.e. complete program, is composed partly of various subroutines. The order pairs of these subroutines are not written in the following program, as all these subroutines are available in the MISTIC library.\*\*

Hence, only the designation and the title as used in the library is given wherever these subroutines are used. The program is prepared for eleven values of Fy and the maximum value of m as 50. But a little modification in the following program will allow one to change the number of values of Fy and the maximum value of m. The value of m as 50 is used for the reasons set forth in the discussion of the convergence of series in Part II of Chapter V.

<sup>\*&</sup>quot;Illiac Programming," <u>Digital Computer Laboratory</u> (Urbana, Illinois: University of Illinois, 1955), pp. 4-9.

<sup>\*\*</sup>MISTIC Library is located at Computer Laboratory, Michigan State University, East Lansing, Michigan.

Orders or Subroutine Designation	Notes
Subroutine XI 218	Decimal order Input (25)
ээ 3к	Directive
))F ))9F	Locations 9 and 10 are floating Accumulators
00F 0011F 00F 00180F 00F 00210F 00F 00240F 00F 00260F	
OO 11K	Directive
Subroutine Al 63	Floating decimal arithmetic routine (168)
ээ 18эк	Directive
Subroutine A3 125	Convert a number from floating decimal representation to normal machine form (27)
JJ 21JK	Directive
Subroutine SA2 127	Exponential Auxiliary for floating decimal (16)
ээ 24эк	Directive
Subroutine SA2-M	Hyperbolic sine and cosine floating point Auxiliary (18)
oo 260 <b>k</b>	Directive
Subroutine TA1 126	Sine Auxiliary for floating decimal (26)
	•

00 305K Directive

Location	Orders	Notes
Э	22L 50L	Transfer control to R.H. of L. Standard subroutine entry.
1	26 S4 88F	Bring the number from the data tape into Acc.
2	8s 290f ok 2f	Store contents of Acc. into 290F. Set the loop for Box 0 by setting $g_0 = 0$ and $c_0 = -2$ .
3	88 F	Bring the number from the data tape
	OS 291F	into Acc. Store the contents of Acc. into designated location.
4	03 3L	If $(c_0 + 1) \leq 0$ , transfer control to
	OK 2F	I.H. of 3L. Set the loop for Box 3 by setting $g_3 = 3$ and $c_3 = -2$ .
5	05 <b>291F</b>	Bring contents of designated location
	87 290F	into Acc. Multiply contents of Acc. by $oldsymbol{\pi}$ .
6	OS 291F	Store contents of Acc.at designated
	03 5L	location. If $(c_0 + 1) \le 0$ , transfer control to L.H. of 5L.
7	8K 2F 8S <b>2</b> 93F	Put 2 into Acc. Store number 2 at 293F.
8	8K F 8S <b>2</b> 94F	Put number 0 into Acc. Store number 0 at 294F.
9	8s 295f 8s 296f	Store number 0 at 295F. Store number 0 at 296F.
10	OK 50F	Set the loop for Box 3 by setting
	85 <b>29</b> 4F	$g_{3} = 0$ and $c_{3} = -50$ . Bring contents of 294F into Acc.
11	84 291F 8S 294F	Add contents of 291F to contents of Acc. Store contents of Acc. at 294F.
12	8J S8 8S 297F	Enter Sine subroutine. Store contents of Acc (Sine value) at 297F.

Location	Orders	Notes
13	85 290F 86 293F	Bring # into Acc.  #/2 into Acc.
14	84 <b>29</b> 4F 8J S8	Add contents of 294F to the Acc. Enter Sine subroutine.
15	87 294F	Multiply contents of 294F by that of
	8s 298f	Acc. Store contents of Acc. at 298F.
16	85 <b>29</b> 7F 80 <b>2</b> 98F	Bring contents of 297F into Acc. Subtract contents of 298F from that of Acc.
17	8s 297f 85 <b>29</b> 6f	Store contents of Acc. at 297F. Bring contents of 296F into Acc.
18	84 <b>29</b> 0F 8 <b>S 29</b> 6F	Add contents of 290F to the Acc. Store contents of Acc. at 296F.
19	85 <b>29</b> 7F 87 <b>29</b> 3F	Bring contents of 297F into Acc. Multiply contents of 293F by that of Acc.
23	86 <b>29</b> 6F 86 <b>29</b> 6F	Divide contents of Acc. by that of 296F. Divide contents of Acc. by that of 296F.
21	8S <b>29</b> 7F 85 <b>29</b> 5F	
22	84 <b>292F</b> 8S <b>29</b> 5F	Add contents of 292F to the Acc. Store contents of Acc. at 295F.
23	8S 295F 8J 24L	Store order. Waste order. Transfer control to L.H. of 24L.
24	22 24L 50 24L	Transfer control to R.H. of 24L. Standard subroutine entry.
25	26 S7	Enter Hyperbolic Sine and Cosine sub-
	50 25L	routine. Standard subroutine entry.
26	26 S4 85 14S7	Re-enter Al subroutine. Bring Hyperbolic sine function into Acc.

Location	Orders	Notes
27	8S 298F 85 15S7	Store contents of Acc. at 298F. Bring Hyperbolic cosine function into Acc.
28	87 295F	Multiply contents of Acc. by that of 295F.
	84 298F	Add contents of 298F to the Acc.
29	8S 299F 85 295F	Store contents of Acc. at 299F. Bring contents of 295F into Acc.
30	87 293F	Multiply contents of Acc. by that of 293F.
	8s 300F	Store contents of Acc. at 300F.
31	8s 300f 8j 32l	Store order. Waste order. Transfer control to L.H. of 32L.
32	22 32L 50 32L	Transfer control to R.H. of 32L. Standard subroutine entry.
33	26 S7	Enter Hyperbolic sine and cosine sub- routine.
	50 33L	Standard subroutine entry.
34	26 S4 85 14S7	Reenter Al routine Bring hyperbolic sine function into Acc.
35	84 300F 8s 300F	Add contents of 300F to the Acc. Store contents of Acc. at 300F.
36	81 299F	Bring negative contents of 299F into
	87 <b>2</b> 97F	Acc. Multiply contents of 297F by that of Acc.
37	86 300F 87 293F	Divide contents of Acc. by that of 300F. Multiply contents of Acc. by that of 293F.
38	0S 350F 85 <b>29</b> 8F	Store $C_{lm}$ starting from 350F. Bring contents of 298F into Acc.
39	87 <b>2</b> 97F	Multiply contents of 297F by that of
	87 293F	Acc. Multiply contents of 293F by that of Acc.

Location	Orders	Notes
40	86 300F 08 450F	Divide contents of Acc. by that of 300F StoreC <sub>2m</sub> starting from 450F.
41	101 20	If $(c_0 + 1) \leq 0$ , transfer control to P.H. of 10L.
	8J 42L	Transfer control to L.H. of 42L.
42	26 600F 0F F	Transfer control to L.H. of 600F. Stop order.
	00 600К	Directive
Э	22 L 50 L	Transfer control to R.H. of L. Standard subroutine entry.
1	26 S4 OK 12F	Reenter Al subroutine. Set the loop for Box 3 by setting $g_0=0$ and $c_0=0$ - 12.
2	88 F OS 699F	Bring the number from the tape. Store contents of Acc. at designated location.
3	03 2L	If $(c_0 + 1) \leq 0$ , transfer control to I. H. of 2L.
	OK 11F	Set the loop for Box 3 by setting $g_3 = 3$ and $c_3 = -11$ .
4	1K 50F	Set the loop for Box 1 by setting
	2K 5F	$g_1 = 0$ and $c_1 = -50$ . Set the loop for Box 2 by setting $g_2 = 0$ and $g_2 = -5$ .
5	8K F 2S 715F	Put 0 into Acc. Store number 0 from 715F onwards.
6	22 5L	If $(c_2 + 1) \angle 0$ , transfer control to R.H. of 5L.
	05 700F	Bring F <sub>y</sub> into Acc.
7	87 <b>2</b> 92F	Multiply contents of 292F by that of Acc.
	8S 720F	Store contents of Acc. at 720F.
8	85 715F 84 <b>72</b> 0F	Bring contents of 715F into Acc. Add contents of 720F to that of Acc.

Location	Orders	Notes
9	8S 715F 8J 10L	Store contents of Acc. at 715F. Transfer control to L.H. of 10L.
10	22 10L 50 10L	Transfer control to R.H. of 10L. Standard subroutine entry.
11	26 S7 50 11L	Enter hyperbolic sine and cosine sub- routine Standard subroutine entry.
12	26 S4 85 15S7	Reenter subroutine Al. Bring hyperbolic function into Acc.
13	17 350F 8S 721F	Multiply contents of designated location by that of Acc. Store contents of Acc. at 721F.
14	85 14S7 17 45)F	Bring hyperbolic sine function into Acc. Multiply contents of designated location by that of Acc.
15	8s 722F 87 715F	Store contents of Acc. at 722F. Multiply contents of Acc. by that of 715F.
16	8s 723F 85 15S7	Store contents of Acc. at 723F. Bring hyperbolic function into Acc.
17	17 450F 8S 724F	Multiply contents of Acc. by that of designated location. Store content of Acc. at 724F.
18	87 715F 8s 725F	Multiply contents of 715F by that of Acc. Store contents of Acc. at 725F.
19	85 14S7 17 350F	Bring hyperbolic sine function into Acc. Multiply contents of Acc. by that of designated location.
20	8s 726F 85 721F	Store contents of Acc. at 726F. Bring contents of 721F into Acc.
21	84 723F 8S 727F	Add contents of 723F to that of Acc. Store contents of Acc. at 727F.
22	87 727F 8S 728F	Multiply contents of 727F by that of Acc. Store contents of Acc. at 728F.

Location	Orders	Notes
23	85 727F 84 724F	Bring contents of 727F into Acc. Add contents of 724F to that of Acc.
24	84 724F 8s 729F	Add contents of 724F to that of Acc. Store contents of Acc. at 729F.
25	87 729F	Multiply contents of 729F by that of Acc.
	8s 730f	Store contents of Acc. at 730F.
26	85 726F 84 725F	Bring contents of 726F into Acc. Add contents of 725F to that of Acc.
27	84 <b>722</b> F 8S 731F	Add contents of 722F to that of Acc. Store contents of Acc. at 731F.
28	87 731F	Multiply contents of 731F by that of Acc.
	8s 732F	Store contents of Acc. at 732F.
29	81 727F	Bring negative contents of 727F into Acc.
	87 729F	Multiply contents of 729F by that of Acc.
30	8s 733F 85 716F	Store contents of Acc. at 733F. Bring contents of 716F into Acc.
31	84 728F 8S 716F	Add contents of 728F to that of Acc. Store contents of Acc. at 716F. <b>\(\Sigma\)</b> dx.
32	85 717F 84 730F	Bring contents of 717 F into Acc. Add contents of 730F to that of Acc.
33	8s 717F 85 718F	Store contents of Acc. at 717F. <b>Z</b> ( $\sigma_{\mathbf{x}}^{2}$ ).dx. Bring contents of 718F into Acc.
34	84 733F 8S 718F	Add contents of 733F to that of Acc. Store contents of Acc. at 718F. \(\sum_{\substack{\sigma}}\) ((\sigma_{\supstack{\sigma}})\) dx
35	85 719F 84 732F	Bring contents of 719F into Acc. Add contents of 732F to that of Acc.
36	8s 719F 13 8L	Store contents of Acc. at 719F. $\sum_{(x_y).dx}^2$ . If $(c_1 + 1) \leq 0$ , transfer control to L. H. of 8L.

Location	Orders	Notes
37	8F 1F 3K 4F	Give a carriage return and line feed. Set the loop for Box 3 by setting $g_3 = 0$ and $c_3 = -4$ .
38	35 716F 89 9F	Bring contents of designated location into Acc. Print contents of Acc.
39	33 38L 81 718F	If $(c_3 + 1) \leq 0$ , transfer control to L.H. of 38L. Bring contents of 718F into Acc.
40	87 293F 87 699F	Multiply contents of Acc. by 2. Multiply contents of Acc. by that of 699F.
41	8s 718f 8k 1f	Store contents of Acc. at 718F. Put number 1 into Acc.
42	84 699F 87 293F	Add contents of 699F to Acc. Multiply contents of Acc. by 2.
43	87 719F 84 718F	Multiply contents of 719F by that of Acc. Add contents of 718F to Acc.
44	84 717F 84 716F	Add contents of 717F to Acc. Add contents of 716F to Acc.
45	89 9F 8F 1F	Print out the number from Acc. (Energy). (2E). Give a carriage return and line feed.
46	03 4L 8J 47L	If $(c_0 + 1) \triangleq 0$ , transfer control to L.H. of 4L. Transfer control to L.H. of 47L.
47	OF F OF F	Stop order. Stop order.
	24 305N	When the program is read in the machine and it comes to symbol N, the machine will be ready to execute the order 24 305F. Hence, after starting with START switch control will be transferred to L.H. of 305F.

# Operation of Program

The program is read into the machine. When the program is read in, the machine will stop at 24 305F. Then the program tape is removed and the data tape is put into the reader. Then START switch is put on. It will take the data in and will do the calculations. Machine will go on until eleven sets of answers are printed out.

# Calculation Time

It takes about 6 minutes for calculation of energy and its components for eleven sets of  $F_y$  values. This time includes the time for reading in the program and data tape and printing out answers.

### BIBLIOGRAPHY

- Allen, D. N. De. G. and Dennis S. C. R. "Graded Nets in Harmonic and Biharmonic Relaxation," Quart. Journal Mech. and Applied Maths., Vol. IV, Pt. 4 (1951), pp. 439-443.
- Allen, D. N. De. G. Relaxation Methods. New York: McGraw-Hill Book Co., Inc., 1954.
- Brahtz, J. H. A. "Stress distribution in re-entrant corner," Transaction of the American Society of Mechanical Engineers, Journal of Applied Mechanics, V. 55 (1933), pp. 31-37.
- Caswell, J. S. "Stresses in short Beams: 1. Experimental Analysis; 2. Theoretical Analysis," Engineering (London) V. 178, (1954), pp. 625-628, 656-658.
- Charlton, T. M. Model Analysis of Structures. New York: John Wiley and Sons, Inc., 1954.
- Computer Laboratory Staff. <u>Illiac Programming</u>. Urbana: Digital Computer Laboratory, University of Illinois, 1955.
- Computer Laboratory Staff. <u>MISTIC Programming Manual</u>. East Lansing: Computer Laboratory, Michigan State University, 1958.
- Evans, I. T. "The Modified Slope Deflection Equations," <u>Proceedings of American Concrete Institute</u>, 28 (September 1931--April 1932), pp. 109-130.
- Fox, I. "Some improvements in the use of relaxation methods for the solution of ordinary and partial differential equations," Proceedings, Royal Society (London), A, Vol. 190 (1947), pp. 31-59.
- Frocht, Max Mark. Photoelasticity. New York: John Wiley and Sons, Inc., 1941.
- Hartman, J. B. and Leven, M. M. "Factors of stress concentration for the bending case of fillets in flat bars and shafts with central enlarged section,"

  Proceedings of the Society of Experimental Stress
  Analysis, IX, No. 1 (1951), pp. 53-62.

- Hayden, Arthur G. The Rigid Frame Bridges. New York: John Wiley and Sons, Inc., Third edition, 1950.
- Lee, George Harmor. An Introduction to Experimental Stress Analysis. New York: John Wiley and Sons, Inc., 1950.
- Lyse, Ing and Black, W. E. "An investigation of Steel Rigid Frames," Transactions of American Society of Civil Engineers, 107 (1942), pp. 127-186.
- Maugh, L. C. Statically Indeterminate Structures. New York: John Wiley and Sons, Inc., 1946.
- Mikishi, Abe. <u>Tests on Rigid Frames, Bulletin 107</u>. Urbana: Engineering Experiment Station, University of Illinois.
- Neuber, Heinz. Theory of Notch Stresses. Ann Arbor: J. W. Edwards, Inc., 1946.
- Olander, Harvy C. "Stresses in the Corners of Rigid Frames,"
  Transactions of American Society of Civil Engineers,
  V. 119 (1954), pp. 797-809.
- Osgood, William R. "A Theory of Flexure for Beams with Non-parallel Extreme Fibers," Transactions of the American Society of Mechanical Engineers, 61 (1939), Journal of Applied Mechanics, pp. A-122--A-126.
- Peterson, R. E. Stress Concentration Design Factors. New York: John Wiley and Sons, Inc., 1955.
- Portland Cement Association. Handbook of Frame Constants. Chicago: Portland Cement A sociation, 1947.
- Richart, F. E., Dolan, T. J. and Olson, T. A. An Investigation of Rigid Frame Bridges, Part I: Tests of Reinforced Concrete Knee Frames and Bakellite Models.

  Bulletin 307. Urbana: Engineering Experiment Station, University of Illinois, 1938.
- Richart, F. E. "Tests of Effects of Brackets in Reinforced Concrete Rigid Frames," Research Paper No. 9, Journal of Research, U. S. Bureau of Standards, Vol. 1 (1928), pp. 189-253.
- Seely, Fred B. and Smith, James O. Advanced Mechanics of Materials. New York: John Wiley and Sons, Inc., 1952.
- Shaw, F. S. An Introduction to Relaxation Methods. New York: Dover Publications, Inc., 1953.

- Shermer, Carl I. Fundamentals of Statically Indeterminate
  Structures. New York: The Ronald Press Company, 1957.
- Sokolnikoff, I. S. <u>Mathematical Theory of Elasticity</u>. New York: McGraw-Hill Book Co., Inc., 1956.
- Spaulding, Ralph E. Discussion on "An Analysis of Stepped-Column Mill Bents," by Daniel S. Ling, Transaction of American Society of Civil Engineers, 113 (1948), pp. 1077-1122.
- Stang, Ambrose H., Greenspan, Martin, and Osgood, William R. "Strength of Riveted Steel Frame having Straight Flanges," Research Paper 1130, Journal of Research, U. S. Bureau of Standards, V-21 (1938), pp. 269-313.
- . "Strength of Riveted Steel Rigid Frame having Curved Inner Flanges," Research Paper No. 1161, Journal of Research, U. S. Bureau of Standards, V. 21 (1938), pp. 853-871.
- Stang, Ambrose H. and Greenspan, Martin. "Strength of Welded Steel Rigid Frame," Research Paper No. 1224, Journal of Research, U. S. Bureau of Standards, V. 23 (1939), pp. 145-150.
- Timoshenko, S. Strength of Materials, Part II. New York: D. Van Nostrand, Inc., 1956.
- Timoshenko, S. and Goodier, J. N. Theory of Elasticity. New York: McGraw-Hill Book Co., Inc., 1951.
- Wang, Chi-Teh. Applied Elasticity. New York: McGraw-Hill Book Co., Inc., 1953.
- Williams, Clifford D. and Cutts, Charles E. Structural

  Design in Reinforced Concrete. New York: The Ronald

  Press Company, Inc., 1954.
- Wise, Joseph A. "Corner Effects in Rigid Frames,"

  Proceedings of American Concrete Institute, 35
  (September 1938--June 1939), pp. 192-1--192-8.

